

การศึกษาประสิทธิภาพของยาแพรมลินไทด์ในมะเร็งกระดูกชนิดออสทีโอซาร์โคมา



นายอภิรักษ์ แสงสิน

จุฬาลงกรณ์มหาวิทยาลัย

CHULALONGKORN UNIVERSITY

บทคัดย่อและแฟ้มข้อมูลฉบับเต็มของวิทยานิพนธ์ตั้งแต่ปีการศึกษา 2554 ที่ให้บริการในคลังปัญญาจุฬาฯ (CUIR)

เป็นแฟ้มข้อมูลของนิสิตเจ้าของวิทยานิพนธ์ ที่ส่งผ่านทางบัณฑิตวิทยาลัย

The abstract and full text of theses from the academic year 2011 in Chulalongkorn University Intellectual Repository (CUIR) are the thesis authors' files submitted through the University Graduate School.

วิทยานิพนธ์นี้เป็นส่วนหนึ่งของการศึกษาตามหลักสูตรปริญญาวิทยาศาสตรดุษฎีบัณฑิต

สาขาวิชาชีวเวชศาสตร์ (สหสาขาวิชา)

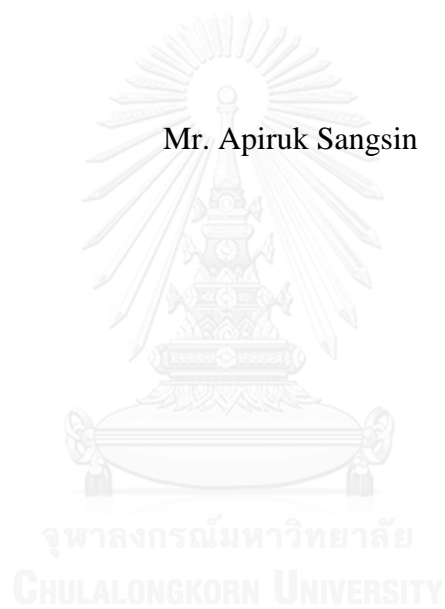
บัณฑิตวิทยาลัย จุฬาลงกรณ์มหาวิทยาลัย

ปีการศึกษา 2559

ลิขสิทธิ์ของจุฬาลงกรณ์มหาวิทยาลัย

IN VITRO STUDY OF EFFICACY OF PRAMLINTIDE IN OSTEOSARCOMA

Mr. Apiruk Sangsin



A Dissertation Submitted in Partial Fulfillment of the Requirements
for the Degree of Doctor of Philosophy Program in Biomedical Sciences
(Interdisciplinary Program)

Graduate School

Chulalongkorn University

Academic Year 2016

Copyright of Chulalongkorn University

Thesis Title	IN VITRO STUDY OF EFFICACY OF PRAMLINTIDE IN OSTEOSARCOMA
By	Mr. Apiruk Sangsin
Field of Study	Biomedical Sciences
Thesis Advisor	Professor Vorasuk Shotelersuk, M.D.
Thesis Co-Advisor	Professor Kanya Suphapeetiporn, M.D., Ph.D.

Accepted by the Graduate School, Chulalongkorn University in Partial Fulfillment of the Requirements for the Doctoral Degree

..... Dean of the Graduate School
(Associate Professor Sunait Chutintaranond, Ph.D.)

THESIS COMMITTEE

..... Chairman
(Professor Apiwat Mutirangura, M.D., Ph.D.)

..... Thesis Advisor
(Professor Vorasuk Shotelersuk, M.D.)

..... Thesis Co-Advisor
(Professor Kanya Suphapeetiporn, M.D., Ph.D.)

..... Examiner
(Professor Ponlapat Rojnuckarin, M.D., Ph.D.)

..... Examiner
(Piti Techavichit, M.D.)

..... External Examiner
(Assistant Professor Dumnoensun Pruksakorn, M.D., Ph.D.)

อภิรักษ์ แสงสิน : การศึกษาประสิทธิภาพของยาแพรมลินไทด์ในมะเร็งกระดูกชนิดออสทีโอซาร์โคมา (IN VITRO STUDY OF EFFICACY OF PRAMLINTIDE IN OSTEOSARCOMA) อ.ที่ปรึกษาวิทยานิพนธ์
หลัก: ศ. นพ. วรศักดิ์ โชติเลอศักดิ์, อ.ที่ปรึกษาวิทยานิพนธ์ร่วม: ศ. ดร. พญ. กัญญา สุภปิณฑิพร, 118 หน้า.

มะเร็งกระดูกชนิดออสทีโอซาร์โคมาเป็นมะเร็งกระดูกที่พบบ่อยที่สุดในเด็กและวัยรุ่น หลังจากการพัฒนาการรักษาด้วยการให้ยาเคมีบำบัดในปี พ.ศ.2513 อัตราการรอดชีวิตของมะเร็งกระดูกชนิดออสทีโอซาร์โคมาเพิ่มขึ้นจากร้อยละ 50 เป็นร้อยละ 70 แต่อย่างไรก็ตามอัตราการรอดชีวิตของมะเร็งกระดูกชนิดออสทีโอซาร์โคมาที่ระดับนี้มากกว่า 30 ปี การศึกษาวิเคราะห์ผลโปรตีนโพรตีโอมิกส์จากการทบทวนวรรณกรรมและอาศัยผลการทดลองในอดีต ร่วมกับการศึกษาการกลายพันธุ์สาเหตุในมะเร็งกระดูกชนิดออสทีโอซาร์โคมา ทำให้ค้นพบยาสองตัวได้แก่ คาร์ดิแอก ไกลโคไซด์ และ แพรมลินไทด์ โดยยาสองตัวนี้ได้ผ่านการรับรองจากองค์การอาหารยาของประเทศสหรัฐอเมริกาให้ใช้ในการรักษาโรคที่ไม่ใช่มะเร็ง ยาทั้งสองได้ถูกนำมาทดสอบประสิทธิภาพการยับยั้งการเจริญเติบโตหรือกระตุ้นให้เกิดการตายของเซลล์มะเร็งกระดูกชนิดออสทีโอซาร์โคมา ด้วยวิธีการทดสอบการเป็นพิษต่อเซลล์ และ โฟล์ว โซโตเมทรี เซลล์ไลน์มะเร็งกระดูกชนิดออสทีโอซาร์โคมาชนิด Saos-2 มีการตอบสนองต่อ คีจ็อกซิน ที่ความเข้มข้นน้อยกว่า 1 ไมโครโมลาร์ เซลล์ไลน์มะเร็งกระดูกชนิดออสทีโอซาร์โคมาชนิด MNNG-HOS และ MG-63 ตอบสนองต่อ คีจ็อกซิน ความเข้มข้นน้อยกว่า 0.1 ไมโครโมลาร์ ร้อยละ 52 ของเซลล์มะเร็งกระดูกชนิดออสทีโอซาร์โคมาปฐมภูมิ ตอบสนองต่อ คีจ็อกซิน ที่ความเข้มข้นน้อยกว่า 1 ไมโครโมลาร์ โดยที่ร้อยละ 25 ตอบสนองต่อ คีจ็อกซิน ความเข้มข้นน้อยกว่า 0.1 ไมโครโมลาร์ สำหรับยาแพรมลินไทด์นั้น งานวิจัยได้ศึกษาเซลล์ไลน์มะเร็งชนิด ได้แก่ NCI-H1299, U-2 OS, Saos-2, และ MMNG/HOS และเซลล์มะเร็งกระดูกปฐมภูมิจำนวน 27 ตัวอย่าง ได้รับการตรวจวัดการแสดงออกของอาร์เอ็นเอเข้ารหัสของยีน *CALCR* และ *RAMP3* ด้วยกระบวนการปฏิกิริยาถูกโซฟอลิเมอเรสแบบเรียลไทม์ เซลล์เหล่านี้ถูกนำไปเลี้ยงในน้ำยาเลี้ยงเซลล์ที่ผสมกับยา แพรมลินไทด์อะซิเตทที่ความเข้มข้น 0.001-100 ไมโครกรัมต่อมิลลิลิตร เป็นเวลา 24, 48, และ 72 ชั่วโมง แล้วจึงนำร้อยละของเซลล์ที่รอดชีวิตมาเปรียบเทียบระหว่างกลุ่มที่ใส่ยาและไม่ใส่ยา จากการทำปฏิกิริยาถูกโซฟอลิเมอเรสแบบเรียลไทม์พบว่า U-2 OS และ เซลล์มะเร็งกระดูกปฐมภูมิตัวอย่างที่หนึ่งมีการแสดงออกของอาร์เอ็นเอเข้ารหัสในยีน *CALCR* และ *RAMP3* ขณะที่ Saos-2, MNNG/HOS, NCI-H1299 และ เซลล์มะเร็งกระดูกปฐมภูมิอีก 26 ตัวอย่างไม่พบการแสดงออก หรือพบการแสดงออกเพียงเล็กน้อย เซลล์มะเร็งกระดูกปฐมภูมิตัวอย่างที่หนึ่งถูกนำมาหาการกลายพันธุ์ในยีน *p53* ด้วยวิธีการถอดรหัสพันธุกรรมทั้งเอ็กโซม โดยพบว่าเซลล์มะเร็งกระดูกปฐมภูมิตัวอย่างที่หนึ่งมีการกลายพันธุ์ของเซลล์ร่างกายซึ่งไม่พบในเม็ดเลือดขาวของผู้ป่วยคนเดียวกัน จากการทดลองพบว่าแพรมลินไทด์อะซิเตทที่ความเข้มข้น 0.001-10 ไมโครกรัมต่อมิลลิลิตร ไม่สามารถกระตุ้นให้เซลล์มะเร็งรวมถึงเซลล์มะเร็งกระดูกชนิดออสทีโอซาร์โคมาเกิดอะพอพโทซิสหรือการตายได้ ไม่ว่าเซลล์นั้นจะมีการกลายพันธุ์ของยีน *p53* หรือ การแสดงออกของยีน *CALCR* และ *RAMP3* อย่างไร ในขณะที่ความเข้มข้น 100 ไมโครกรัมต่อมิลลิลิตรทำให้เกิดการตายของเซลล์มะเร็งเนื่องจากความเป็นกรดของอะซิเตทในยา ไม่ได้เกิดจากแพรมลินไทด์ โดยสรุปพบว่าการศึกษาที่แพรมลินไทด์ไม่มีคุณสมบัติในการต่อต้านมะเร็งกระดูกชนิดออสทีโอซาร์โคมาในหลอดทดลอง

สาขาวิชา ชีวเวชศาสตร์

ปีการศึกษา 2559

ลายมือชื่อนิสิต

ลายมือชื่อ อ.ที่ปรึกษาหลัก

ลายมือชื่อ อ.ที่ปรึกษาร่วม

5787824220 : MAJOR BIOMEDICAL SCIENCES

KEYWORDS: OSTEOSARCOMA, P53, TARGETED THERAPY, PRAMLINTIDE

APIRUK SANGSIN: IN VITRO STUDY OF EFFICACY OF PRAMLINTIDE IN OSTEOSARCOMA. ADVISOR: PROF. VORASUK SHOTELERSUK, M.D., CO-ADVISOR: PROF. KANYA SUPHAPEETIPORN, M.D., Ph.D., 118 pp.

Osteosarcoma (OS) is the most common primary bone cancer in young adults and children. After the development of chemotherapy in 1970, the survival rate improved from 50 to 70%; however, it has reached its plateau at 70% for almost 30 years. Using comprehensive analysis of proteomic studies, our in-house proteomic database, and underlying pathogenic genetic studies of OS, cardiac glycosides and pramlintide were identified as potential targeted therapeutic agents in OS. Cytotoxic assay and flow cytometry were performed to test *in vitro* efficacy against OS cells. OS cell lines including Saos-2 responded to digoxin at the concentrations of less than 1 μM . MNNG-HOS and MG-63 responded to digoxin at the concentrations of less than 0.1 μM . 52% of primary OS (11/21) responded at the concentrations of less than 1 μM . 25% (5/21) responded at the concentrations of less than 0.1 μM . *For the pramlintide*, mRNA expression levels of the *CALCR* and *RAMP3*, which are *pramlintide receptors*, were measured by real-time PCR (qRT-PCR) in four known p53 status cancer cell lines including NCI-H1299, U-2 OS, Saos-2, and MMNG/HOS and 27 primary osteosarcoma lines. They were co-cultured with pramlintide acetate at various concentrations ranging from 0.001-100 $\mu\text{g/ml}$ for 24, 48, and 72 hours. qRT-PCR showed that NCI-H1299, U-2 OS, and a primary osteosarcoma cell line expressed *CALCR* and *RAMP3* while Saos-2, MNNG/HOS, and other 26 primary osteosarcoma cell cultures did not express or expressed at very low levels. Whole exome sequencing (WES) revealed a p53 somatic missense mutation in one primary osteosarcoma cell culture expressing *CALCR* and *RAMP3*. At the concentration of 0.001-10 $\mu\text{g/ml}$, pramlintide acetate could not induce cancer cell apoptosis or cell death including osteosarcoma cells regardless of p53 status or *CALCR* and *RAMP3* expressions. At the concentration of 100 $\mu\text{g/ml}$, more cells were found to die in the pramlintide acetate treatment group compared to the non-treatment group. However, this was resulted from acidity of the acetate group, not pramlintide *per se*. In conclusion, this is the first study that demonstrates an *in vitro* antiosteosarcoma effect of digoxin. These findings should prompt further *in vivo* and clinical studies to verify its effectiveness.

Field of Study: Biomedical Sciences

Academic Year: 2016

Student's Signature

Advisor's Signature

Co-Advisor's Signature

ACKNOWLEDGEMENTS

“As a surgeon, you may help some patients throughout your life, but as a researcher you may help millions of them”, Prof. Vorasuk Shotelersuk, my beloved advisor, once said to me. This sentence ensured me to be his Ph.D. student. Throughout my years under supervision of Prof. Vorasuk, he said and did profound things that provided me a guiding light, not only academic but also realistic life. His mercy and kindness always expresses to everyone including his patients and students. I would like to express my deepest gratitude to him, Prof. Vorasuk Shotelersuk, by being a merciful doctor and a faithful researcher.

I am really grateful to my co-advisor Prof. Kanya Suphapeetiporn and colleagues in Center of Excellence for Medical Genetics for their guidance, helps, and support. My works in this thesis would not accomplish without these persons. Thank you all committee for your valuable time. Most importantly, thank you my patients who participated in this study.

Finally, I would like to express my sincere thanks to my parents who are my role models.

Financial support was provided by National Science and Technology Development Agency (NSTDA)

CONTENTS

	Page
THAI ABSTRACT	iv
ENGLISH ABSTRACT.....	v
ACKNOWLEDGEMENTS.....	vi
CONTENTS.....	vii
LIST OF FIGURES	1
LIST OF TABLES	4
CHAPTER 1 INTRODUCTION	5
1.1 Background and rationale.....	5
1.2 Research questions	6
1.3 Hypothesis	7
1.4 Objectives	7
1.5 Key words.....	7
1.6 Ethical consideration	8
1.7 Expected benefit	8
CHAPTER II REVIEW OF RELATED LITERATURES	9
2.1 Osteosarcoma	9
2.2 Current treatment in osteosarcoma	11
2.3 Molecular pathologies in osteosarcoma	12
2.4 Restoration of p53 functions	13
2.5 Selection of targeted therapy in osteosarcoma	18
2.6 Proteomic studies were used to identify targeted drugs in osteosarcoma	19
2.7 A novel anti-cancer applications of cardiac glycosides	24
2.8 The use of primary cell culture for in vitro targeted therapy testing.....	26
Partial enzymatic degradation of stromal cells	28
CHAPTER III MATERIALS AND METHODS	30
3.1 Subjects and clinical data	30

	Page
3.2 Pramlintide acetate and digoxin were selected to test their <i>in vitro</i> anticancer effects in primary osteosarcoma cell cultures and cancer cell lines. 30	
3.3 Primary osteosarcoma cell cultures	31
3.4 Cell line	32
3.4.1 NCI-H1299 (ATCC; CRL 5803).....	32
3.4.2 U-2 OS (ATCC; HTB-96), Saos-2 (ATCC; HTB-85), MNNG/HOS (ATCC; CRL-1547), and MG-63 (ATCC; CRL-1427)	33
3.5 Genomic DNA and RNA extraction of primary osteosarcoma cell cultures and cancer cell lines.....	33
3.5.1 Total RNA purification	34
3.5.2 Genomic DNA purification	35
3.6 Real-time quantitative reverse transcription PCR (qRT-PCR) of <i>CALCR</i> , <i>RAMP3</i> , and <i>ATP1B1</i> expression in primary osteosarcoma cells and cancer cell lines.....	35
3.7 Whole exome sequencing (WES) to determine p53 status in a primary osteosarcoma primary cell culture	36
3.8 Flow cytometry.....	37
3.9 Cytotoxicity assay (Resazurin microplate assay) (100)	38
CHAPTER IV RESULTS	40
4.1 U-2 OS and osteosarcoma primary cell culture No. 1 express <i>CALCR</i> and <i>RAMP3</i> at mRNA level	40
4.2 By WES, a somatic missense variant in p53 was found in primary osteosarcoma cell culture No.1.....	41
4.3 By using flow cytometry, pramlintide acetate at 10 µg/ml could not induce apoptosis in primary osteosarcoma cell culture and cell lines expressing <i>CALCR</i> and <i>RAMP3</i>	42
4.4 Pramlintide has no anticancer activity at concentration of 0.001-100 µg/ml in primary osteosarcoma cell culture and cancer cell lines.	44
4.5 Digoxin has anticancer effect in a half of primary osteosarcoma cell cultures and all osteosarcoma cell lines.....	56
4.6 Responses to digoxin do not correlate with <i>ATP1B1</i> expression levels.....	74

	Page
4.6 5-year survival rate in and chemotherapy response of patients recruited in this study are very low.....	75
CHAPTER V DISCUSSION.....	77
REFERENCES	83
APPENDIX A.....	103
THE USE OF NEXT-GENERATION SEQUENCING IN DIAGNOSIS AND MANAGEMENT OF SKELETAL DYSPLASIAS.....	103
A.1 BACKGROUND AND RATIONALE	103
A.2 REVIEW OF RELATED LITERATURES	104
A.2.1 Molecular pathology and phenotypic spectrum in osteogenesis imperfecta.....	104
A.2.2 Molecular pathology and phenotypic spectrum in type II collagenopathies	105
A.2.3 The use of whole-exome sequencing as a molecular diagnostic tool in skeletal dysplasias	105
A.2.4 Synthesis approach NGS by Illumina technology.....	106
A.3 MATERIALS AND METHODS.....	108
A.3.1 Study subjects.....	108
A.3.2 Genomic DNA preparation and Truseq Custom Amplicon sequencing in the patient with OI.....	108
A.3.3 Genomic DNA preparation and WES in the patient with type II collagenopathy.....	109
A.3.3A diagnosis of type II OI was made in the first child.....	110
A.3.4A diagnosis of type II OI was made in the first child.....	112
A.4 Results	113
A.4.1 Truseq Custom Amplicon sequencing revealed a novel homozygous one base pair frameshift deletion in <i>WNT1</i> in OI child.....	113
A.4.2 WES revealed a <i>de novo</i> missense mutation in <i>COL2A1</i>	114
A.5 Discussion	115
VITA.....	118

LIST OF FIGURES

Figure 1	The flow chart illustrated the approaching to improve the survival rate in osteosarcoma.....	6
Figure 2	Photomicrograph of a hematoxylin and eosin stain of a conventional high-grade osteosarcoma	10
Figure 3	Illustration of locations of p53 alterations in osteosarcoma	13
Figure 4	Δ -N isoform of p63 and p73 causes dominant negative effect on p53, p63, and p73 which promotes tumor growth and progression.....	14
Figure 5	CALCR and RAMP3 expression is critical for pramlintide function.	15
Figure 6	Magnetic resonance imaging of a mouse treated with three weekly injection of pramlintide.....	16
Figure 7	Histology of normal colon epithelial cell and carcinomastain with anti-RAMP3 antibody.....	17
Figure 8	Pramlinitde function is independent from p53, TAp63 or TAp73 status.	17
Figure 9	Diagram shows protein targets of FDA-approved for anti-cancer drugs, FDA-approved for non-anticancer drugs, and non-FDA-approved chemical agents.	22
Figure 10	The possible anticancer mechanisms of cardiac glycosides	26
Figure 11	CALCR and RAMP3 express obviously in U-2 OS and primary cell culture No. 1.....	40
Figure 12	BAM file of WES reveal a somatic mutation of p53 in tumor.....	41
Figure 13	Flow cytometry of U-2 OS cells stain with Annexin-FITC and PI.....	42
Figure 14	Flow cytometry of primary osteosarcoma cell culture No.1 stain with Annexin-FITC and PI.	43
Figure 15	Flow cytometry of NCI-H1299 cells stain with Annexin-FITC and PI. ...	43
Figure 16	Percentage of NCI-H1299 cell viability treated with various concentration of pramlintide acetate.	47
Figure 17	At the concentration of 100 μ g/ml, pramlintide acetate inhibited cell proliferation of NCI-H1299 cells at 24, 48, and 72 hours.	48
Figure 18	Flow cytometry of NCI-H1299 cells stain with Annexin-FITC and PI. ...	49

Figure 19	Percentage of U-2 OS cell viability (CALCR and RAMP3 expression) treated with various concentration of pramlintide acetate.	50
Figure 20	Percentage of primary cell culture No. 1 cell viability (CALCR and RAMP3 expression) treated with various concentration of pramlintide acetate.	51
Figure 21	Percentage of Saos-2 cell viability (CALCR and RAMP3 expression) treated with various concentration of pramlintide acetate.....	52
Figure 22	Percentage of MNNG/HOS cell viability (no CALCR and RAMP3 expression) untreated with various concentration of pramlintide acetate.	53
Figure 23	Percentage of NCI-H1299 (CALCR expression with no RAMP3 expression) cell viability treated with various concentration of pramlintide.	54
Figure 24	Illustration of the molecular structure of pramlintide.....	55
Figure 25	Percentage of primary cell culture case 1 cell viability treated with various concentration of acetic acid.....	56
Figure 26	Digoxin inhibits the viability of OS cells. Four greatest digoxin responsiveness OS cell lines and primary cell cultured are shown.	57
Figure 27	Percentage of primary cell culture No. 1 cell viability treated with various concentration of digoxin.	58
Figure 28	Percentage of primary cell culture No. 2 cell viability treated with various concentration of digoxin.	59
Figure 29	Percentage of primary cell culture No. 3 cell viability treated with various concentration of digoxin.	59
Figure 30	Percentage of primary cell culture No. 4 cell viability treated with various concentration of digoxin.	60
Figure 31	Percentage of primary cell culture No. 5 cell viability treated with various concentration of digoxin.	61
Figure 32	Percentage of primary cell culture No. 6 cell viability treated with various concentration of digoxin.	62
Figure 33	Percentage of primary cell culture No. 7 cell viability treated with various concentration of digoxin.	62
Figure 34	Percentage of primary cell culture No. 8 cell viability treated with various concentration of digoxin.	63
Figure 35	Percentage of primary cell culture No. 9 cell viability treated with various concentration of digoxin.	63

Figure 36	Percentage of primary cell culture No. 10 cell viability treated with various concentration of digoxin.	64
Figure 37	Percentage of primary cell culture No. 11 cell viability treated with various concentration of digoxin.	65
Figure 38	Percentage of primary cell culture No. 12 cell viability treated with various concentration of digoxin.	65
Figure 39	Percentage of primary cell culture No. 13 cell viability treated with various concentration of digoxin.	66
Figure 40	Percentage of primary cell culture No. 14 cell viability treated with various concentration of digoxin.	67
Figure 41	Percentage of primary cell culture No. 15 cell viability treated with various concentration of digoxin.	68
Figure 42	Percentage of primary cell culture No. 16 cell viability treated with various concentration of digoxin.	68
Figure 43	Percentage of primary cell culture No. 17 cell viability treated with various concentration of digoxin.	69
Figure 44	Percentage of primary cell culture No. 18 cell viability treated with various concentration of digoxin.	70
Figure 45	Percentage of primary cell culture No. 19 cell viability treated with various concentration of digoxin.	70
Figure 46	Percentage of primary cell culture No. 21 cell viability treated with various concentration of digoxin.	71
Figure 47	Percentage of MG-63 cell viability treated with various concentration of digoxin.	71
Figure 48	Percentage of MNNG-HOS cell viability treated with various concentration of digoxin.	72
Figure 49	Percentage of Saos2 cell viability treated with various concentration of digoxin.	73
Figure 50	Percentage of U-2OS cell viability treated with various concentration of digoxin.	73
Figure 51	Relative ATP1B1 mRNA expression levels in OS cell lines and primary cell cultures.....	74
Figure 52	5 year-survival graph of patients in this study.....	75

Figure 53	Percentage of tumor necrosis obtained from post-chemotherapy pathological reports of patients recruited in this study.	76
Figure 54	Physical examination reveals short stature with complex long bone deformities. Radiograph of lower extremities revealed varus deformity of the femurs and valgus deformity of the tibias.....	111
Figure 55	Clinical and radiographic feature of the patient with SEDC	113
Figure 56	Mutation analysis.....	115

LIST OF TABLES

Table 1	Summary of proteomics studies of osteosarcoma in Pubmed database ...	20
Table 2	p53 status of each cell line included in this study	33
Table 3	Percentage of growth inhibition of cancer cells treated with various concentrations of pramlintide acetate and time.	45

CHAPTER 1

INTRODUCTION

1.1 Background and rationale

Osteosarcoma is the most common primary bone cancer in young adults and children. Incidence peaks during the second decade of life, with a second peak during the seventh and eighth decades. In children, osteosarcoma accounts for 5-10% of all new pediatric cancers in the United States. Incidence of osteosarcoma in the United States is about 4:100,000 while the incidence in Thailand is much lower at about 1.9:100,000 (1). The lower incidence in Thailand may be due to lacking of complete database collection. The leading cause of death in osteosarcoma is the distant metastases to vital organs especially lung metastases. Treatment of osteosarcoma needs the multidisciplinary approaches from oncologic orthopedists, medical oncologists, physical therapists, and prosthetists which are very limited in Thailand. Osteosarcoma causes mortality and disability in young patients. Patients suffer from side effects of chemotherapy and aggressive surgery. Standard treatment guidelines of osteosarcoma, which consist of pre-operative chemotherapy, wide excision, and post-operative chemotherapy, have not changed for over 20 years. Standard treatment of osteosarcoma consists of neo-adjuvant chemotherapy, wide surgical excision, and adjuvant chemotherapy. After 1970, development of chemotherapy improved the survival rate of osteosarcoma patients from 50% to 70%. Chemotherapy regimens usually combines with methotrexate (response rate 30-40%), cisplatin (response rate 30%), doxorubicin (response rate 30-40%), and ifosfamide (response rate 30%) (2). Despite the development of new chemotherapy and surgical techniques, survival rate

after treatment remains unchanged for almost 30 years (3). In the non-metastases group, the survival rate is at 60-70% while of metastases group is only 30% (3). To improve the survival rate in osteosarcoma, the responder and non-responder to conventional should have biomarkers to distinguish between these two groups. The non-responder should have a new treatment protocol or a protocol that is adjunct to the conventional guidelines (Figure 1). We therefore propose to explore a possibility of a novel approach to treat osteosarcoma by testing potential drugs in primary osteosarcoma cell cultures and osteosarcoma cell lines.

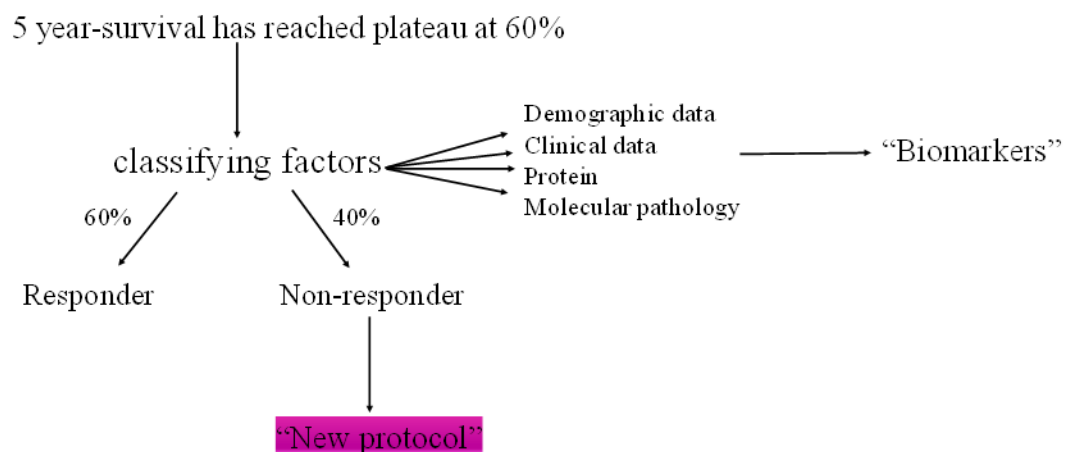


Figure 1 The flow chart illustrated the approaching to improve the survival rate in osteosarcoma.

1.2 Research questions

1.2.1 Can pramlintide inhibit cell proliferation and induce apoptosis in osteosarcoma primary cell cultures and osteosarcoma cell lines?

1.2.2 Does pramlintide function depend on p53 status?

- 1.2.3 Does pramlintide function depend on *CALCR* and *RAMP3* expressions?
- 1.2.4 Can proteomic approaches using previous databases and in-house database identify FDA approved non-anticancer drugs that have antiosteosarcoma properties in osteosarcoma primary cell cultures and osteosarcoma cell lines?

1.3 Hypothesis

- 1.3.1 Pramlintide induces apoptosis in cancer cells expressing *CALCR* and *RAMP3* independently of p53 status.
- 1.3.2 Proteomic approaches can identify upregulated targeted proteins in osteosarcoma that have matched FDA approved non-anticancer drugs and antiosteosarcoma properties in primary osteosarcoma cell cultures and osteosarcoma cell lines.

1.4 Objectives

- 1.4.1 To evaluate the efficacy of pramlintide in cancer with *CALCR* and *RAMP3* expression.
- 1.4.2 To identify FDA-approved non-anticancer drugs that have antiosteosarcoma properties in osteosarcoma primary cell cultures and osteosarcoma cell lines.

1.5 Key words

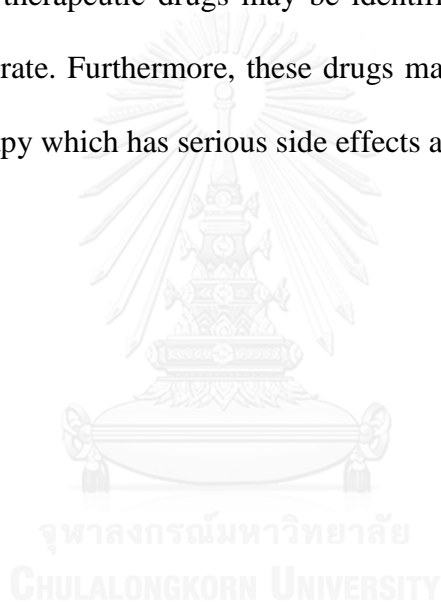
Osteosarcoma, targeted therapy, proteomic, pramlintide, *IAPP*, *p53*, cardiac glycoside, digoxin

1.6 Ethical consideration

The study was approved by the institutional review board of Faculty of Medicine, Chiang Mai University. Written informed consent was obtained from the parents who participated in this study.

1.7 Expected benefit

New targeted therapeutic drugs may be identified in osteosarcoma that may improve the survival rate. Furthermore, these drugs may reduce the dosage or avoid the use of chemotherapy which has serious side effects and complications.



CHAPTER II

REVIEW OF RELATED LITERATURES

2.1 Osteosarcoma

Osteosarcoma peaks during second and seventh and eighth decade of life. In elderly, osteosarcoma often occurs as a result of radiation therapy or underlying bone diseases such as Paget disease. In children, osteosarcoma have linked to rapid growth or growth spurt so incidence peaks during the second decade of life. Osteosarcoma has a predilection for the metaphyseal regions where the growth plate taking place. The two most common location are distal femur and proximal tibia accounting for 50% of all osteosarcoma (4). Osteosarcoma classified as primary or secondary osteosarcoma. Primary osteosarcoma are subdivided into intramedullary and surface osteosarcomas (5).

Conventional osteosarcoma is a primary intramedullary, high grade malignant tumor in which neoplastic cells produce osteoid (Figure 2). Conventional osteosarcoma has also been classified into osteoblastic, chondroblastic, and fibroblastic subtypes based on histologic appearance.

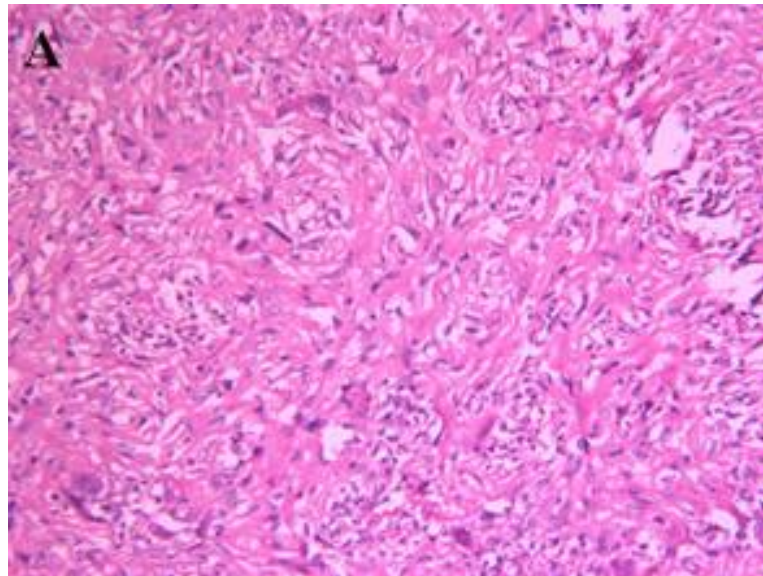


Figure 2 Photomicrograph of a hematoxylin and eosin stain of a conventional high-grade osteosarcoma (6)

Telangiectatic osteosarcoma is a subtype that mimics aneurysmal bone cyst which characterized by radiolucent bone destruction and blood-filled spaces with minimal solid tissue but presence of nuclear polymorphism and spindle cells producing osteoid distinguish telangiectatic osteosarcoma from aneurysmal bone cyst.

Small cell osteosarcoma composed of small round cells with osteoid production which is used as a clue to distinguish small cell osteosarcoma from Ewing sarcoma. This subtype has worse prognosis than conventional type (7, 8)

Low-grade central osteosarcoma is composed of low to moderate cell stroma with osteoid production (7, 9). Its histologic appearance mimics fibrous dysplasia so clinical and radiographic correlation is crucial to obtain diagnosis.

Surface osteosarcomas consist of parosteal and periosteal osteosarcoma. Parosteal osteosarcoma refers to low-grade osteosarcoma that occurs on the surface of the bone. The most common location is posterior surface of distal femur. Periosteal

osteosarcoma is an intermediate-grade chondroblastic osteosarcoma arising on the surface of the bone. The cartilaginous component can show cytologic atypia.

High-grade surface osteosarcoma is a high-grade bone malignancy originated from surface of the bone. The histologic features are the same as conventional type.

Secondary osteosarcoma occurs at the bone parts with preexisting conditions such as Paget disease, radiation, bone infraction, osteomyelitis, and fibrous dysplasia (7, 10)

2.2 Current treatment in osteosarcoma

Patient diagnosed non-metastases osteosarcoma should receive treatment with combination of chemotherapy using a regimen that contains at least three agents. The three most common drugs including doxorubicin, cisplatin, and high-dose methotrexate. The regimens can achieve a 5-year event free survival at 70% in non-metastases patients. Surgery is the key to obtain local control in patients with osteosarcoma. The optimal timing is usually after two cycles of preoperative chemotherapy. Obtaining free margin by limb salvage (Figure 3) or amputation (Figure 4) is based on the possibility of performing complete removal of the primary tumor and preserving a functional limb for the patients. Postoperative chemotherapy should resume within three weeks after surgery if no complications such as infections or wound dehiscence.

2.3 Molecular pathologies in osteosarcoma

The exact cause of osteosarcoma is still unclear. *p53* pathway thought to be a cause. Many lines of evidence suggests that *p53* is the key factor gene tumorigenesis. A germ line mutation in *p53*, Li-Fraumeni syndrome, has 107 times higher risk of osteosarcoma than normal population (11) while one allele loss of *p53* in mice can cause osteosarcoma (12). *p53* is named “guardian of the genome” due to its tumor suppressive function including DNA repair, controlling cell division, and induction of apoptosis (13, 14). In the past, many studies tried to identify the correlation of alterations in *p53* and the clinical course of the patients but most of them could not demonstrate clear correlation. There are only two studies demonstrated that overexpression of *p53* correlated with chemoresistance and low survival rate (15, 16). In 2005, 196 osteosarcoma samples were underwent Sanger sequencing. Only 19.4% carried alterations in *p53* because structural variations and other genes in *p53* pathway especially *MDM2*, a potent *p53* inhibitor, did not include in the study (17). Until recently in 2014, 20 osteosarcoma samples underwent whole genome sequencing and fluorescence *in situ* hybridization (Figure 3). The results showed that all osteosarcoma have alterations in *p53* pathway. 95% of them are *p53* structural variations or mutations while 5% are *MDM2* amplification (18). These aforementioned data support that *p53* alteration is a cause of tumorigenesis in osteosarcoma.

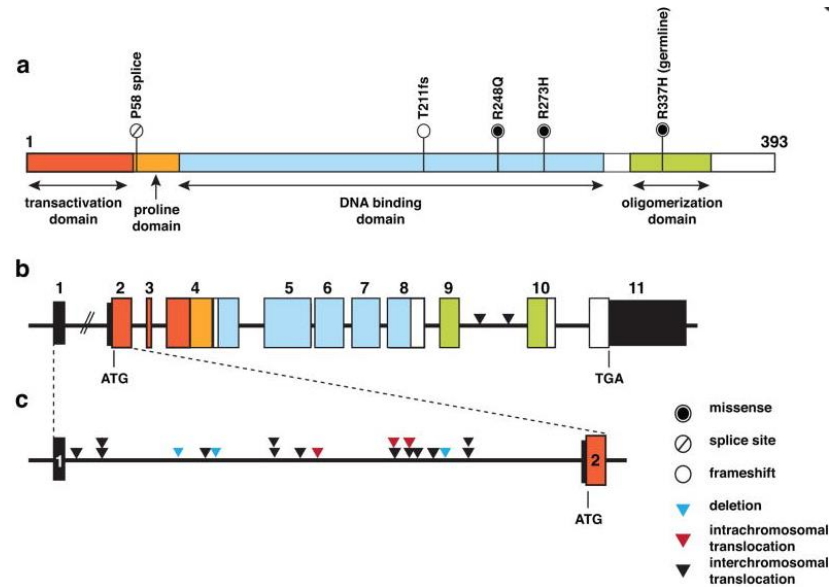


Figure 3 Illustration of locations of p53 alterations in osteosarcoma (18).

2.4 Restoration of p53 functions

Like osteosarcoma, Human cancers usually carry alterations in *p53*. In mouse model, restoration of *p53* function inhibited tumor progression. However, restoration of *p53* function in human is complicate because most of alterations result in loss of gene function. Recently, Venkatanarayan et al (19) focused on restoration of p53 functions using alternative genes in *p53* family, *p63* and *p73*. *p63* and *p73* have two different structures consisting of acidic transactivation-domain-bearing (TA) isoform which structurally and functionally resemble *p53* and Δ -N isoform (without acidic transactivation domain) which usually overexpresses in many cancers. Δ -N isoform causes dominant negative effect with p53, TAp63, and TAp73 which leads to loss of tumor progression function in these genes (20-24) (Figure 4).

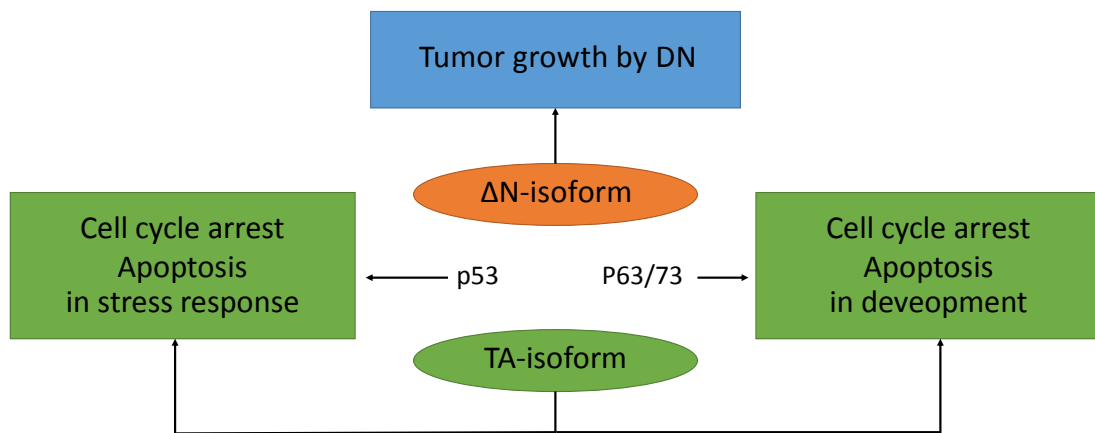


Figure 4 Δ -N isoform of p63 and p73 causes dominant negative effect on p53, p63, and p73 which promotes tumor growth and progression (19)

p53, *p63*, and *p73* are member of *p53* family which control the development and progression of cancer via apoptosis and autophagy. Acutely removed Δ -N isoform by intratumoral injection with adeno-Cre-mCherry in Δ Np63^{fl/fl}p53^{-/-}, Δ Np73^{fl/fl}p53^{-/-} mice at 10 weeks of age, mice deficient for either Δ Np63 or Δ Np73 and p53 showed marked decreases in tumor burden. Absence of Δ -N isoform of p63 and p73 caused metabolism reprogramming leading to tumor regression via overexpression of *IAPP* because TAp63 and TAp73 are transcription factor of *IAPP* gene. *IAPP* encodes amylin, a 37 amino acid protein, which is secreted from beta-cells of pancreas. Amylin inhibits glycolysis and induces reactive oxygen species which cause apoptosis via calcitonin receptor (*CALCR*) and receptor activity modifying protein 3 (*RAMP3*). When media containing amylin were used to treat H1299 cells (non-small cell lung cancer) with knockdown of *CALCR* or *RAMP3*,

glycolysis was not inhibited and ROS and apoptosis were not induced, indicating that the CALCR and RAMP3 receptors are critical for *IAPP* function (Figure 5). Amylin has a synthetic analogue named “pramlintide”.

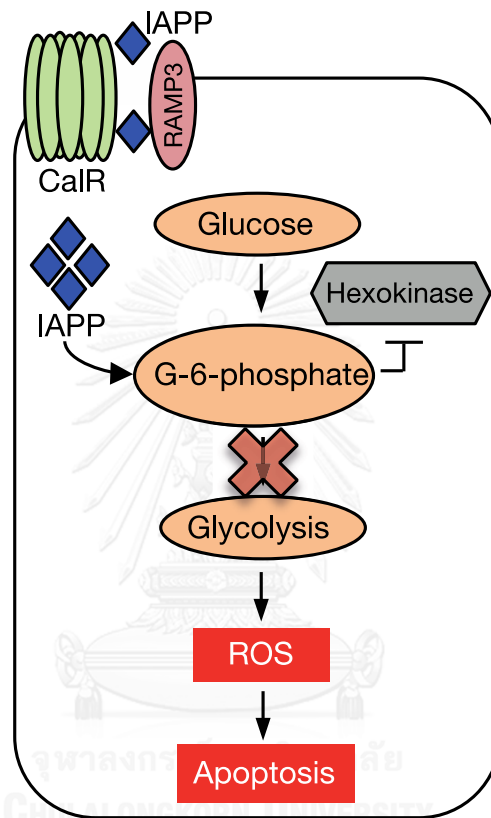


Figure 5 CALCR and RAMP3 expression is critical for pramlintide function (19).

In mouse model, mouse receiving pramlintide showed marked decrease in tumor volume while mouse receiving pramlintide and calcitonin receptor inhibitor showed tumor progression (19) (Figure 6).

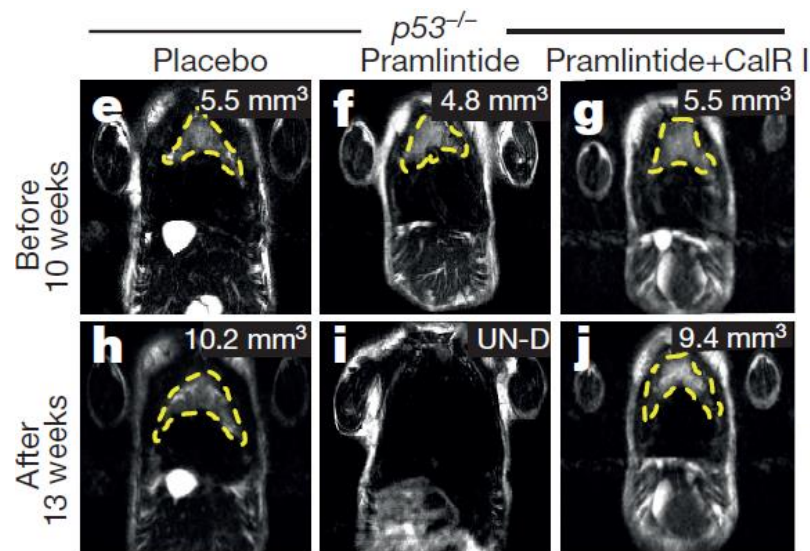


Figure 6 Magnetic resonance imaging of a mouse treated with three weekly injections of pramlintide (Middle column). Tumor volume reduction was statistically significant different between the mouse treated with pramlintide and placebo (Left column). A mouse treated with pramlintide plus calcitonin receptor inhibitor showed tumor progression (Right column).

In the normal colons, *RAMP3* expresses in colorectal carcinoma but not epithelial cells (Figure 7). This observation was repeated in 5 different tumors such as colon, breast, and gastric cancer (25) so pramlintide may be a potential anticancer drug that do no harm to normal tissues. As aforementioned, action of pramlintide may be independent to p53 status of tumor but dependent to *CALCR* and *RAMP3* expression. *p53* deficiency leading to up-regulation of TA p63 and 73 isoform. TAp63 and TAp73 are transcription factors of amylin so inhibition of glycolysis and induction of reactive oxygen species depend on p 53 status but when pramlintide is administered, mechanism of action is independent from p53, TAp63, or TAp73 (Figure 8).

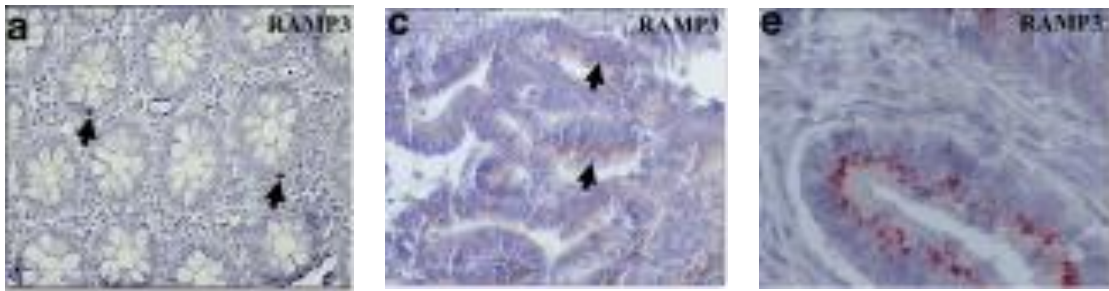


Figure 7 a. shows histology of normal colon epithelial cell stain with anti-RAMP3 antibody. c. Only neuroendocrine cells were stained while in carcinoma in picture and e. almost all of the epithelial cells shows RAMP3 expression so pramlintide may be a targeted therapy that do no harm to normal tissue (25) .

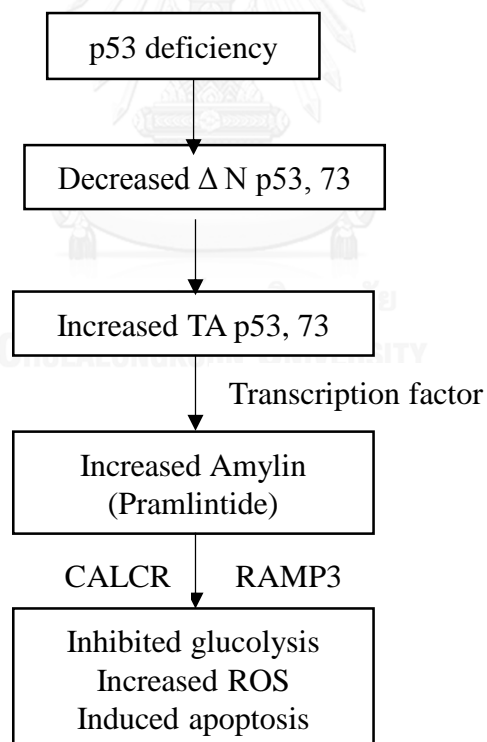


Figure 8 Pramlintide function is independent from p53, TAp63 or TAp73 status.

Pramlintide, a synthetic analogue of amylin, has been used for treatment of

type I and II diabetes. Pramlintide was approved by U.S. FDA so if its efficacy for osteosarcoma treatment is proved, end-state osteosarcoma may have a therapeutic approach and overall survival in osteosarcoma patients may improve.

2.5 Selection of targeted therapy in osteosarcoma

The most challenging issue in identifying an actionable target drug is to distinguish between driver mutations and passenger mutations. The goal is to maximize the anticancer properties while minimize the toxicity to normal tissues. The era of single gene testing is substituted with –omic era. The use of NGS gives us the alterations in known oncogenes or tumor suppressor genes. Factors that may help us to distinguish between driver and passenger mutations including

- Silent or non-silent mutation.
- The depth of sequencing.

By WGS or transcriptomic studies, we may identify structural variations that resulted from the instability of cancers. These abnormal genes may produce abnormal proteins that do not have in normal process in the body but it may or may not involve in tumorigenesis. Copy number variations may be also detected by comprehensive analysis of the read depths. Increasing in read depths in an oncogenes may be a cause that leads us to a targeted drug.

Besides NGS, several methods using public database can be used to identify upregulated genes that may involve in tumorigenesis. Using The Gene Expression Omnibus (GEO), a public repository for high-throughput gene expression data by microarray of cancers including osteosarcoma, is a source to identify upregulated

genes that may have novel anticancer protein inhibitors. Apiwat et al, created Connection up- and down-regulation expression analysis of microarrays (CU-DREAM) (26), a powerful tool for comparing the expression levels from microarrays. The resulting list of significantly upregulated genes can be cross-referenced with all targeted drugs or chemical substances.

Proteomics is a major technique of choice for studying proteins expressed by certain types of cancer. Aberrant protein expression is an important characteristic of malignant transformation that involves in changes of various cellular processes. In fact, not does proteomics only determine an alteration of protein abundance, it also serves as a valuable tool to investigate diversity of proteomes which largely arises from alternative splicing and post-translational modification. Therefore, this technique allows scientists to understand more insight into molecular mechanisms that relate to oncogenic pathways. Several proteomics studies of osteosarcoma cells have been performed mainly through gel-based approach. Most of them aim to study biological mechanisms of the disease as well as to seek for potential diagnostic biomarkers and novel therapeutic targets. The identification of aberrant-expressed proteins in osteosarcoma cells comparing to osteoblastic cells, thereby, enables further study on the targeted treatment of osteosarcoma.

2.6 Proteomic studies were used to identify targeted drugs in osteosarcoma

By literature mining from PubMed database (early 2016), proteomics studies of osteosarcoma have been performed both in cell cultures and clinical specimens including the studies of (1) osteoblastic and osteosarcoma cells, (2) benign and osteosarcoma tissues, (3) phenotypic characteristics of osteosarcoma cells including

metastasis, and chemoresistance, (4) responsiveness to various medicines or specific induction, (5) osteosarcoma cell lines, and (6) serum or plasma from osteosarcoma patients as summarized in table 2. This study aims to find candidate proteins that serve as targets of available medicines. Therefore, we particularly focus on proteomics data showing differentially-expressed proteins in osteosarcoma comparing to normal. However, thus far, proteomics studies of osteosarcoma tissues have been relied on a comparison with benign tumors, which did not represent actual normal tissues. This is not relevant to the objective of this study, thereby they were excluded.

Table 1 Summary of proteomics studies of osteosarcoma in Pubmed database

Proteomics of osteosarcoma	Number of literatures	Reference
Osteoblastic and osteosarcoma cells	8	(27-34)
Benign and osteosarcoma tissues	5	(35-39)
Metastasis	3	(40-42)
Chemoresistance	2	(43, 44)
Responsiveness to various medicines	6	(45-50)
Responsiveness under specific conditions	2	(51, 52)
Osteosarcoma cell lines	5	(53-57)
Serum or plasma	5	(58-62)
Total	36	

Proteomics studies of osteosarcoma and osteoblastic cells have been reported in publications during 2006 to early 2016 (Table 1). By using 1DE, 2DE and gel-free approaches, approximately 1900 proteins, which were upregulated in osteosarcoma

cells, were successfully identified (27-34). According to DAVID bioinformatics database, sub-cellular localizations of these identified proteins are membrane > nucleus > cytoplasm > mitochondria > ER. The biggest proportion of identified proteins from proteomics studies is membrane protein, since most data was mainly derived from the proteomics studies of membrane protein (30, 32). From our previous works, we have performed proteomics studies of primary osteosarcoma cell cultures and tissue samples of osteosarcoma. Results showed that expression levels of 24 and 37 proteins were significantly increased in osteosarcoma cells and tissues, respectively. To generate a list of upregulated proteins in osteosarcoma, proteomics data from literature mining and in-house results were combined. Then, to match available medicines and chemical agents to aberrantly expressed proteins in osteosarcoma cells, all upregulated protein names were converted to gene symbols and matched with lists of FDA-approved for anticancer drugs, FDA-approved for non-anticancer drugs, and non-FDA-approved chemical agents (Figure 9).

Sample		Technique	Reference
Osteoblastic cells	Osteosarcoma cells		
Primary cells: Bone samples	Osteosarcoma cell line: SaOS-2	2DE, MALDI-TOF	Spreafico <i>et al.</i> , 2006, Proteomics. (34)
Osteoblastic cell line: hFOB1.19	Osteosarcoma cell lines: U2OS, SaOS-2, and IOR/OS9	2DE, MALDI-TOF	GUO <i>et al.</i> , 2007, Acta Pharmacologica Sinica (27)
Primary cells: Biopsy of patients underwent surgery	Primary osteosarcoma cells: Paired samples of chemo-naive high- grade patients	2DE-DIGE, LC-ESI-MS/MS	Folio <i>et al.</i> , 2009, Journal of proteome research (28)
Primary cells: Bone sample	Osteosarcoma cell line: SaOS-2	2DE, MALDI-TOF	Liu <i>et al.</i> , 2009, Cancer Investigation (29)
Osteoblastic cell line: hFOB1.19	Osteosarcoma cell line: MG-63	iTRAQ labeling LC-MS/MS	Zhang <i>et al.</i> , 2010, BMC cancer (30)
Osteoblastic cell line: hFOB1.19	Osteosarcoma cell line: MG-63	2DE, ESI-MS/MS	Hua <i>et al.</i> , 2011, Tumor biology (31)
Primary osteoblastic cells: ORT-1, Hum31, Hum54	Osteosarcoma cell lines: MG-63, U2OS, Cal-72, SaOS-2, and LM7	1DE, LC-MS/MS, Label-free quantitative protein analysis	PosthumaDeBoer <i>et al.</i> , 2013, British journal of cancer (32)

Sample		Technique	Reference
Osteoblastic cells	Osteosarcoma cells		
Osteoblastic cell line: hFOB1.19	Osteosarcoma cell lines: Hs 39.T, Hs 184.T, and Hs 188.T	2DE, Ultraflex-TOF/TOF	Gemoll <i>et al.</i> , 2015, Oncotarget (33)

We focused on targeted protein inhibitors that have been proved by FDA for non-anticancer treatments because they have passed clinical trials for their safety and toxicity. If they are proven to have anti-cancer properties, they may novel targeted treatments in osteosarcoma which improve overall survival in osteosarcoma. ATP1B1 is a protein that has upregulation. It encodes Na⁺/K⁺-transporting ATPase subunit beta-1 which belongs to Na⁺/K⁺ ATPase subfamily. Na⁺/K⁺ ATPase has its inhibitors collectively called “cardiac glycosides”.

2.7 A novel anti-cancer applications of cardiac glycosides

Back in 1980s, breast cancer cells obtained from women who received digitalis had more benign characteristics when compared with control patients. These patients underwent mastectomy. Patients received digitalis have lower recurrence and mortality rate (63-65). These articles by Stenkvis triggered attention in anti-cancer effects of cardiac glycosides. After that, more than a thousand articles described anticancer properties of cardiac glycosides, with most describing *in vitro*. apoptotic effects of cardiac glycosides confirmed in many cancers including breast (66),

prostate (67-69), leukemia (70-74), melanoma (75), pancreatic (76), lung (77, 78), neuroblastoma (79), and renal cell adenocarcinoma (80). Many potential mechanisms that increased the susceptibility of cancer cells to cardiac glycosides are not yet elucidated. Possible mechanisms are proposed and summarized below and figure.

- Leakage theory: The differential expression and activity of Na^+/K^+ ATPase in tumor and normal tissues. Tumor significantly increase the expression level and activity of Na^+/K^+ ATPase (81)
- Activation of SRC-epidermal growth-factor receptor (EGFR)-mitogen-activated protein kinase (MAPK): Activation these pathways by cardiac glycosides in cancers results in growth arrest through an overexpression of the cyclin-dependent kinase inhibitor 1A (p21) (82)
- Inhibition of DNA topoisomerase activity: Digitoxin, at the concentration found in heart failure treatment, can induce DNA topoisomerase II cleavable complexes similar to etoposide which is a chemotherapy that inhibits topoisomerase (80).
- Inhibition of glycolysis: Cardiac glycosides can inhibit aerobic glycolysis. It is known that cancer cells have high rate of glycolysis. Inhibition of aerobic

glycolysis reduces the capacity of cancer cells to eliminate H_2O_2 (83).

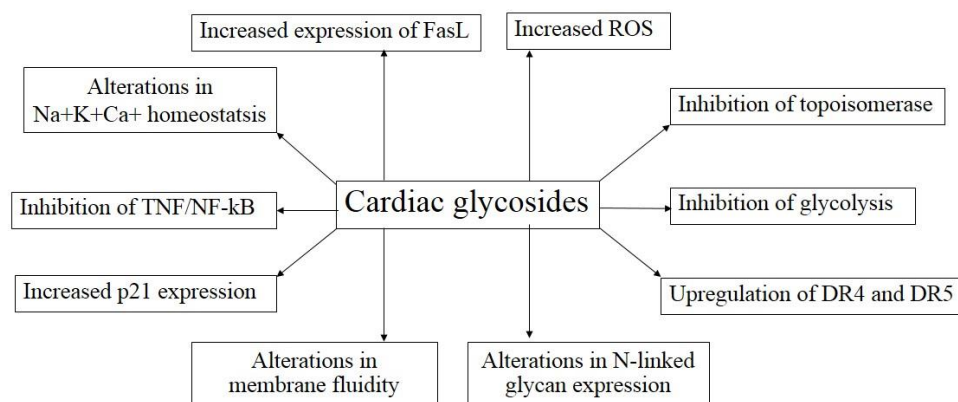


Figure 10 The possible anticancer mechanisms of cardiac glycosides (66, 74, 78, 80, 84-88)

2.8 The use of primary cell culture for *in vitro* targeted therapy testing

In vitro studies using cancer cell lines have role in understanding of tumor biology, in order to screen potential drugs. However, accumulation of genetic alterations of cancer cell lines limit clinical correlation (89, 90) so these cell lines do not represent clinical scenarios. Patients in clinical practice have genetic and epigenetic diversities that cannot be comprehended by a small number of cancer cell lines. Development of generating and culturing technologies from primary tumor cells from patients will be an effective *in vitro* to *in vivo* translation.

Isolation and culturing tumor cells from solid tumors are challenge and require specific techniques in each type of tumor. Isolation of tumor cells from a solid tumor depend on disruption of extracellular matrix (ECM) by specific enzyme because ECM

of each solid tumor has specific mixture of cohesive factors (91, 92). Moreover, after isolation of cancer cells, there are some additional complications that should be concerned including contamination of non-tumor cell, few viable cancer cells, and contamination of normal stromal cell. These complications are the main obstacles of using primary cell culture. Several methods are generated to provide essential tools from primary cell culture development.

2D monolayer culture

Plate is coated with collagen, Matrigel, fibronectin, or mixture components. The aim is to promote cancer cells to produce ECM and adhere to the plate. However, this methods do not represent tissue specific characteristic and lack of architecture diversities. In vitro drug test by 2D culture have quite variable results than 3D method (93).

Explant-cell culture system

Tumor tissue is cut into a smaller pieces ($<2 \text{ mm}^3$) and then placed in six-well plate that was coated with FBS. The tissue pieces must have a contact surface with plate and not float in the medium. The explants with overgrowth fibroblast are discarded while monolayer of cancer is preserved. The monolayer of cancer cells will form a halo. The explants should be moved to a new culture dish or plate to subculture. Several subculture will derive a primary tumor cell lines. This method reflects better *in vivo* molecular interactions. However, long-term culture creates genetic alteration and variability (94).

Precision-cut slice cultures

This method is the same as explant culture methods, however; the thickness of tissue cut is $160 \mu\text{m}$ and the size is 0.5 cm^3 . This method increasing the percentage of

viable cell at about 50% at 24 and 48 hours. This method is not suitable for tumor cell that usually from specific architecture such as melanoma (95).

3D cell culture

This method aims to develop organoids that resemble *in vivo* environment. Cells growth on ECM that consists of mixture glycoproteins, proteoglycan, and collagens. These make up the scaffold to stabilize and support the cell attachment (96). Biological scaffold facilitates cell proliferation, factors secretions, immune invasion strategies, hypoxic condition, angiogenesis, and metastatic ability. However, reagents are more expensive and tissue specific choice of matrix is needed.

Partial enzymatic degradation of stromal cells

Tumors are suspended in medium containing collagenase type I and hyaluronidase and incubated at 37°C for 1-6 hours until the medium becomes turbid. Then medium is filtered and centrifuged to obtain cell pellet. Cell pellet is cultured in medium with low calcium and nutrients. Fibroblast contamination is removed by differential trypsinization (97). This method is effective when using with mammary tissue. However, contamination of normal stromal and epithelial cells makes heterogeneity of cell culture by this method.

Sandwich culture

This method provides nutrition support environment for cancer cells while normal cells cannot survive. Organoids and clumps of the cancer cell will be isolated from the tumor by mechanical or enzymatic dissociation. Then single cell suspension is made by trypsinization. Cells are plated on a glass slide. After 24 hours, Cells will attach to the slide. Another slide is placed on the top of the first slide. A thin layer of medium supplies the nutrition for cancer cells. Cells will grow in clonal patches of 8-

16 cells. Discrete Patches are cultured by regular methods for 2-4 weeks, then are ready for large amount of culture (98).

Cancer stem cell isolation

Surface markers on cancer cell surface can be used to source pre-cancer stage of cells based on autofluorescence. However, cancer stem cells express surface marker heterogeneously in the same tumor mass. Identification of markers for cancer diversities is growing. By this method, scientist will get several primary cancer cell lines from one tumor mass that represent its heterogeneity (99).



CHAPTER III

MATERIALS AND METHODS

3.1 Subjects and clinical data

27 primary osteosarcoma cell cultures were collected from diagnostic incisional biopsies at Faculty of Medicine, Chiang Mai University from 2012-2015.

3.2 Pramlintide acetate and digoxin were selected to test their *in vitro* anticancer effects in primary osteosarcoma cell cultures and cancer cell lines.

From the literature reviews, all osteosarcomas have alterations in p53 pathway. The alternative pathway including TAp63 and TAp73 may be a potential therapeutic pathway. Tap63 and Tap73 cause metabolic reprogramming via upregulation of IAPP, a gene encode amylin protein. Amylin has a synthetic analogue named pramlintide so pramlintide acetate, a FDA approved drug for DM type I and II was selected to study its efficacy in osteosarcoma by using primary osteosarcoma cell cultures.

From the reviews of proteomic studies and analysis of our in-house database by using primary osteosarcoma cell cultures and fresh-frozen tissues. Four upregulated genes matched FDA approved non-anticancer drugs consisting of *ATP1B1*, *DHODH*, *IMPDH1*, *IMPDH2*, and *PPAT*. We focused on *ATP1B1* because it has cardiac glycosides as its inhibitors which were known to have anticancer properties both *in vitro* and *in vivo*. One of the most well-known cardiac glycoside is digoxin. Its dosages and therapeutic levels in heart conditions are well-established. Moreover, its availability in every hospital and research institutes made digoxin is the

most frequent cardiac glycoside that has been tested its anticancer properties so we have chosen digoxin as a representative of cardiac glycosides.

3.3 Primary osteosarcoma cell cultures

After biopsy tissues were obtained from the operating room, they will be soaked in 0.9% normal saline. The fresh tissue culture protocol was done as below.

1. Tissue was cut into a small pieces in a 50 ml tube and washed with 1X PBS 4-5 times repeatedly.
2. The tube containing tissue was centrifuged briefly then supernatant was discarded.
3. Collagenase was added to the 3 ml medium then this medium was poured to the tissue.
4. The tube was incubated at 37 °C in shaking water bath for 20 minutes.
5. The supernatant was kept in a new 50 ml tube and 3 ml of 10% DMEM was added to stop reaction.
6. 3 ml of medium containing collagenase was added to the tissue part.
7. The tube was incubated at 37 °C in shaking water bath for 20 minutes.
8. The supernatant was collected to the 50 ml tube containing supernatant from step 5.
9. 3ml of 0.25% trypsin was added to the tissue part.
10. The tube was incubated at 37 °C in shaking water bath for 20 minutes.
11. The supernatant was collected to the 50 ml tube containing supernatant from step 5 and 8.
12. 3ml of medium containing collagenase was added to the tissue part.

13. The tube was incubated at 37 °C in shaking water bath for 20 minutes.
14. The supernatant was collected to the 50 ml tube containing supernatant from step 5, 8, and 11 then centrifuged at 2,000 RPM for 3 minutes.
15. The tissue part was washed with 1X PBS for 2 times
16. Tissue was seeded on a T25 flask then 5 ml 20% DMEM medium was added.
17. Flask was incubated at 37 °C for a week.
19. After that the cells were ready for future experiments.

After a week, these primary osteosarcoma cells then were cultured in DMEM with high glucose, with L-Glutamine, without Sodium Pyruvate (Hyclone, GE Healthcare Life Science, Utah, USA). Supplemented with 10% FBS, 100 units/ml penicillin, and 100 µg/ml streptomycin (Gibco, Life Technologies, New York, USA). Cells were incubated at 37°C in 5%CO₂-95% air atmosphere. Passaging were achieved using Trypsin-EDTA solution (Hyclone).

3.4 Cell line

Cancer cell lines with known p53 status (table 1) were cultured using medium and methods as following;

3.4.1 NCI-H1299 (ATCC; CRL 5803)

cells were cultured in RPMI-1640 Medium (Hyclone, GE Healthcare Life Science, Utah, USA) supplemented with 10% FBS, 100 units/ml penicillin, and 100 µg/ml streptomycin (Gibco, Life Technologies, New York, USA). Cells were

incubated at 37°C in 5%CO₂-95% air atmosphere. Passaging were achieved using Trypsin-EDTA solution (Hyclone).

3.4.2 U-2 OS (ATCC; HTB-96), Saos-2 (ATCC; HTB-85), MNNG/HOS (ATCC; CRL-1547), and MG-63 (ATCC; CRL-1427)

cells were cultured in DMEM with high glucose, with L-Glutamine, without Sodium Pyruvate (Hyclone, GE Healthcare Life Science, Utah, USA) supplemented with 10% FBS, 100 units/ml penicillin, and 100 µg/ml streptomycin (Gibco, Life Technologies, New York, USA). Cells were incubated at 37°C in 5%CO₂-95% air atmosphere. Passaging were achieved using Trypsin-EDTA solution (Hyclone).

Table 2 p53 status of each cell line included in this study

Wild type p53	Mutant/ deficient p53
U-2 OS (MDM2 amplification)	NCI-H1299 (Partial deletion)
	Saos-2 (Entire gene deletion)
	MNNG/HOS (Missense)
	MG-53 (Rearrangement)

3.5 Genomic DNA and RNA extraction of primary osteosarcoma cell cultures and cancer cell lines

DNA and RNA were extracted from primary osteosarcoma cell cultures or osteosarcoma cell lines in the same passage using AllPrep DNA/RNA Mini kit following manufacturer's protocols.

1. Cells were trypsinized from T75 flask using 0.1% trypsin-EDTA solution (Hyclone) and washed with PBS.
2. Cells were centrifuged at 300xg for 5 minutes. Supernatant was aspirated
3. Cells were disrupted by adding 600 μ l and mixed homogeneously.
4. Lysate was pipetted into QIAshredder spin column placed in a 2 ml collection tube and centrifuge at maximum speed.
5. Homogenized lysate was transfer to AllPrep DNA spin column placed in 2 ml collection tube. Closed the lid gently, and centrifuge for 30 seconds at \geq 8,000xg
6. AllPrep DNA spin column was placed in a new collection tube, and store at room temperature for later DNA purification. The flow through was used for RNA purification.

3.5.1 Total RNA purification

1. 600 μ l of 70% ethanol was added to the flow through, and mixed by pipetting.
2. Sample was transfer to an RNeasy spin column placed in a 2 ml tube. Centrifuge at \geq 8,000xg for 15 seconds.
3. 700 μ l of Buffer RW1 was added to the RNeasy spin column. Column was centrifuged Centrifuge at \geq 8,000xg for 15 seconds.
4. 500 μ l of Buffer RPE was added to the RNeasy spin column, and Centrifuge at \geq 8,000xg for 15 seconds to wash the spin column membrane.
5. 500 μ l of Buffer RPE was added to the RNeasy spin column, and Centrifuge at \geq 8,000xg for 2 minutes to wash the spin column membrane.
6. RNeasy spin column was placed in a new 2 ml tube, and centrifuged at full

speed for 1 minute.

7. RNeasy spin column was placed in 1.5 ml collection tube. 30 μ l RNase-free water was added directly to the spin column membrane. Column was centrifuged at $\geq 8,000xg$ for 1 minute to elute the RNA.

3.5.2 Genomic DNA purification

1. 500 μ l of Buffer AW1 was added to the AllPrep DNA column, and Centrifuge at $\geq 8,000xg$ for 15 seconds to wash the spin column membrane. Flow through was discarded.
2. 500 μ l of Buffer AW2 was added to the AllPrep DNA column, and Centrifuge for 2 minutes to wash the spin column membrane.
3. AllPrep DNA column was placed in a new 1.5 ml collection tube. 100 μ l of Buffer EB was added directly to the spin column membrane. Column was incubated at room temperature for 1 minute, and centrifuged at $\geq 8,000xg$ for 1 minute to elute the DNA.

3.6 Real-time quantitative reverse transcription PCR (qRT-PCR) of *CALCR*, *RAMP3*, and *ATP1B1* expression in primary osteosarcoma cells and cancer cell lines.

Reverse transcription was performed using ImProm-II[™] RT (Promega, Madison, Wisconsin, USA). RNA levels of *CALCR*, *RAMP3*, and *ATP1B1* were quantified in primary osteosarcoma cell cultures and osteosarcoma cell lines by quantitative real-time (qRT) analysis using TaqMan probes of the StepOnePlus Real-

time PCR system (Applied Biosystems, CA, USA). The probes will be run in triplicate two times in separate tubes. Relative expression analysis will be calculated in terms of $\Delta\Delta C_t$ normalised to glyceraldehyde 3-phosphate dehydrogenase (*GAPDH*) transcription levels.

3.7 Whole exome sequencing (WES) to determine p53 status in a primary osteosarcoma primary cell culture

Genomic DNA from primary osteosarcoma cell culture No.1 that expressed *CALCR* and *RAMP3* and leukocytes from the same patient were sent to Macrogen, Inc., South Korea for WES. DNA was captured using a SureSelect Human All Exon version 4 kit (Agilent Technologies, Santa Clara, CA) and sequenced on a HiSeq2000 instrument. Base calling was performed and quality scores were analyzed using Real Time Analysis software version 1.7. Sequence reads were aligned against the University of California Santa Cruz human genome assembly hg19 using Burrows-Wheeler Alignment software (bio-bwa.sourceforge.net/). Single-nucleotide variants (SNVs) and insertions/deletions (Indels) were detected by SAMTOOLS (samtools.sourceforge.net/) and annotated against dbSNP & the 1000 Genomes Project. After quality filtering, we looked for somatic mutations by comparing side by side at each locus of variants to identify discordant variants between DNA derived from osteosarcoma cell and leukocytes especially in p53.

3.8 Flow cytometry

Primary osteosarcoma cells or cancer cell lines were seeded (5×10^5 cells/well) on 6 well plate for 12 hours. Cells will be treated pramlintide acetate (SymlinPen®) at concentration 0, 0.001, 0.01, 0.1, 1, 10, and 100 $\mu\text{g/ml}$ for 24, 48, and 72 hours (NCI-H1299) and 10 $\mu\text{g/ml}$ for 48 hours (NCI-H1299, U-2OS, Saos2, and MNNG/HOS). 0.9% NaCl solution was used to perform control experiment (untreated group). After desired period of time, cells were harvested and washed in cold phosphate-buffered saline (PBS). Then FITC AnnexinV/Dead cell Apoptosis kit with annexinV and propidium iodide (PI), for flow cytometry (Molecular Probes, OR, USA) was used according to the modified manufacturer's instructions.

1. 1x annexin-binding buffer was prepared by adding 1 ml of annexin binding buffer to 4 ml of deionized water (for 10 assays).
2. 100 $\mu\text{g/ml}$ working PI solution was prepared by diluting 5 μl of the 1 mg/ml PI stock solution in 45 μl 1x annexin binding buffer.
3. Re-centrifuge the washed cells, discard the supernatant, and resuspend the cells in 1x annexin binding buffer. (Determine the cell density and dilute in 1x annexin binding buffer to $\sim 1 \times 10^6$ cells/ml, preparing a sufficient volume to have 100 μl per assay)
4. Add 2 μl of FITC annexinV and 1 μl of the 100 $\mu\text{g/ml}$ PI working solution were added to each 100 μl of cell suspension.
5. Cells were incubated at room temperature for 15 minutes.
6. After the incubation period, 400 μl of 1x annexin binding buffer were added and mixed with the samples in ice.
7. Stained cells were analyzed by flow cytometry. The fluorescence emission

at 530 nm and >575nm was measured.

3.9 Cytotoxicity assay (Resazurin microplate assay) (100)

This assay is performed in triplicate wells of 96-well plate. 5×10^3 primary osteosarcoma cells or cancer cell lines were seeded to each well in culture medium for 24 hours. After that, medium was replaced with drug containing culture medium at concentration varied from 0.001-100 $\mu\text{g/ml}$. Plate is then incubated at 37°C in a humidified incubator with 5% CO_2 for 24, 48, or 72 hours. After desired period of time, 25 μl of 0.0625 mg/ml resazurin solution is filled to each well and the plate is further incubated at 37°C for 4 hours. Fluorescence is measured at 530 nm excitation and 590 nm emission wavelengths by using the bottom-reading mode of fluorometer. The signal is subtracted with blank before calculation. The percentage of growth inhibition is calculated by the following equation:

$$\% \text{ Inhibition} = [1 - (\text{FU}_T / \text{FU}_C)] \times 100$$

Where FU_T and FU_C represent the fluorescence units of cells treated with test compound and negative control agent, respectively.

The % inhibition can be interpreted to anti-cancer activity by our cutoff criteria:

If % inhibition is $< 50\%$, the activity is reported as “Inactive”

If % inhibition is $\geq 50\%$, the activity is reported as “Active”.

IC_{50} value can be determined.

The IC_{50} value is derived from dose-response-curve that is plotted between % inhibition against the sample concentrations by using Microsoft Excel (Microsoft Corporation, WA, USA)



CHAPTER IV

RESULTS

4.1 U-2 OS and osteosarcoma primary cell culture No. 1 express *CALCR* and *RAMP3* at mRNA level

qRT-PCR showed that U-2 OS, and osteosarcoma primary cell culture No. 1 expressed *CALCR* and *RAMP3* while NCI-H1299 expressed only *CALCR*. Other osteosarcoma cell lines and primary cell cultures expressed *CALCR* and *RAMP3* at very low level or do not express (Figure 10.)

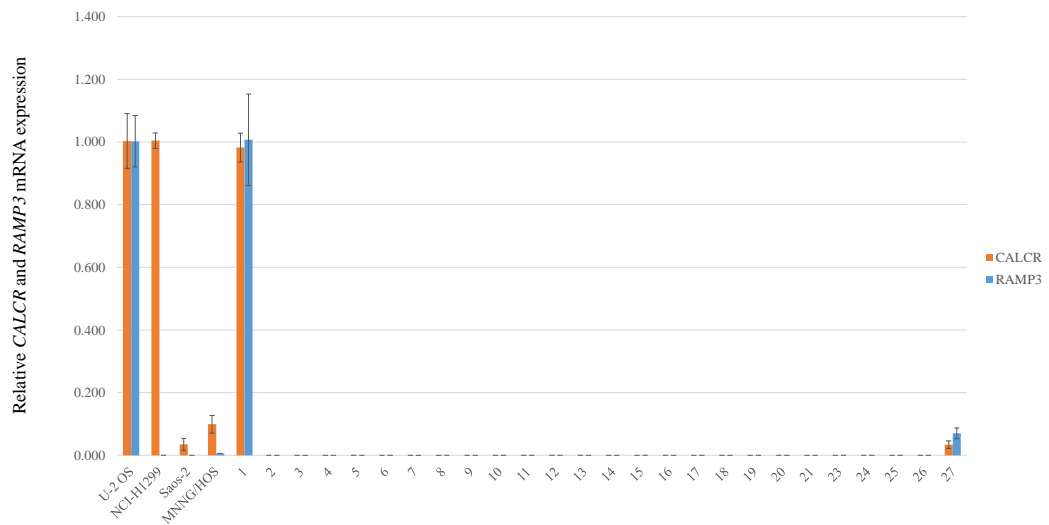


Figure 11 CALCR and RAMP3 express obviously in U-2 OS and primary cell culture No. 1.

4.2 By WES, a somatic missense variant in p53 was found in primary osteosarcoma cell culture No.1

WES revealed a heterozygous missense variant c.C841T in p53 causing amino acid change p.Asp281Asn in genomic DNA from a primary osteosarcoma cell culture while genomic DNA from blood leukocytes did not (Figure 11). The total read depth was 73. The reference base (C) read depth was 50 while the alternative base (T) read depth was 23. The allele frequency of this variant is 0.000008318 (ExAC.org). This variant is absent in 165 in-house Thai exome database. Prediction software including SIFT (sift.jcvi.org) and PolyPhen (genetics.bwh.harvard.edu/pph2/) predicted that this variant is deleterious with a score 0.01 and probably damaging with a score 0.991 respectively.



Figure 12 BAM file of WES reveal a somatic mutation of p53 in tumor.

4.3 By using flow cytometry, pramlintide acetate at 10 µg/ml could not induce apoptosis in primary osteosarcoma cell culture and cell lines expressing CALCR and RAMP3

Pramlintide acetate at a concentration of 10 µg/ml which was previously described to induce extensive apoptosis in p53 deficient and mutant tumor by Venkatanarayan et al. (19), could not lead to cell death in cancer cells expressing *CALCR* and *RAMP3* including U-2 OS (Figure 12), and primary cell culture No. 1 (Figure 13). Moreover, NCI-H1299, a non-small cell lung cancer cell lined, that claimed to be induced apoptosis by pramlintide acetate in Venkatanarayan report (19), did not respond to pramlintide acetate in our experiment (Figure 14).

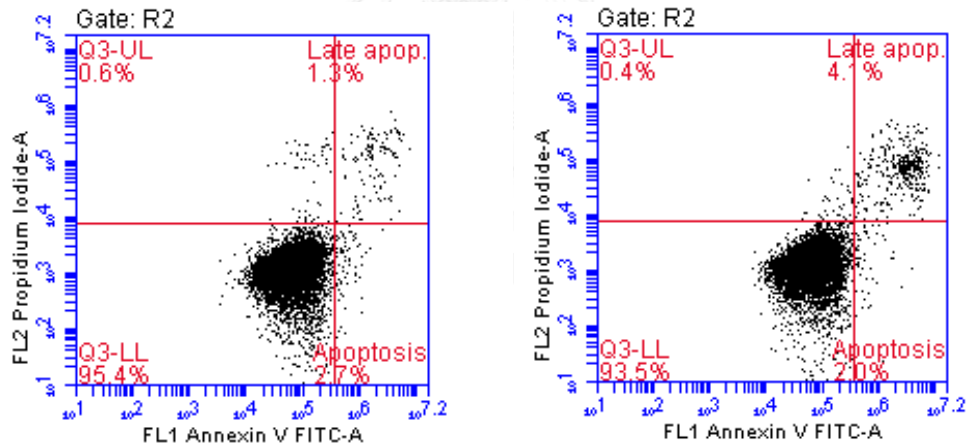


Figure 13 Flow cytometry of U-2 OS cells stain with Annexin-FITC and PI. The percentage apoptotic cell (Q2 UR and LR) in untreated (left) group was not differ from those co-cultured with pramlintide acetate at a concentration of 10 µg/ml (right).

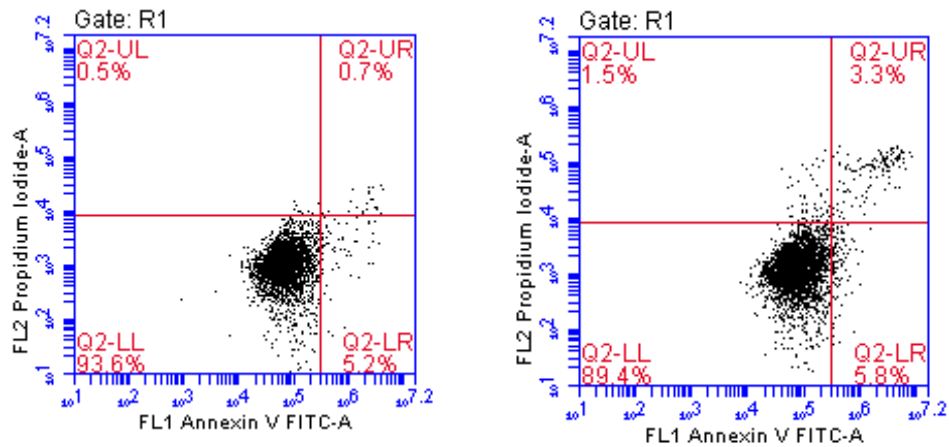


Figure 14 Flow cytometry of primary osteosarcoma cell culture No.1 stain with Annexin-FITC and PI. The percentage of apoptotic cell (Q2 UR and LR) in untreated (left) group was not differ from those co-cultured with pramlintide acetate at a concentration of 10 µg/ml (right).

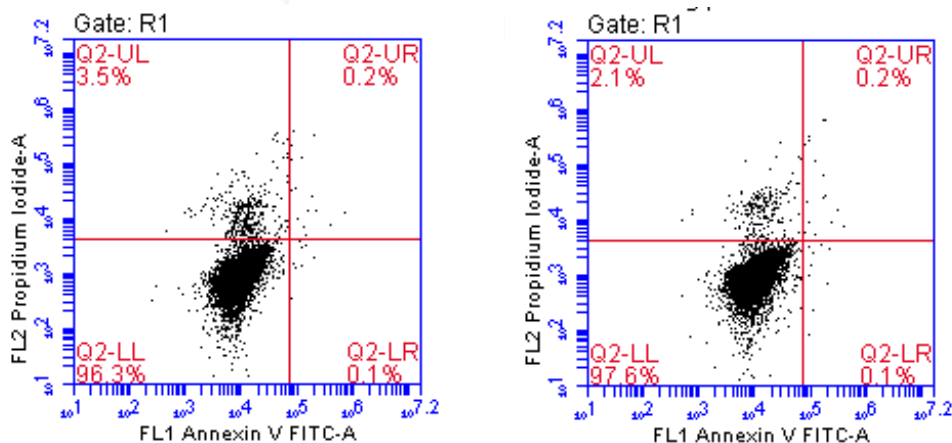


Figure 15 Flow cytometry of NCI-H1299 cells stain with Annexin-FITC and PI. The percentage of apoptotic cell (Q2 UR and LR) in untreated (left) group was not

differ from those co-cultured with pramlintide acetate at a concentration of 10 $\mu\text{g/ml}$ (right).

4.4 Pramlintide has no anticancer activity at concentration of 0.001-100 $\mu\text{g/ml}$ in primary osteosarcoma cell culture and cancer cell lines.

Resazurin microplate assay was used to identify the concentration of pramlintide acetate that could lead to cancer cell death by varying the concentration from 0.001-100 $\mu\text{g/ml}$. The fluorescent levels which represented the percentage of viable cell in U-2 OS, NCI-H1299, primary cell culture No. 1, Saos2, and MNNG/HOS cells cultured in medium containing pramlintide acetate at concentration 0.001, 0.01, 0.1, 1, and 10 $\mu\text{g/ml}$ at 24, 48, and 72 hours were not differ from those of control regardless of *CALCR* and *RAMP3* RNA expression (Figure 15, 18-21). The percentage of growth inhibition was calculated and showed in table 4.

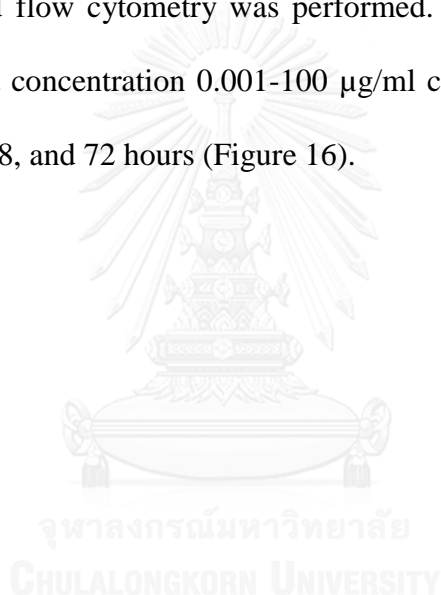
Table 3 Percentage of growth inhibition of cancer cells treated with various concentrations of pramlintide acetate and time.

Cancer cells	Time (hours)	Percentage of growth inhibition (%) at various pramlintide concentration					
		0.001	0.01	0.1	1	10	100
		$\mu\text{g/ml}$	$\mu\text{g/ml}$	$\mu\text{g/ml}$	$\mu\text{g/ml}$	$\mu\text{g/ml}$	$\mu\text{g/ml}$
U-2 OS	24	1.36	0.67	-1.29	-3.30	3.70	13.34
	48	-2.50	-4.90	-5.34	-2.70	7.51	20.06
	72	-5.40	-1.99	-4.08	-1.69	-7.74	37.74
NCI-H1299	24	-2.07	-15.95	-16.85	-11.34	-4.21	21.65
	48	3.17	-1.19	-5.38	-3.45	1.10	33.32
	72	2.89	-1.42	4.55	0.30	6.50	52.55
Primary osteosarcoma cell No. 1	24	-1.85	-0.51	-1.31	-3.03	2.08	14.19
	48	0.63	0.39	0.29	-0.18	1.54	15.77
	72	4.60	3.37	-0.17	-1.47	3.01	14.16
Saos2	24	-10.16	-10.70	-2.98	-6.31	-0.44	-5.20
	48	-6.20	-6.20	-7.17	2.78	2.00	9.03
	72	-9.22	-3.99	-8.11	-4.44	5.70	15.62
MNNG/HOS	24	-3.06	-9.40	-12.07	-9.42	3.30	6.30
	48	-5.86	-4.72	-7.49	-8.56	-3.90	-4.70
	72	0.96	3.31	1.17	3.53	26.51	30.38

At the concentration of 100 $\mu\text{g/ml}$, as soon as pramlintide acetate was added to the medium containing phenol red as a pH indicator, the color of the medium changed

from pink to yellow indicating acidity of the pramlintide acetate. At this concentration, percentage of cell viability reduced significantly compared with untreated groups (Figure 16, 17, 19-22).

To confirm the result of resazurin microplate assay in NCI-H1299 (positive control cell line) which was reported by Venkatanarayan et al. (19) that pramlintide acetate led to extensive apoptosis in this cell line. NCI-H1299 cells co-cultured with pramlintide acetate at concentration of 0.001-100 $\mu\text{g/ml}$ were stained with annexinV and PI and flow cytometry was performed. Flow cytometry showed that pramlintide acetate at concentration 0.001-100 $\mu\text{g/ml}$ could not induced NCI-H1299 cell apoptosis at 24, 48, and 72 hours (Figure 16).



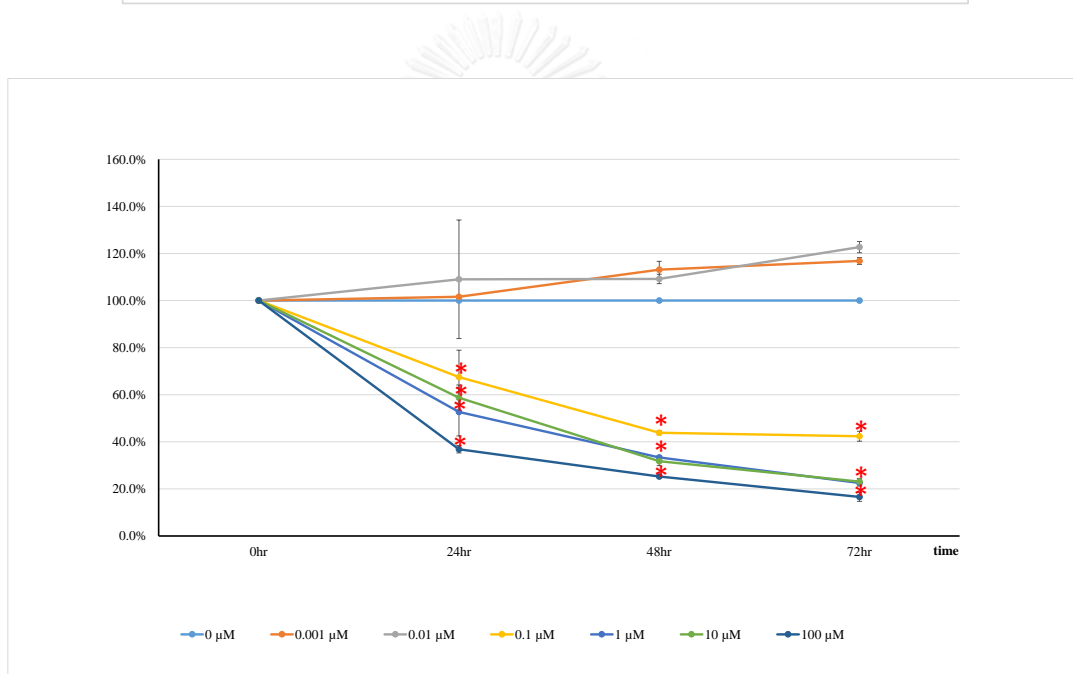
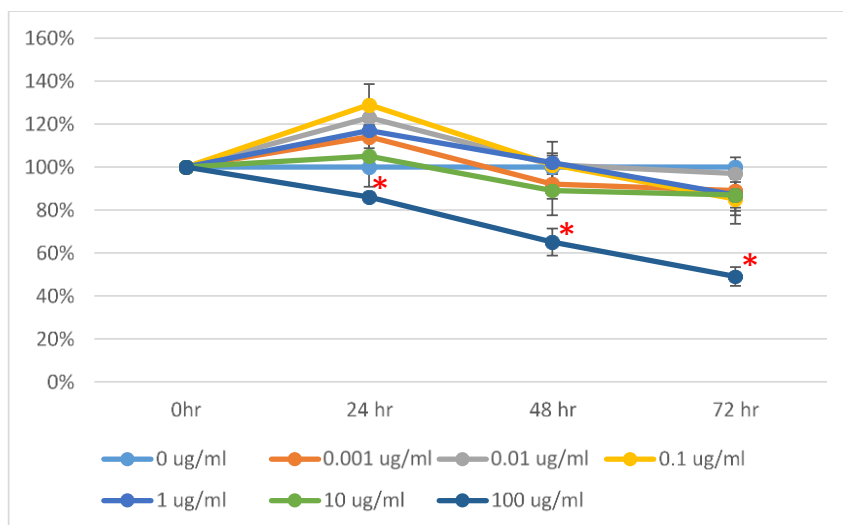


Figure 16 Percentage of NCI-H1299 cell viability treated with various concentration of pramlintide acetate. Results are expressed as mean \pm SD. The student t test was used to analyze the difference between treated group vs untreated group. Asterisks indicate significant different at p-value < 0.05 when compared with untreated group. NCI-H1299 cells treated with doxorubicin was used as a positive control (Lower picture)

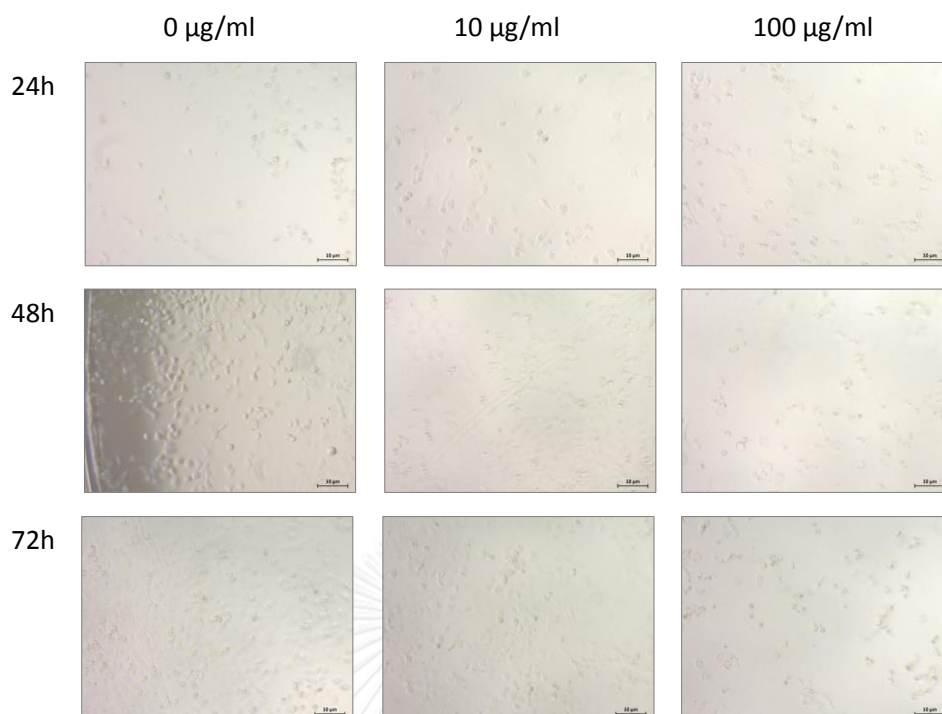


Figure 17 At the concentration of 100 $\mu\text{g/ml}$, pramlintide acetate inhibited cell proliferation of NCI-H1299 cells at 24, 48, and 72 hours.

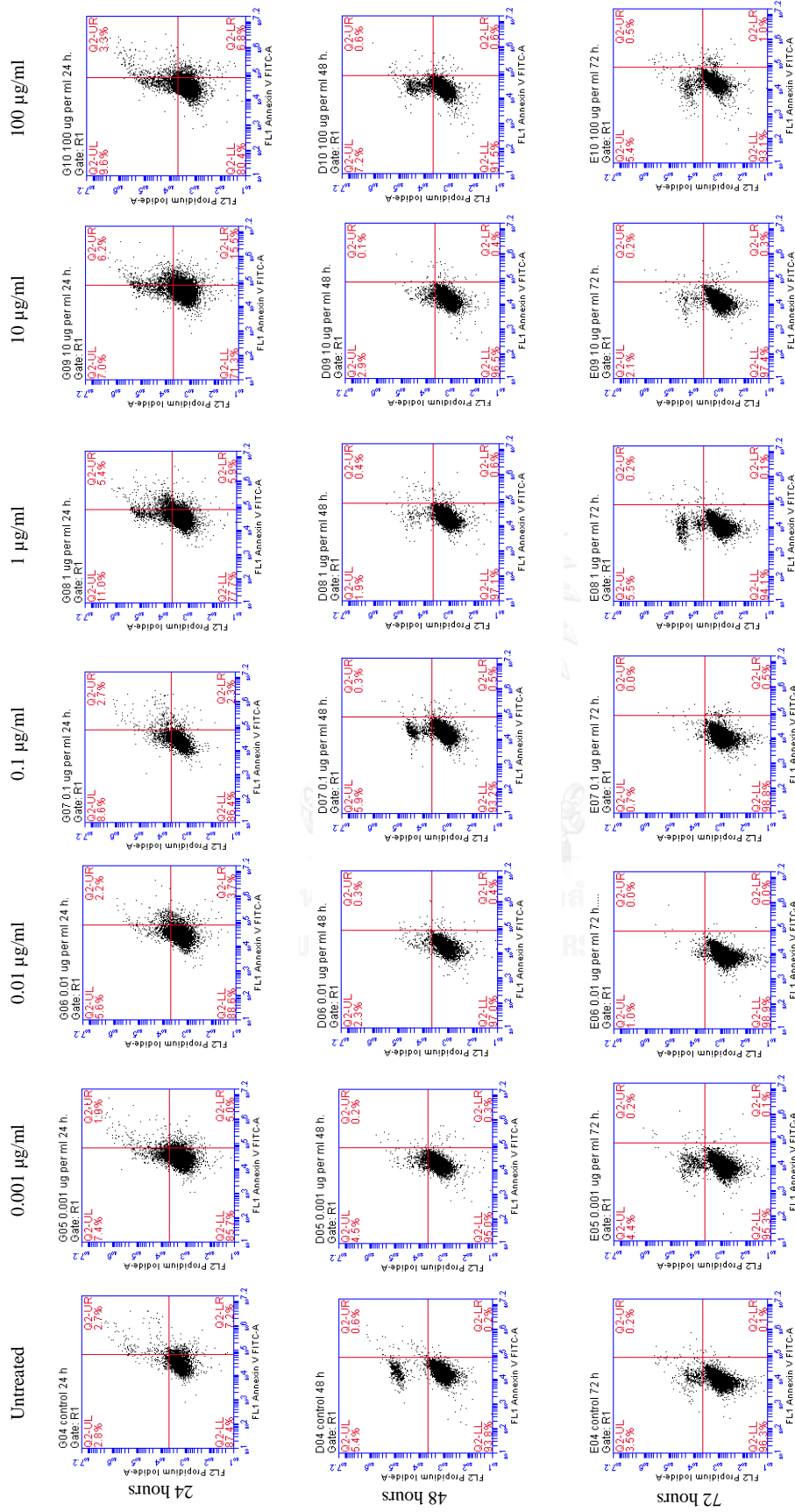


Figure 18 Flow cytometry of NCI-H1299 cells stain with Annexin-FITC and PI. The percentage of apoptotic cell in untreated group was not differ from those co-cultured with pramlintide acetate at a concentration of 0.001-100 µg/ml at 24, 48, and 72 hours.

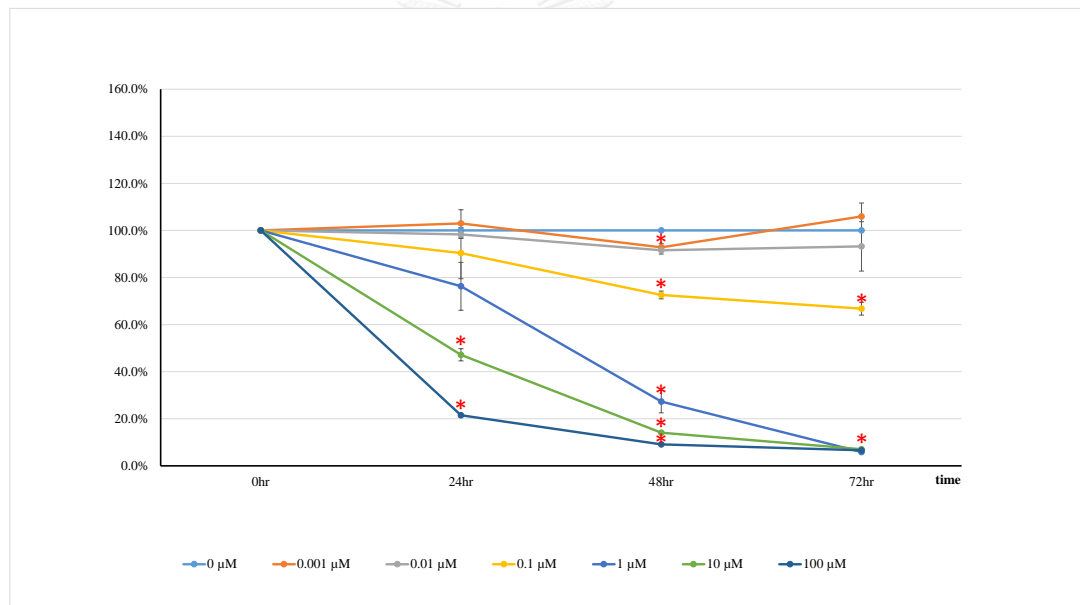
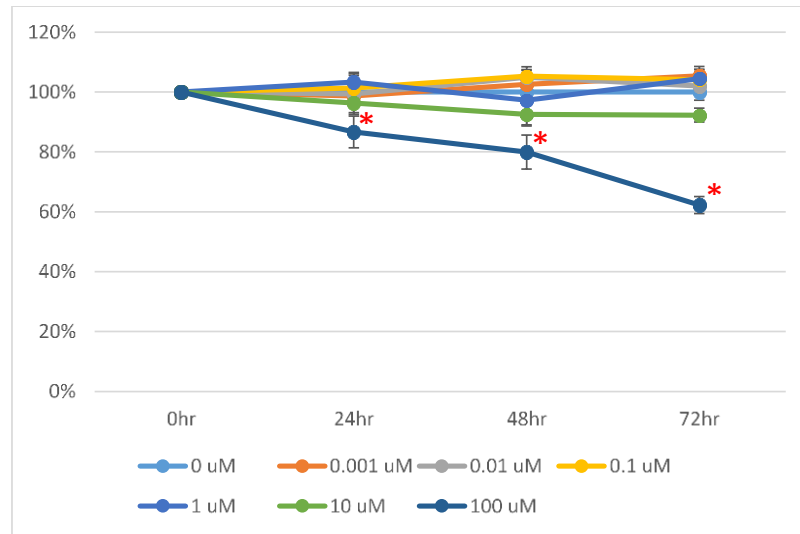


Figure 19 Percentage of U-2 OS cell viability (CALCR and RAMP3 expression) treated with various concentration of pramlintide acetate. Results are expressed as mean \pm SD. The student t test was used to analyze the difference between treated group vs untreated group. Asterisks indicate significant different at p-value < 0.05 when compared with untreated group. U-2 OS cells treated with doxorubicin was used as a positive control (Lower picture)

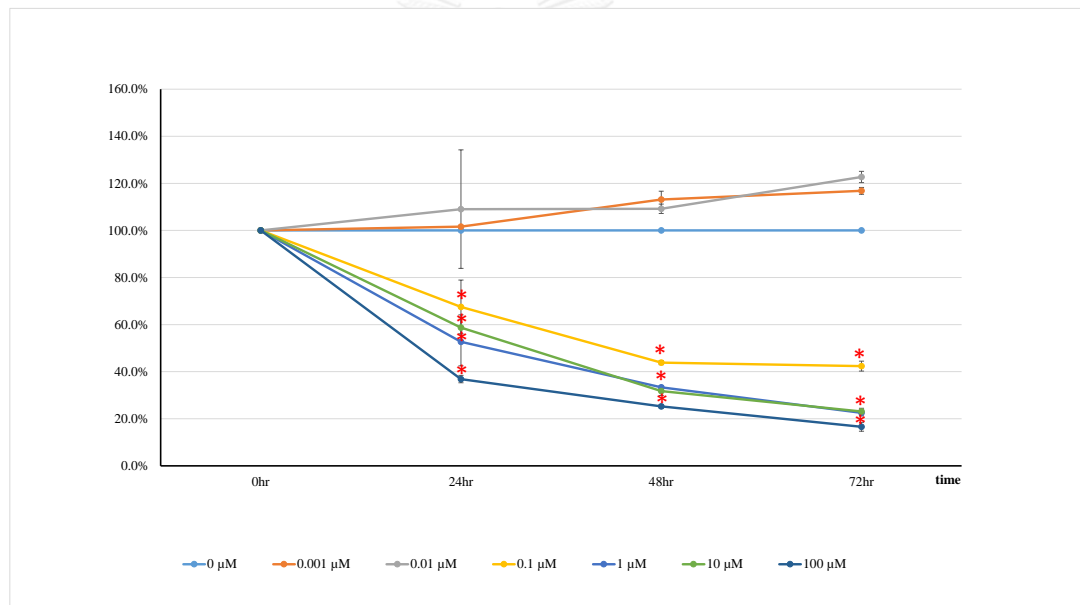
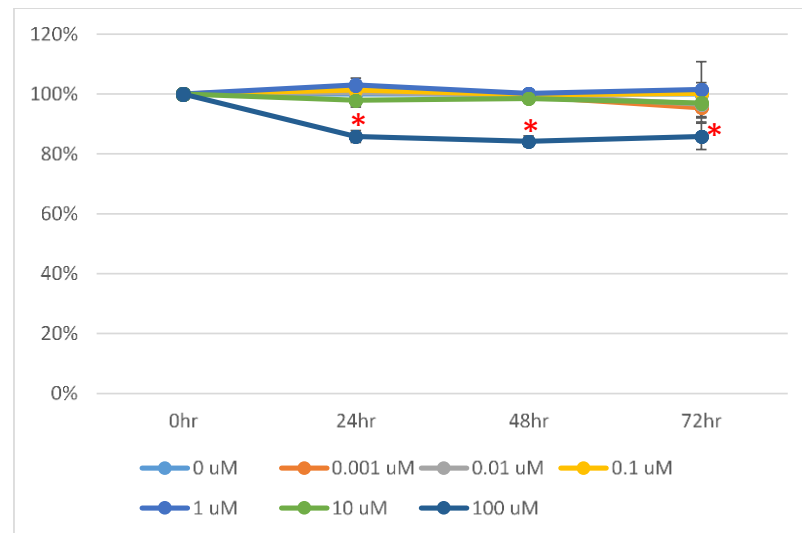


Figure 20 Percentage of primary cell culture No. 1 cell viability (CALCR and RAMP3 expression) treated with various concentration of pramlintide acetate. Results are expressed as mean \pm SD. The student t test was used to analyze the difference between treated group vs untreated group. Asterisks indicate significant different at p-value < 0.05 when compared with untreated group. Primary cell culture No. 1 cells treated with doxorubicin was used as a positive control (Lower picture).

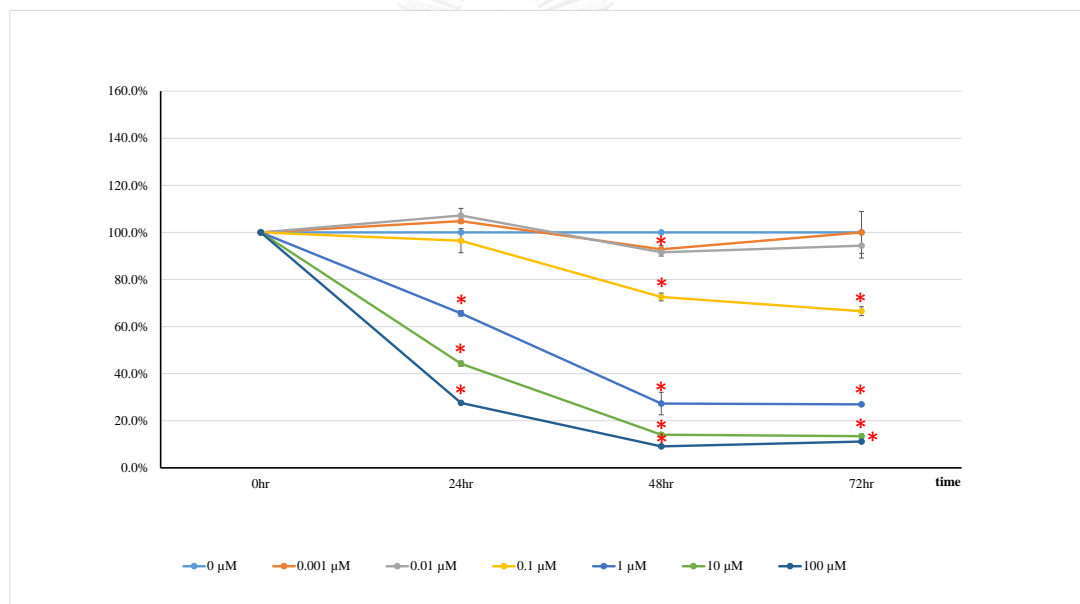
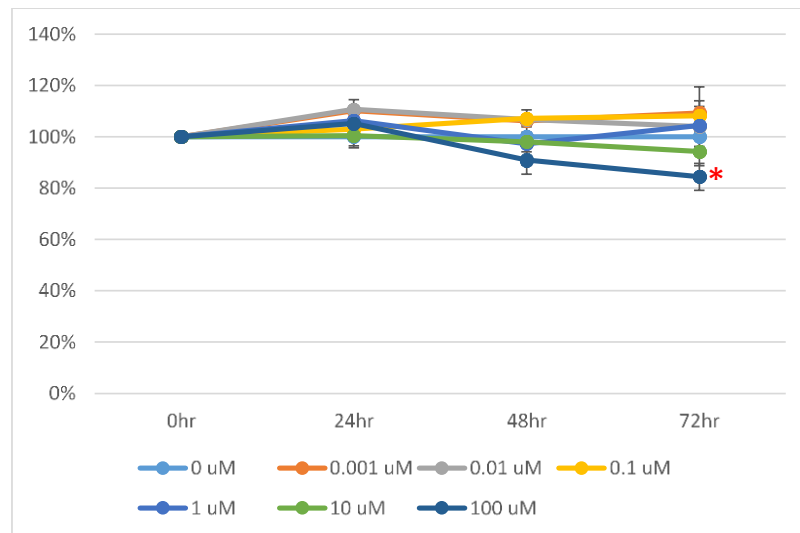


Figure 21 Percentage of Saos-2 cell viability (CALCR and RAMP3 expression) treated with various concentration of pramlintide acetate. Results are expressed as mean \pm SD. The student t test was used to analyze the difference between treated group vs untreated group. Asterisks indicate significant different at p-value < 0.05 when compared with untreated group. Saos-2 cells treated with doxorubicin was used as a positive control (Lower picture).

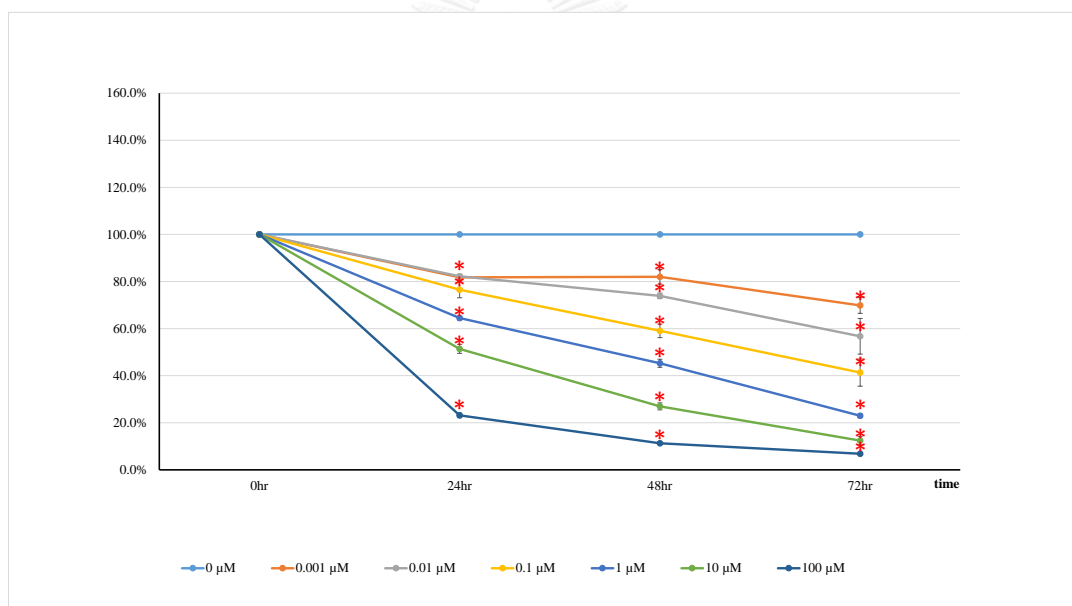
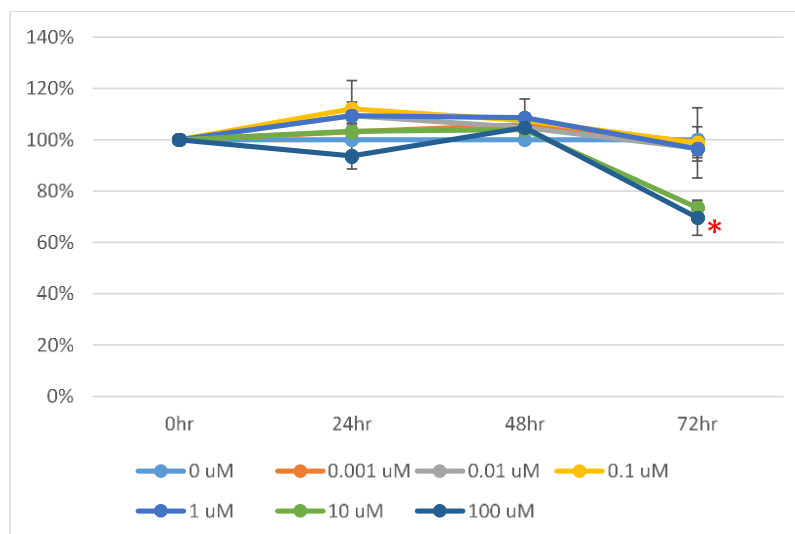


Figure 22 Percentage of MNNG/HOS cell viability (no CALCR and RAMP3 expression) untreated with various concentration of pramlintide acetate. Results are expressed as mean \pm SD. The student t test was used to analyze the difference between treated group vs untreated group. Asterisks indicate significant different at p-value < 0.05 when compared with untreated group. MNNG/HOS cells treated with doxorubicin was used as a positive control (Lower picture).

To test whether pramlintide acetate at concentration of 100 $\mu\text{g/ml}$ could induce cancer cell death by pramlintide itself or acetate in the compound. Pramlintide (Tocris Bioscience, Bristol, UK) and acetic acid with various concentrations were co-cultured with NCI-H1299 cells.

Pramlintide could not induced cell death at concentration 0.001, 0.01, 0.1, 1, 10, and 100 $\mu\text{g/ml}$ at 24, 48, and 72 hours in NCI-H1299 cells (Figure 23).

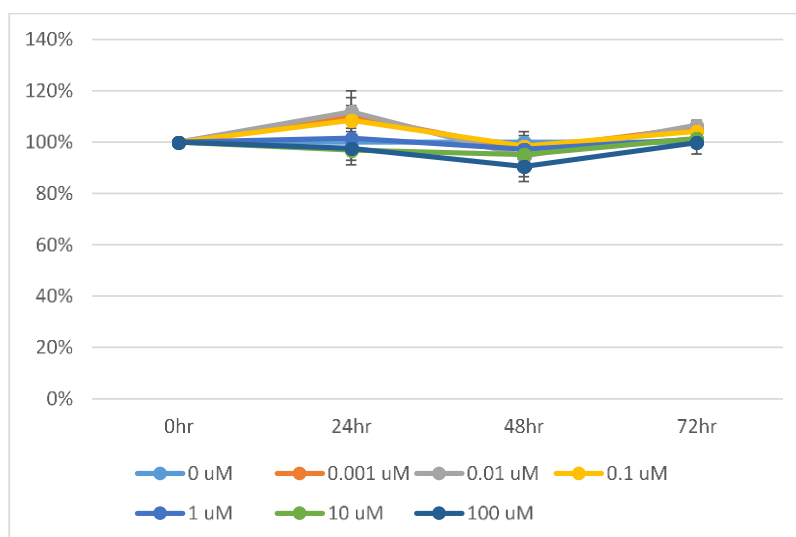


Figure 23 Percentage of NCI-H1299 (CALCR expression with no RAMP3 expression) cell viability treated with various concentration of pramlintide. Results are expressed as mean \pm SD. The student t test was used to analyze the difference between treated group vs untreated group. There is no significant different at p-value < 0.05 when compared treated vs untreated group.

Pramlintide acetate is a white powder that has a molecular formula of $\text{C}_{17}\text{H}_{26}\text{N}_5\text{O}_5\text{S}_2 \cdot x \text{C}_2\text{H}_4\text{O}_2$; the molecular weight is 3949.4. In one molecule

of pramlintide contains 3-8 molecule of acetate as described in the leaflet of the Symlin® (Figure 24).

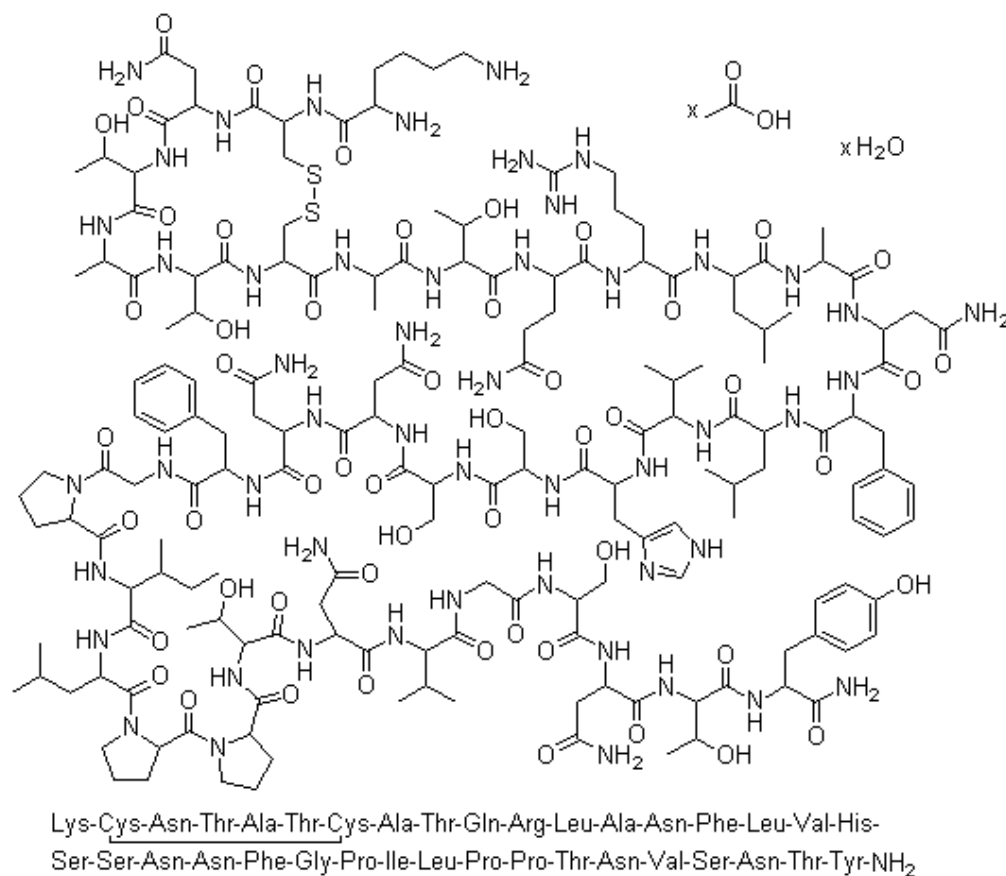


Figure 24 Illustration of the molecular structure of pramlintide

Three molecules of acetate per one molecule of pramlintide acetate were used to calculate concentration of acetic acid in each concentration of pramlintide acetate. In 0.001, 0.01, 0.1, 1, 10, and 100 µg/ml of pramlintide acetate contain acetic acid approximately equals to 0.0000456, 0.000456, 0.00456, 0.0456, 0.456, and 4.56 µg/ml respectively so glacial acetic acid were added to standard medium to achieve these concentrations.

Acetic acid at concentration 4.56 $\mu\text{g/ml}$ reduced NCI-H1299 cell viability to 60 and 39% at 48 and 72 hours respectively. (Figure 25).

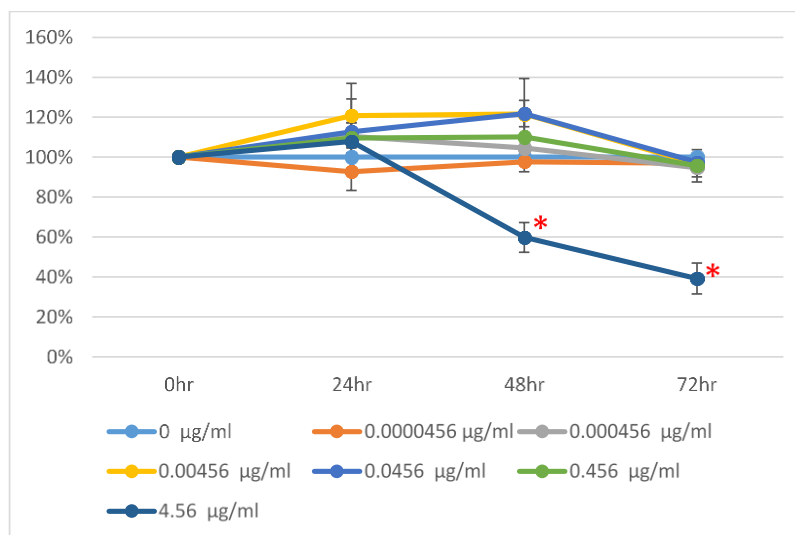


Figure 25 Percentage of primary cell culture case 1 cell viability treated with various concentration of acetic acid. Results are expressed as mean \pm SD. The student t test was used to analyze the difference between treated group vs untreated group. Asterisks indicate significant different at p-value < 0.05 when compared with untreated group.

4.5 Digoxin has anticancer effect in a half of primary osteosarcoma cell cultures and all osteosarcoma cell lines

All OS cell lines and 11/21 primary OS cell cultures (52%) responded to digoxin at the concentration $\leq 1 \mu\text{M}$. Saos2, MG-63, MNNG/HOS, and four (25%) OS primary cell culture responded at the concentration $\leq 0.1 \mu\text{M}$. The greatest effects were noted in MNNG/HOS cells ($\text{IC}_{50} = 0.667, 0.543, \text{ and } 0.425$), and the second greatest effects were noted in MG-63 cells ($\text{IC}_{50} = 4.11, 0.66, \text{ and } 0.56$). The results

showed that cell viability was affected in a dose- and time- dependent manner. Four greatest digoxin responsiveness osteosarcoma cell lines and primary cell cultures are shown in figure 26. Percentage of cell viability graphs of other osteosarcoma cell lines and primary cell cultures are shown in figure 27-50.

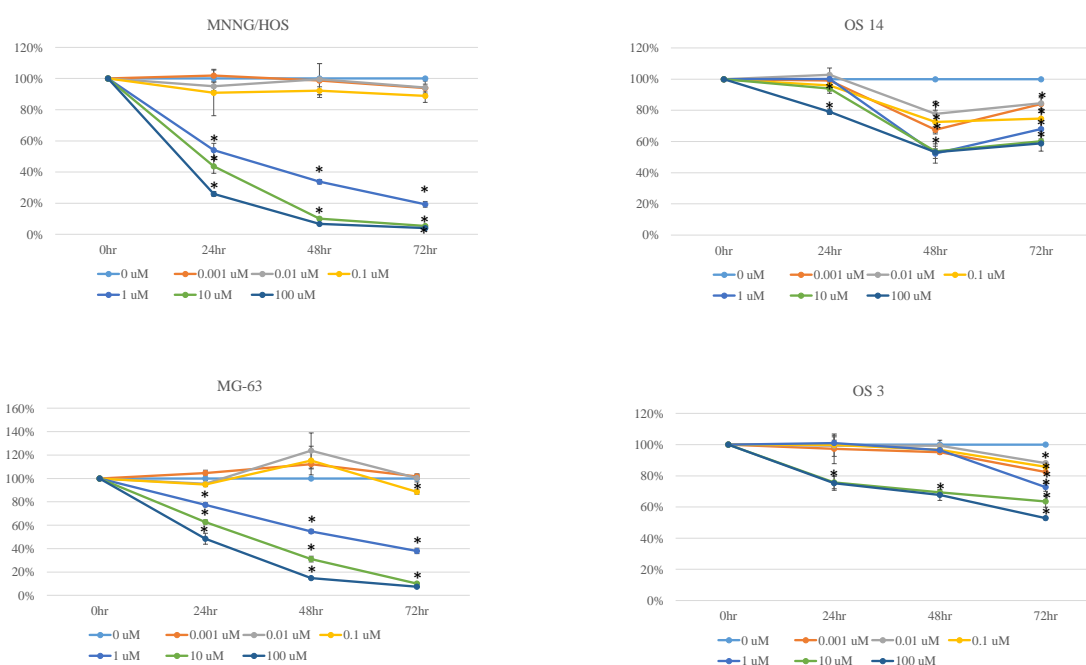


Figure 26 Digoxin inhibits the viability of OS cells. Four greatest digoxin responsiveness OS cell lines and primary cell cultured are shown. These cell were treated with 6 different doses (0.001, 0.01, 0.1, 1, 10, and 100 μM) of digoxin at different time points (0, 24, 48, and 72 h) Cell viability was measured using REMA after treatment. Quantitative data are presented as mean \pm SD. Asterisks indicate significant different at p-value < 0.05 when compared with with untreated group (0.9% NaCl solution).

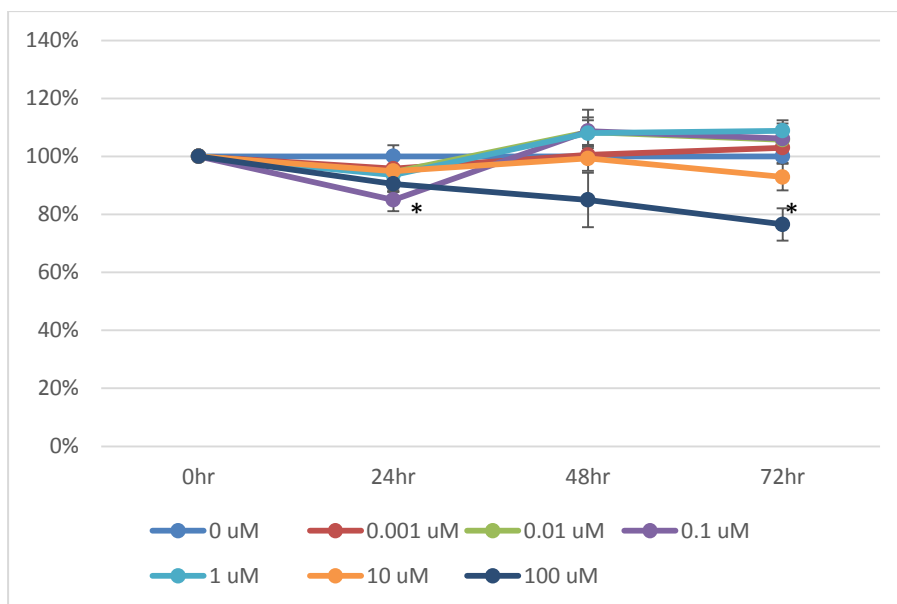


Figure 27 Percentage of primary cell culture No. 1 cell viability treated with various concentration of digoxin. Results are expressed as mean \pm SD. The student t test was used to analyze the difference between treated group vs untreated group. Asterisks indicate significant different at p-value < 0.05 when compared with untreated group.

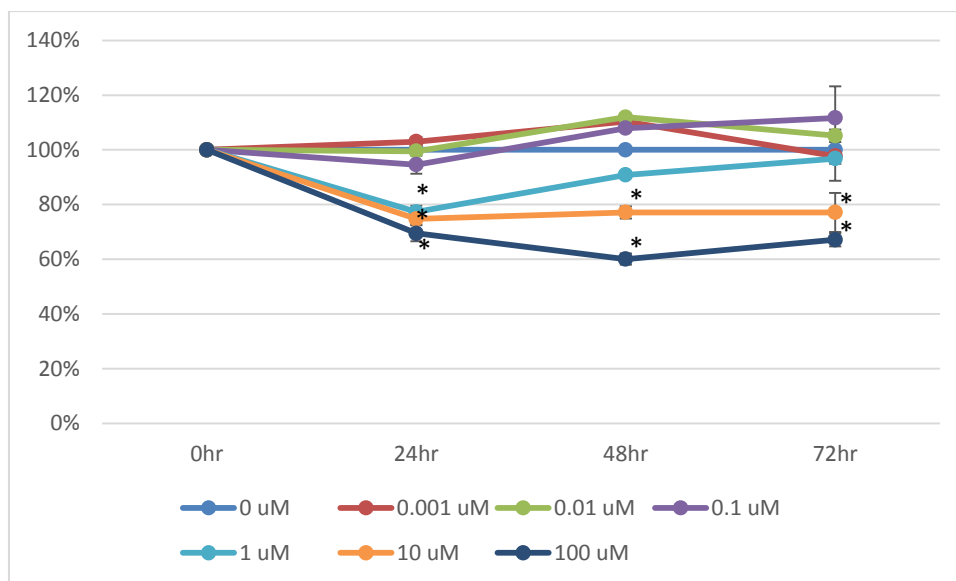


Figure 28 Percentage of primary cell culture No. 2 cell viability treated with various concentration of digoxin. Results are expressed as mean \pm SD. The student t test was used to analyze the difference between treated group vs untreated group. Asterisks indicate significant different at p-value < 0.05 when compared with untreated group.

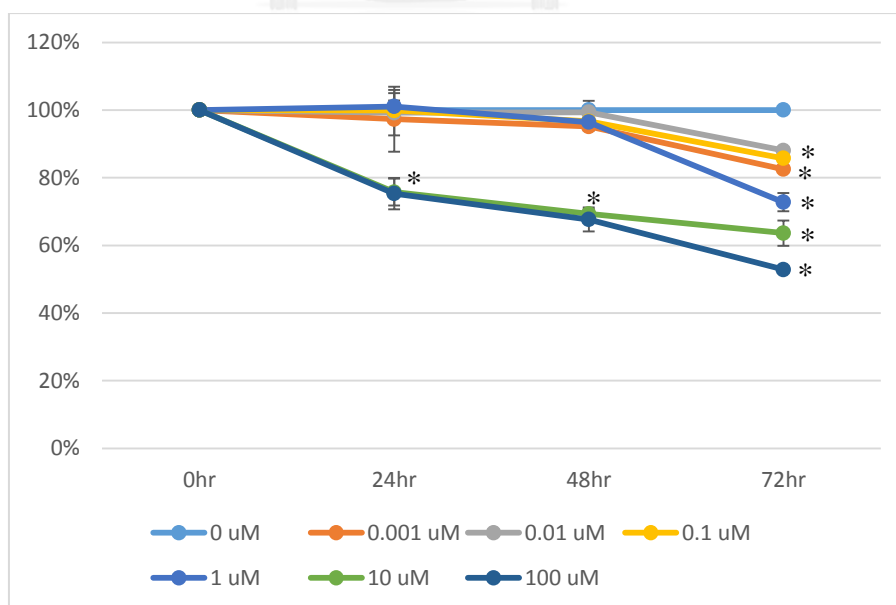


Figure 29 Percentage of primary cell culture No. 3 cell viability treated with various concentration of digoxin. Results are expressed as mean \pm SD. The student t

test was used to analyze the difference between treated group vs untreated group. Asterisks indicate significant different at p-value < 0.05 when compared with untreated group.

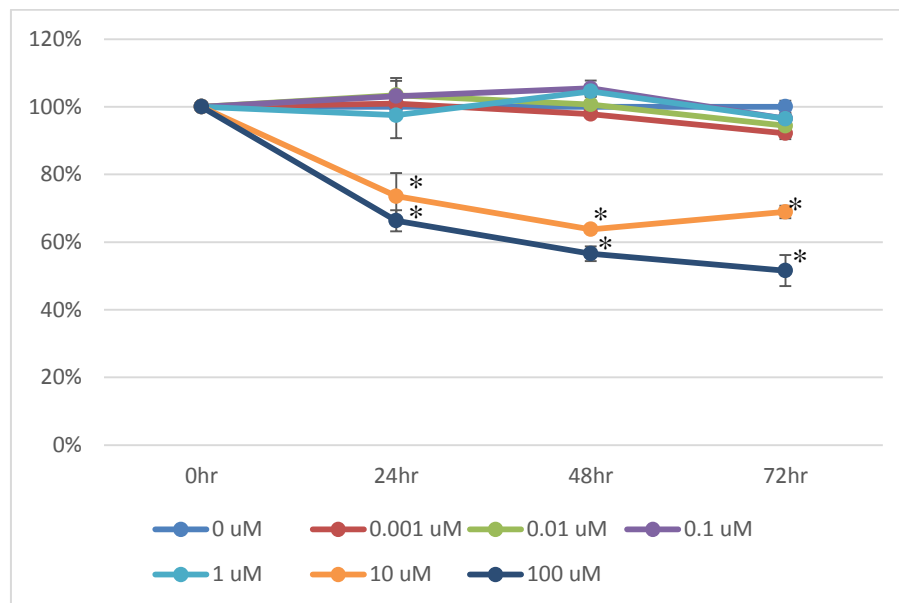


Figure 30 Percentage of primary cell culture No. 4 cell viability treated with various concentration of digoxin. Results are expressed as mean \pm SD. The student t test was used to analyze the difference between treated group vs untreated group. Asterisks indicate significant different at p-value < 0.05 when compared with untreated group.

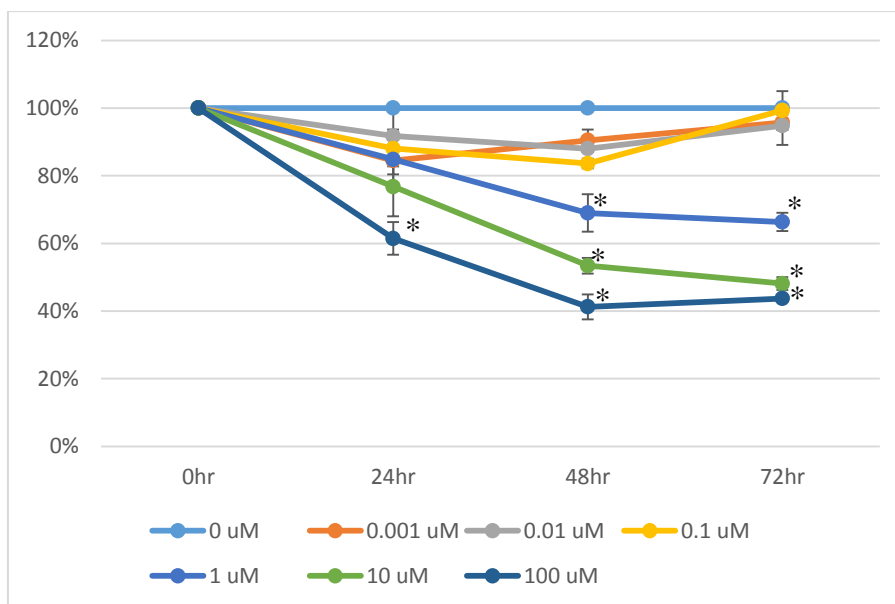


Figure 31 Percentage of primary cell culture No. 5 cell viability treated with various concentration of digoxin. Results are expressed as mean \pm SD. The student t test was used to analyze the difference between treated group vs untreated group. Asterisks indicate significant different at p-value < 0.05 when compared with untreated group.

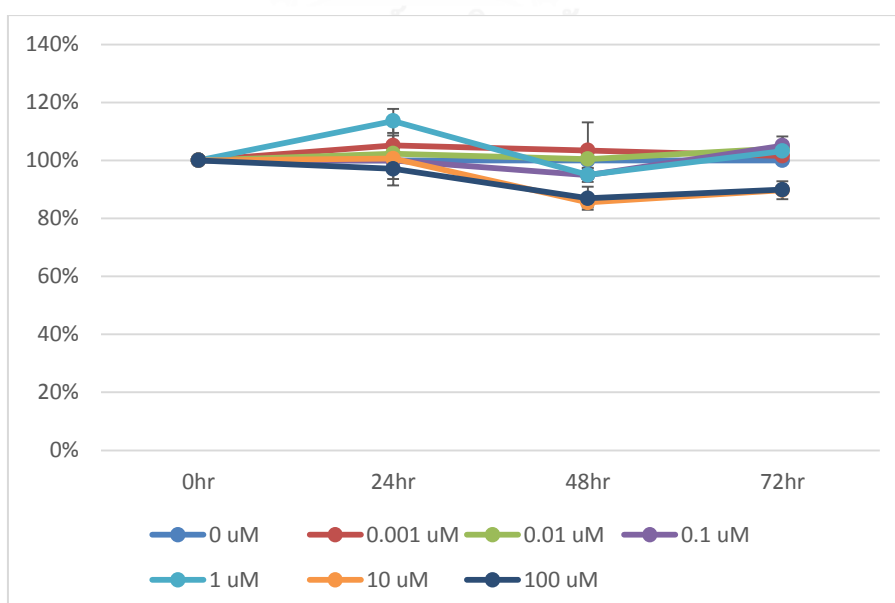


Figure 32 Percentage of primary cell culture No. 6 cell viability treated with various concentration of digoxin. Results are expressed as mean \pm SD. The student t test was used to analyze the difference between treated group vs untreated group. Asterisks indicate significant different at p-value < 0.05 when compared with untreated group.

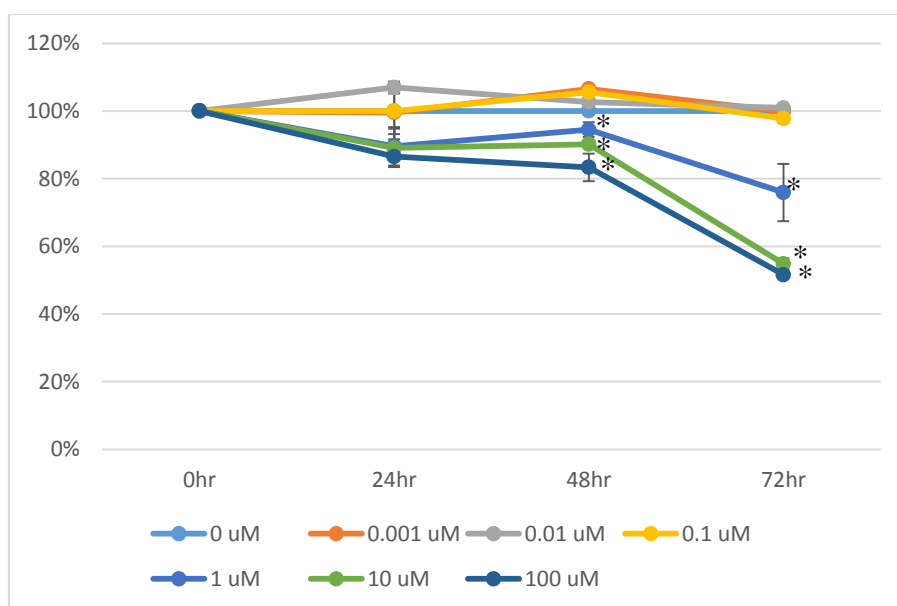


Figure 33 Percentage of primary cell culture No. 7 cell viability treated with various concentration of digoxin. Results are expressed as mean \pm SD. The student t test was used to analyze the difference between treated group vs untreated group. Asterisks indicate significant different at p-value < 0.05 when compared with untreated group.

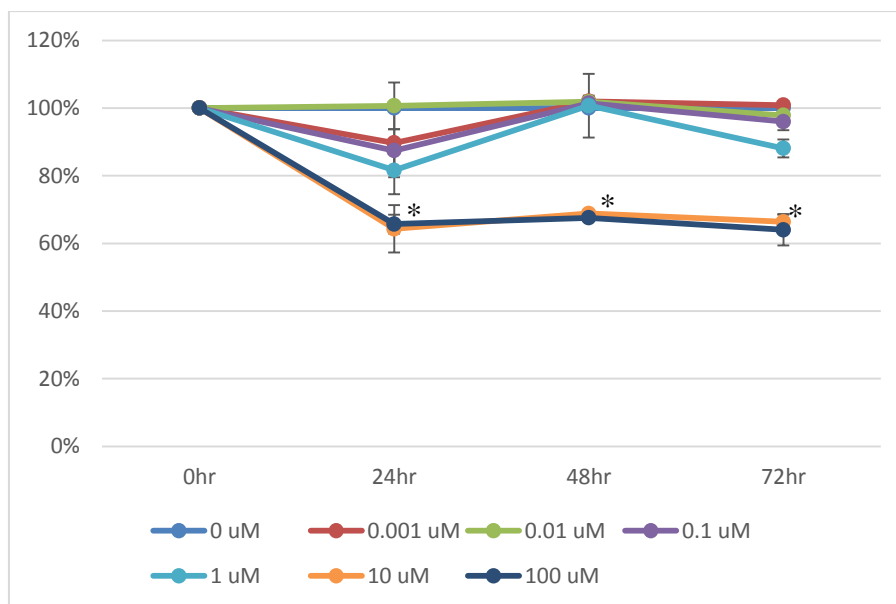


Figure 34 Percentage of primary cell culture No. 8 cell viability treated with various concentration of digoxin. Results are expressed as mean \pm SD. The student t test was used to analyze the difference between treated group vs untreated group. Asterisks indicate significant different at p-value < 0.05 when compared with untreated group.

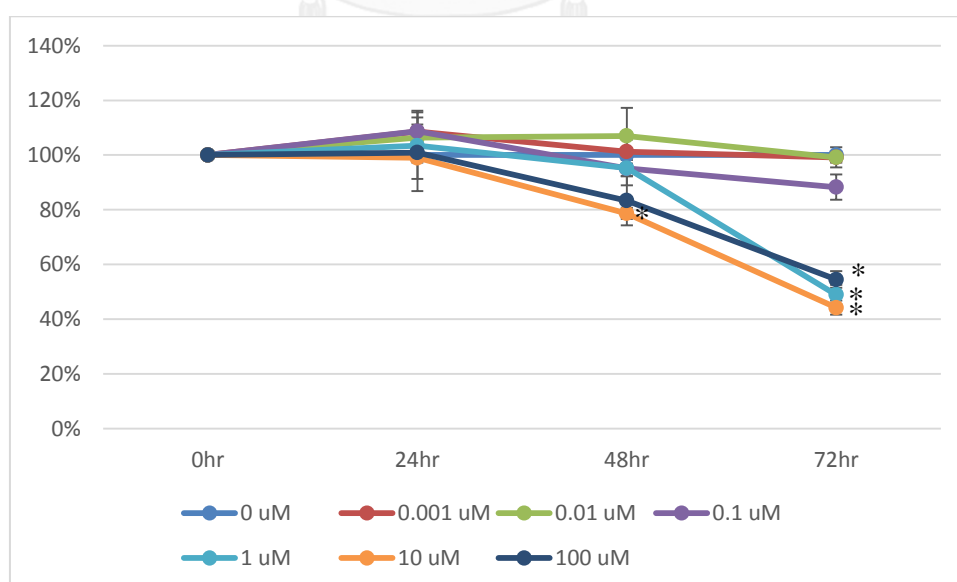


Figure 35 Percentage of primary cell culture No. 9 cell viability treated with various concentration of digoxin. Results are expressed as mean \pm SD. The student t

test was used to analyze the difference between treated group vs untreated group. Asterisks indicate significant different at p-value < 0.05 when compared with untreated group.

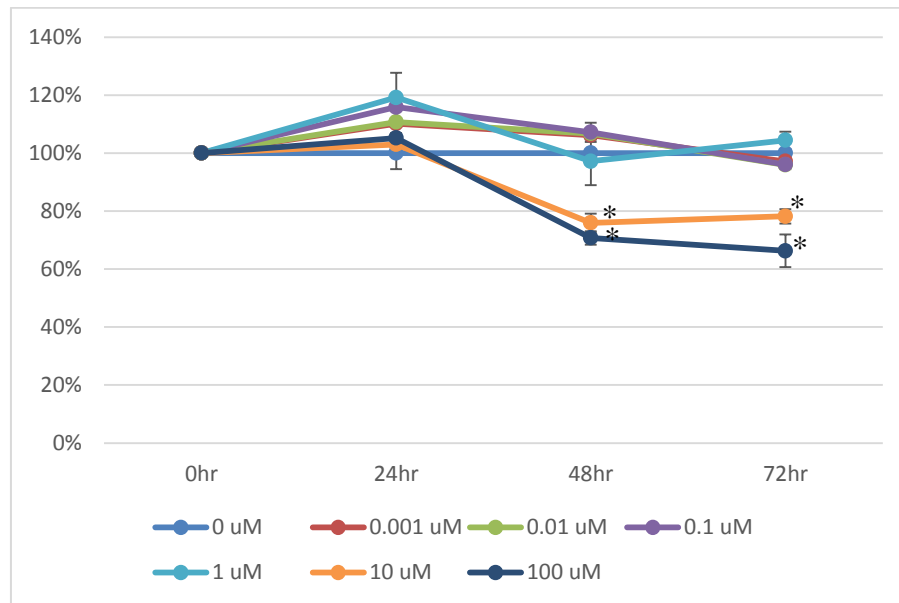


Figure 36 Percentage of primary cell culture No. 10 cell viability treated with various concentration of digoxin. Results are expressed as mean \pm SD. The student t test was used to analyze the difference between treated group vs untreated group. Asterisks indicate significant different at p-value < 0.05 when compared with untreated group.

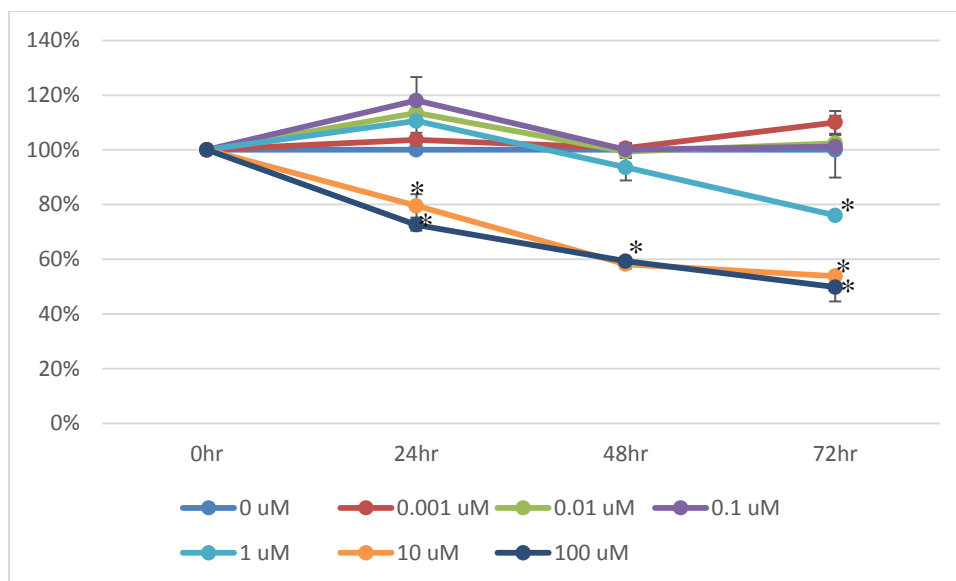


Figure 37 Percentage of primary cell culture No. 11 cell viability treated with various concentration of digoxin. Results are expressed as mean \pm SD. The student t test was used to analyze the difference between treated group vs untreated group. Asterisks indicate significant different at p-value < 0.05 when compared with untreated group.

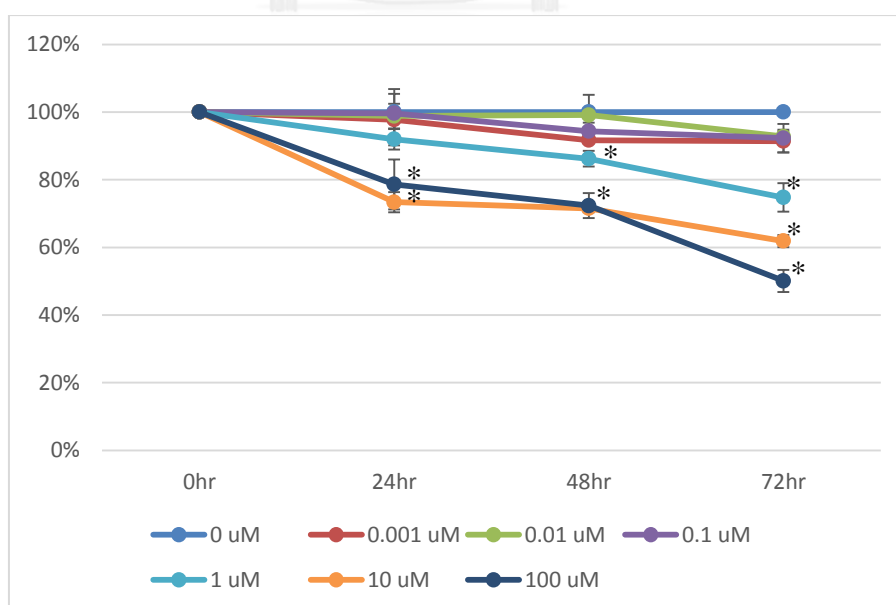


Figure 38 Percentage of primary cell culture No. 12 cell viability treated with various concentration of digoxin. Results are expressed as mean \pm SD. The student t

test was used to analyze the difference between treated group vs untreated group. Asterisks indicate significant different at p-value < 0.05 when compared with untreated group.

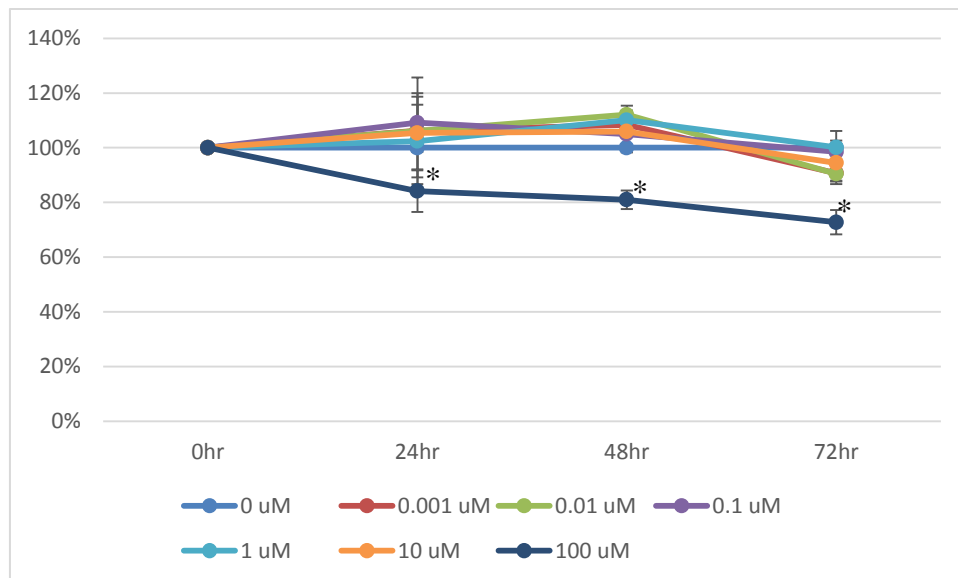


Figure 39 Percentage of primary cell culture No. 13 cell viability treated with various concentration of digoxin. Results are expressed as mean \pm SD. The student t test was used to analyze the difference between treated group vs untreated group. Asterisks indicate significant different at p-value < 0.05 when compared with untreated group.

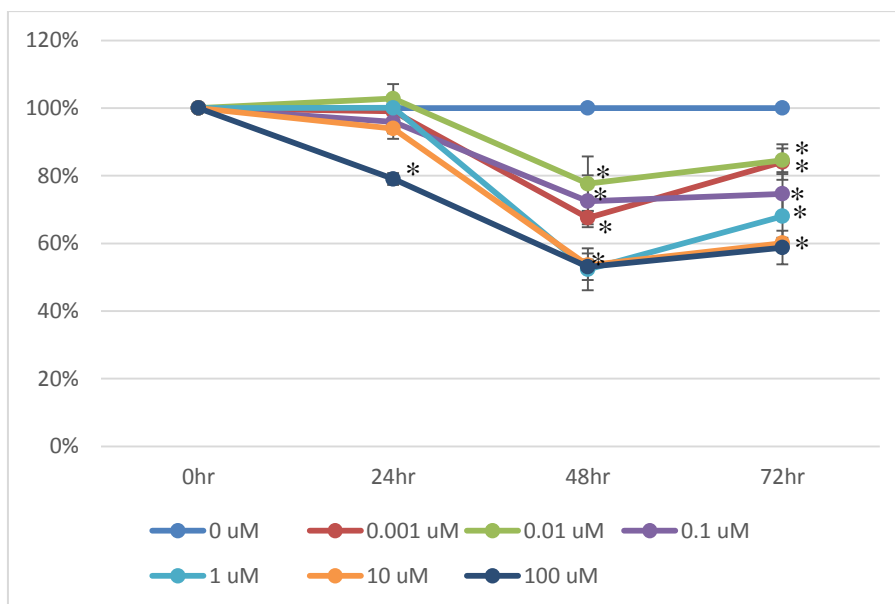


Figure 40 Percentage of primary cell culture No. 14 cell viability treated with various concentration of digoxin. Results are expressed as mean \pm SD. The student t test was used to analyze the difference between treated group vs untreated group. Asterisks indicate significant different at p-value < 0.05 when compared with untreated group.

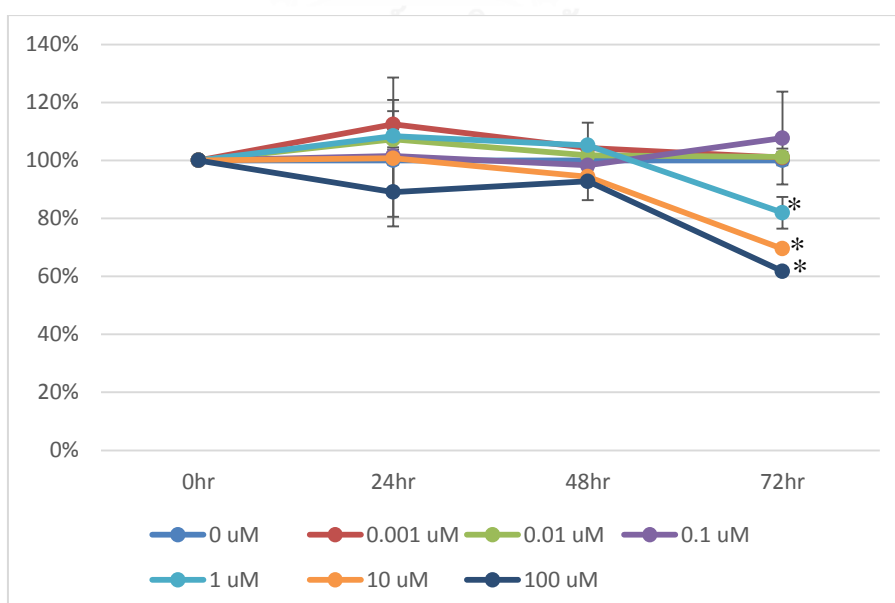


Figure 41 Percentage of primary cell culture No. 15 cell viability treated with various concentration of digoxin. Results are expressed as mean \pm SD. The student t test was used to analyze the difference between treated group vs untreated group. Asterisks indicate significant different at p-value < 0.05 when compared with untreated group.

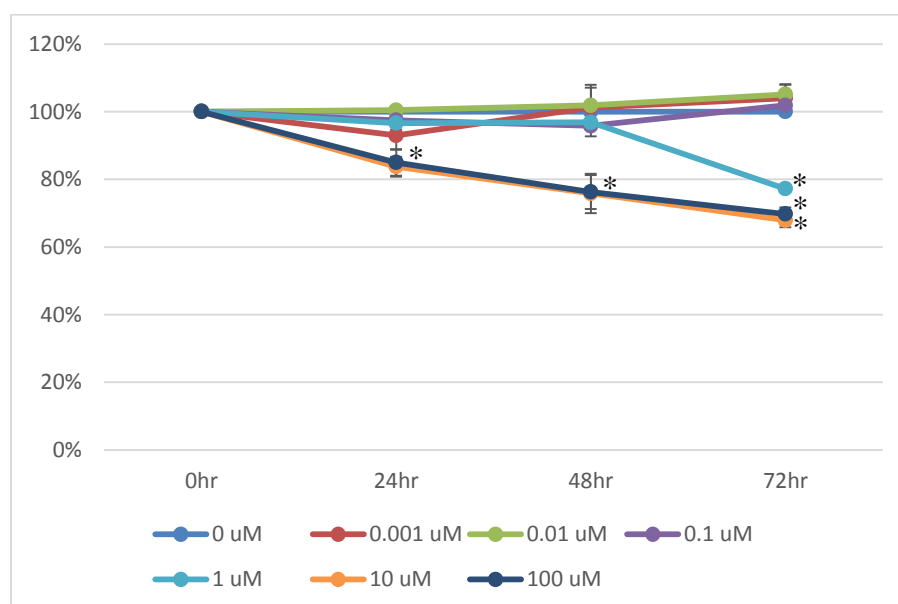


Figure 42 Percentage of primary cell culture No. 16 cell viability treated with various concentration of digoxin. Results are expressed as mean \pm SD. The student t test was used to analyze the difference between treated group vs untreated group. Asterisks indicate significant different at p-value < 0.05 when compared with untreated group.

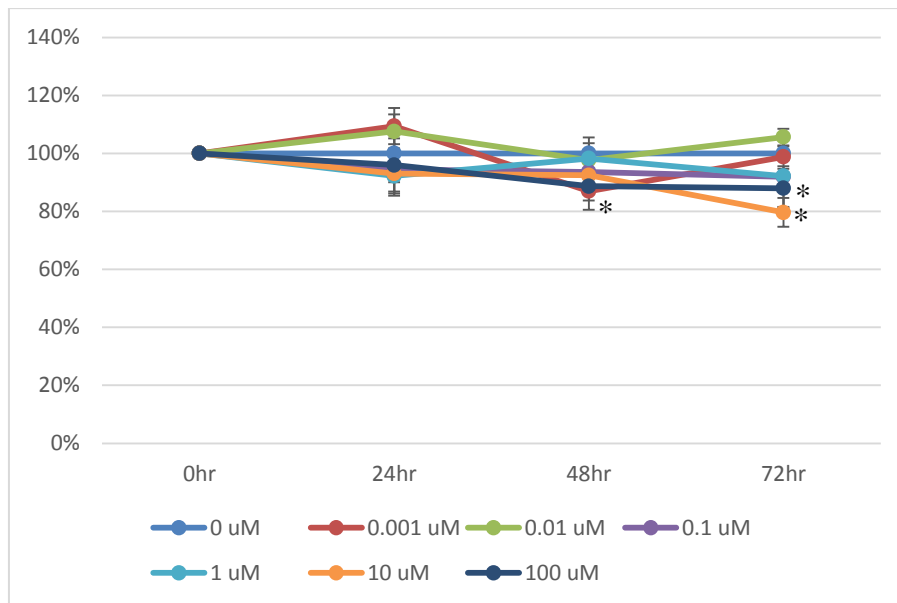


Figure 43 Percentage of primary cell culture No. 17 cell viability treated with various concentration of digoxin. Results are expressed as mean \pm SD. The student t test was used to analyze the difference between treated group vs untreated group. Asterisks indicate significant different at p-value < 0.05 when compared with untreated group.

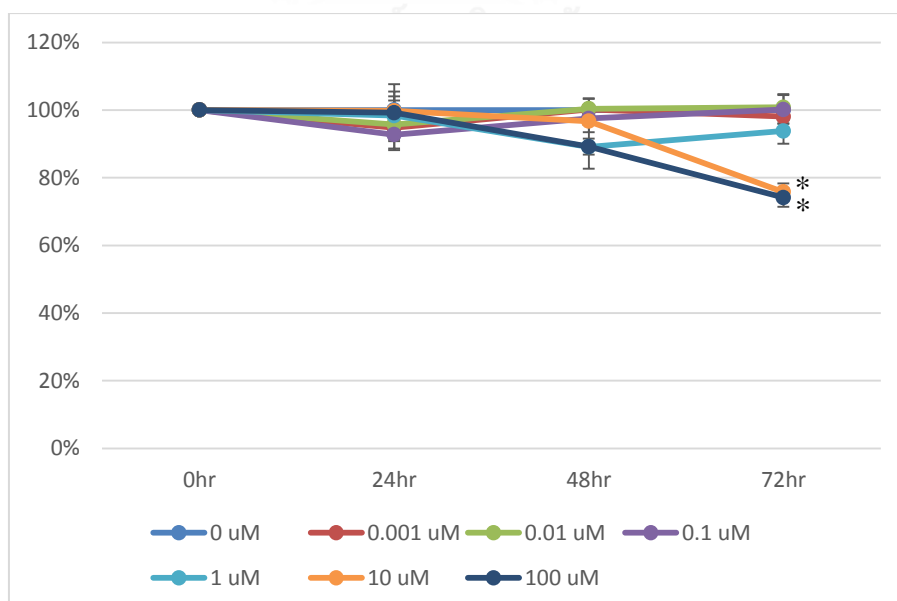


Figure 44 Percentage of primary cell culture No. 18 cell viability treated with various concentration of digoxin. Results are expressed as mean \pm SD. The student t test was used to analyze the difference between treated group vs untreated group. Asterisks indicate significant different at p-value < 0.05 when compared with untreated group.

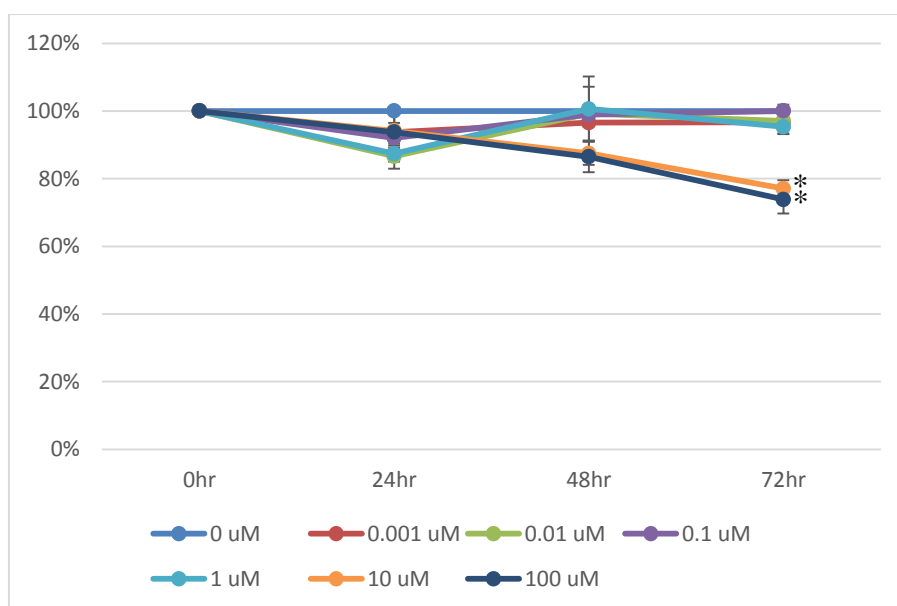


Figure 45 Percentage of primary cell culture No. 19 cell viability treated with various concentration of digoxin. Results are expressed as mean \pm SD. The student t test was used to analyze the difference between treated group vs untreated group. Asterisks indicate significant different at p-value < 0.05 when compared with untreated group.

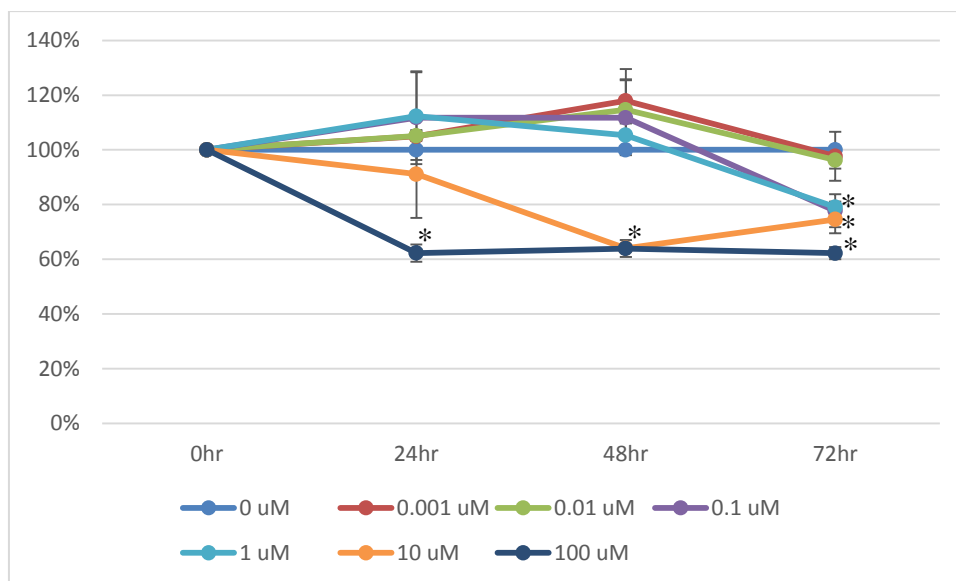


Figure 46 Percentage of primary cell culture No. 21 cell viability treated with various concentration of digoxin. Results are expressed as mean \pm SD. The student t test was used to analyze the difference between treated group vs untreated group. Asterisks indicate significant different at p-value < 0.05 when compared with untreated group.

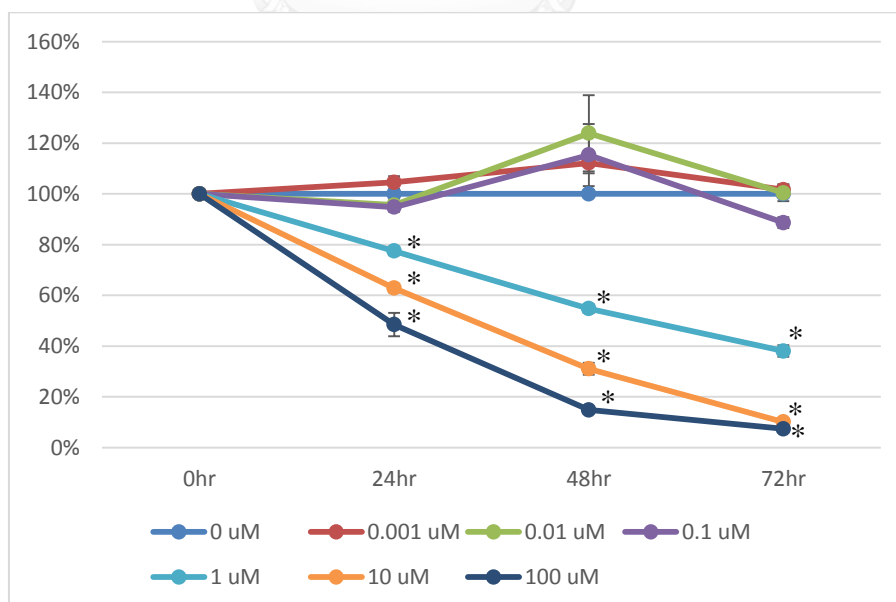


Figure 47 Percentage of MG-63 cell viability treated with various concentration of digoxin. Results are expressed as mean \pm SD. The student t test was used to analyze

the difference between treated group vs untreated group. Asterisks indicate significant different at p -value < 0.05 when compared with untreated group.

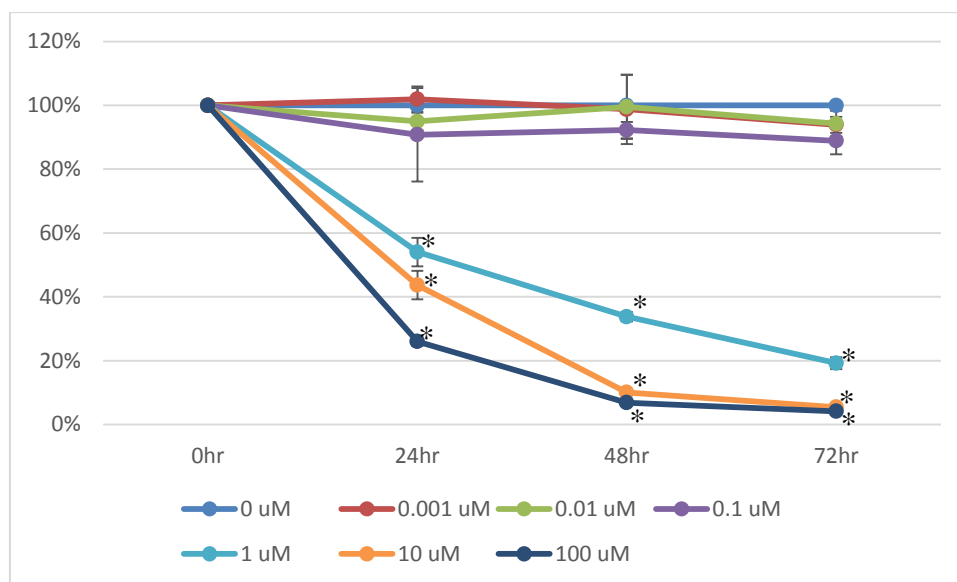


Figure 48 Percentage of MNNG-HOS cell viability treated with various concentration of digoxin. Results are expressed as mean \pm SD. The student t test was used to analyze the difference between treated group vs untreated group. Asterisks indicate significant different at p -value < 0.05 when compared with untreated group.

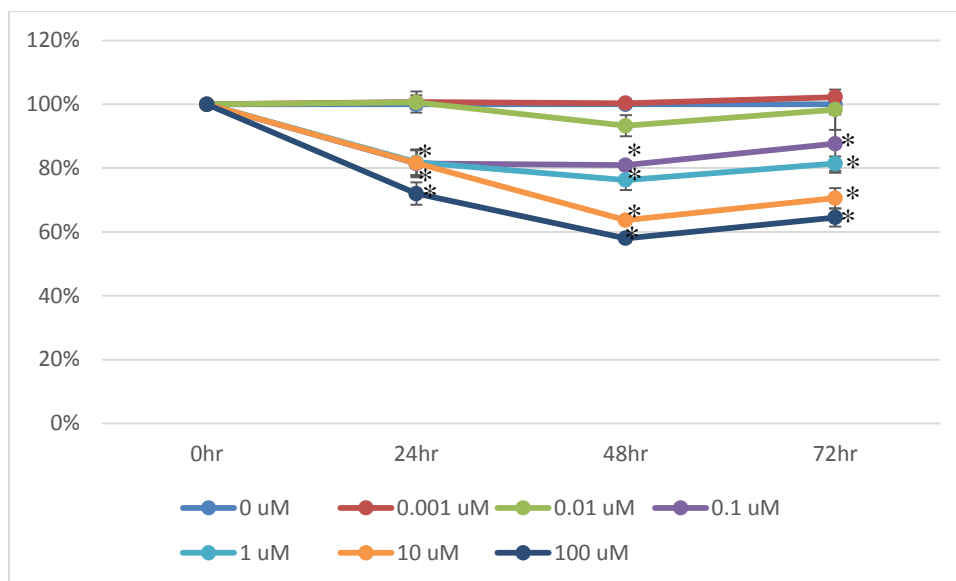


Figure 49 Percentage of Saos2 cell viability treated with various concentration of digoxin. Results are expressed as mean \pm SD. The student t test was used to analyze the difference between treated group vs untreated group. Asterisks indicate significant different at p-value < 0.05 when compared with untreated group.

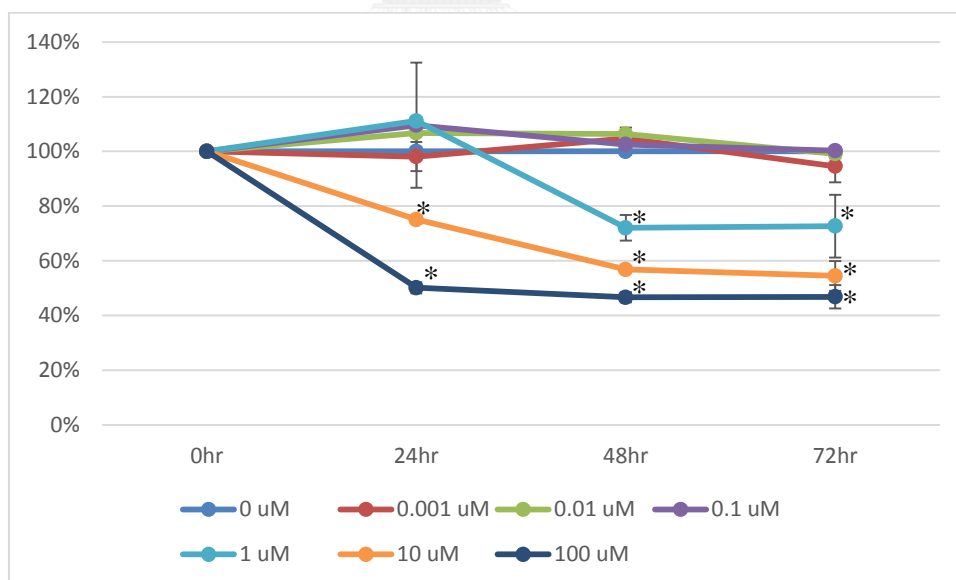


Figure 50 Percentage of U-2OS cell viability treated with various concentration of digoxin. Results are expressed as mean \pm SD. The student t test was used to analyze

the difference between treated group vs untreated group. Asterisks indicate significant different at p -value < 0.05 when compared with untreated group.

4.6 Responses to digoxin do not correlate with *ATP1B1* expression levels.

All osteosarcoma cell lines and primary osteosarcoma cell cultures express *ATP1B1* at mRNA level. However, the levels of expressions do not correlate with responses to digoxin by using Pearson's correlation test. (Figure 26)

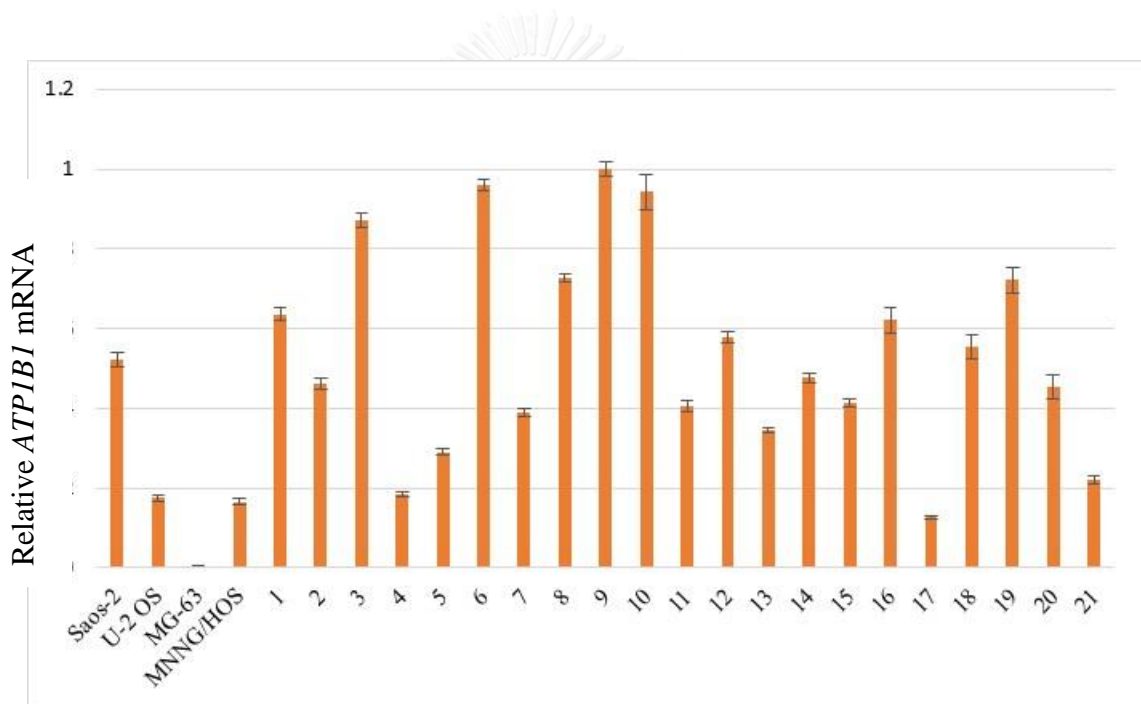


Figure 51 Relative *ATP1B1* mRNA expression levels in OS cell lines and primary cell cultures.

4.6 5-year survival rate in and chemotherapy response of patients recruited in this study are very low.

When we perform a retrospective review the clinical data of patients, we found that 5-year survival rate is only 7%. 52% of them (10/19) died within one year after first diagnosis (Figure 52).

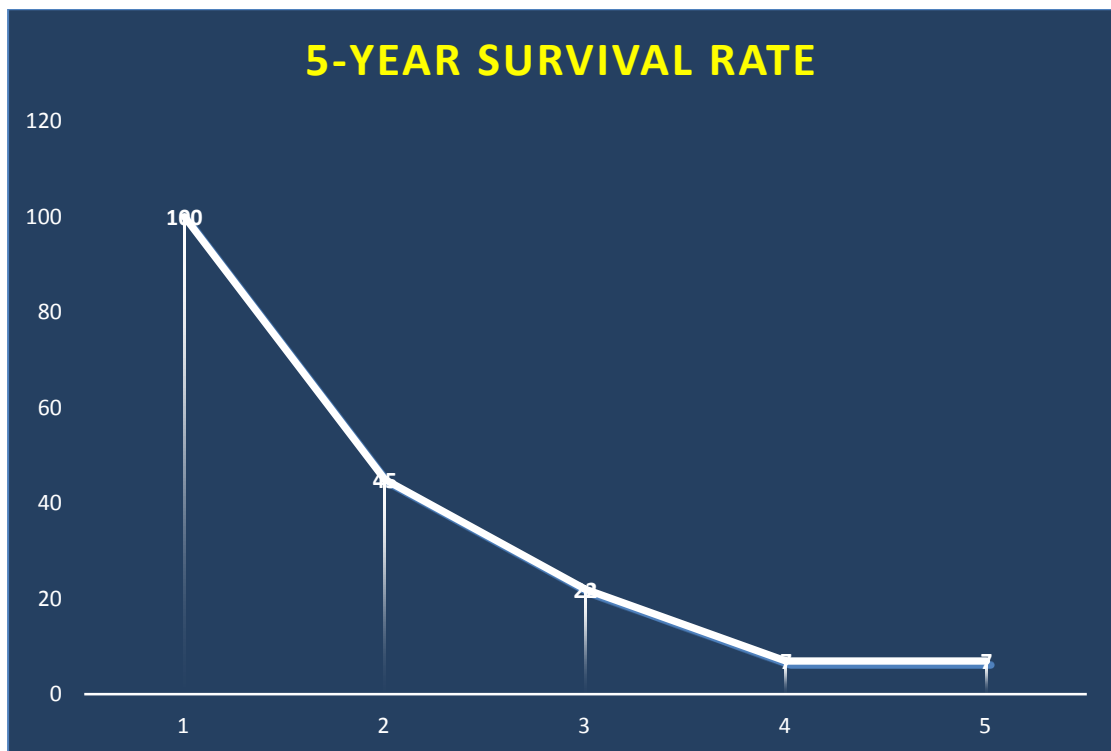


Figure 52 5 year-survival graph of patients in this study.

Most of them respond to chemotherapy evaluated by percentage of in vivo tumor necrosis by post-chemotherapy pathological reports less than 50% (Figure 53). When we take a look at the levels of response in primary cell cultures of these patients, we found that 50% of primary osteosarcoma cell cultures in patients who have survival time less than a year respond to digoxin at concentrations $< 1 \mu\text{M/ml}$. 25% of them respond to digoxin at concentrations $< 0.1 \mu\text{M/ml}$.

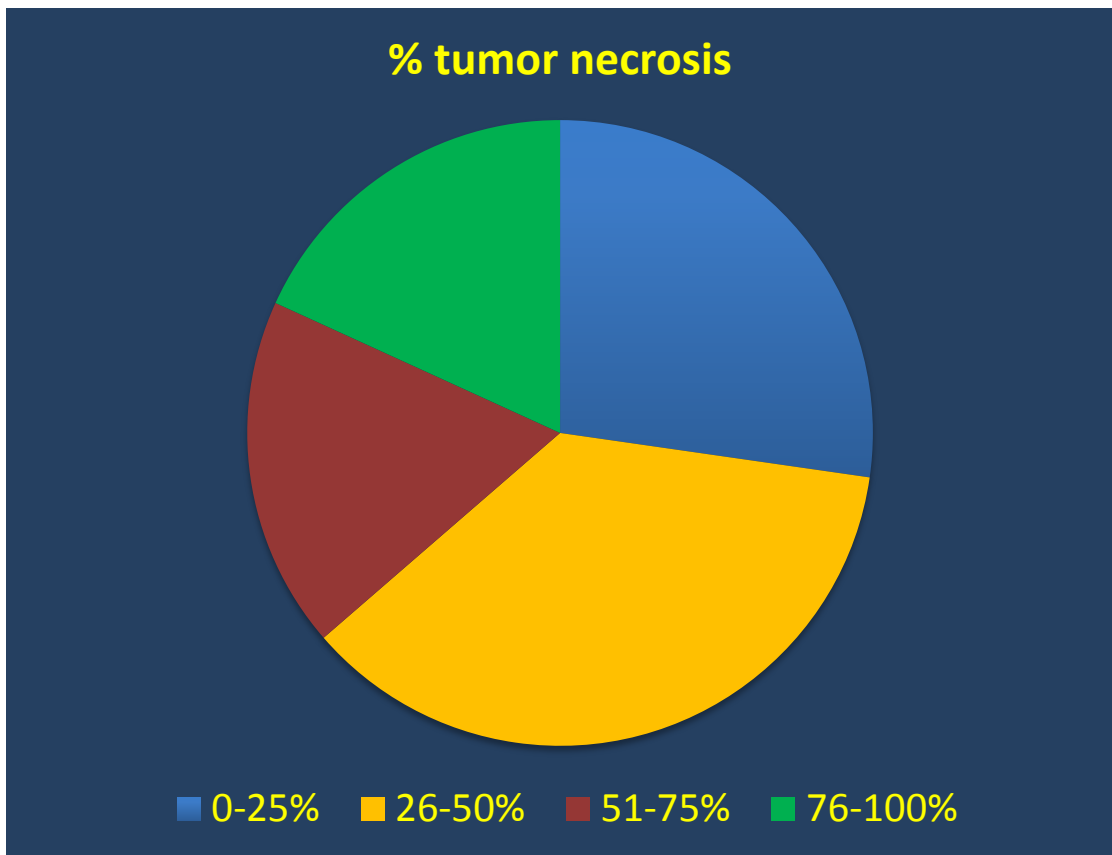


Figure 53 Percentage of tumor necrosis obtained from post-chemotherapy pathological reports of patients recruited in this study.

CHAPTER V

DISCUSSION

p53 is known as “guardian of the genome” because of its tumor suppressive function. *p53* loss of function believed to be a major genetic alteration in that leads to osteosarcoma (12, 18). *p53* pathway alterations account for 100% of osteosarcoma (18). Unlike gain of function alterations, restoration of *p53* function remains challenging. In 2015, Venkatanarayan claimed a therapeutic intervention to treat tumors with *p53* alterations by manipulation of *p53* family members, *p63* and *p73*. Inhibition of their ΔN isoforms in tumors led to restore function of TA isoforms which are tumor suppressor by elimination of dominant negative manner of ΔN isoforms against TA isoform. These TA isoforms are transcriptional factor of a metabolic regulator and metabolic reprogramming, *IAPP* which mediate its anti-cancer effect via two receptors, *CALCR* and *RAMP3* (19). *IAPP* has a synthetic analogue named “pramlintide acetate” (Symlin®) currently approved by US FDA for treatment of diabetes mellitus. We therefore propose to test its efficacy in osteosarcoma using primary osteosarcoma cell cultures.

At the concentration of 10 $\mu\text{g/ml}$ pramlintide acetate which was claimed its efficacy against *p53* deficient and mutant tumor by Venkatanarayan et al.(19), the percentage of apoptotic cells between treated and untreated groups were not differ in both U-2 OS and primary osteosarcoma cell No. 1 by flow cytometry.

Moreover, by using resazurin microplate assay, pramlintide acetate with various concentrations ranging from 0.001-100 $\mu\text{g/ml}$, could not lead to cell apoptosis in

U-2 OS cell line, which carries *MDM2* amplification (a *p53* inhibitor), and primary osteosarcoma cell culture No. 1 carrying a missense mutation in *p53*. Both of them express *CALCR* and *RAMP3* at mRNA level. At the concentration of 100 µg/ml, there was decreasing in percentage of cell viability detected by resazurin microplate assay. We hypothesized that due to acidity of pramlintide acetate caused cell death so pramlintide and acetic acid were used to confirm the hypothesis. Pramlintide alone could not lead to cell apoptosis or death while acetic acid led to significant cell death at concentration of 4.56 µg/ml which is about equal to its concentration in 100 µg/ml pramlintide acetate. These data from resazurin microplate assay and flow cytometry indicate that pramlintide has no anti-cancer effect in osteosarcoma regardless of *p53* status, and *CALCR* and *RAMP3* expression.

NCI-H1299 cell was used as a positive control as previously described by Venkatanarayan (19). *CALCR* and *RAMP3* expression levels were measured by qRT-PCR and showed that NCI-H1299 cell line expresses only *CALCR* but not *RAMP3* so pramlintide acetate should induce apoptosis in this cell line. We performed the experiment as the same as performing in osteosarcoma cells. Unfortunately, results in our hand differ from those reported by Venkatanarayan (19). At the concentration of 0.001-10 µg/ml of pramlintide acetate, we observed no statistical significant difference in percentage of cell viability using resazurin microplate assay, but at the concentration of 100 µg/ml, cell viability was decreased due to acidity of pramlintide acetate but not by the anti-cancer effect of the pramlintide. The efficacy of pramlintide acetate against NCI-H1299 cells was also confirmed by flow cytometry which showed that pramlintide acetate could not induce apoptosis in NCI-H1299 cells.

In conclusion, our study cannot demonstrate an *in vitro* antiosteosarcoma effect of pramlintide.



ATP1B1 encodes Na⁺/K⁺-transporting ATPase subunit beta-1 which belongs to Na⁺/K⁺ ATPase subfamily. Na⁺/K⁺ ATPase has its inhibitors collectively called “cardiac glycoside”. Cardiac glycosides inhibits Na⁺/K⁺ ATPase causing increased sodium ions in cardiac myocytes , which leads to increased intracellular calcium concentrations and contractile force of cardiac muscle. Cardiac glycosides showed anticancer effects. After first report in 1967, antiproliferative and apoptotic effects of cardiac glycosides confirmed in many cancers including breast (66), prostate (67-69), leukemia (70-74), melanoma (75), pancreatic (76), lung (77, 78), neuroblastoma (79), and renal cell adenocarcinoma (80). Right now, many cardiac glycoside-based compound are in the clinical studies as both single and combined administrations (NCT01887288, NCT01763931, NCT01162135, NCT00281021, NCT02138292, NCT02212639, NCT01562301, NCT00837239, and NCT01715532; ClinicalTrials.gov).

Digoxin, a cardenolides cardiac glycoside that has been long described for treatment of congestive heart failure was used in our experiments. Firstly, *ATP1B1* expression levels were measured using qRT-PCR. All osteosarcoma cell lines and primary cell cultures expresses *ATP1B1* at RNA level. Then cytotoxic assays were performed using REMA. This study demonstrates that the cardiac glycoside, particularly digoxin, are able to inhibit cell proliferation and induce osteosarcoma cell death. However, *ATP1B1* expression levels do not associated with the digoxin responsiveness. Anticancer mechanisms of digoxin including other cardiac glycosides have been purposed for many decades. In osteosarcoma, the mechanism of action of cardiac glycosides may via increased expression of the cyclin-dependent kinase inhibitor 1A (p21). Ouabain and digoxin activated Src kinase and stimulated the

interaction of Src and Na⁺/K⁺-ATPase with epidermal growth factor receptor-2 (EGFR2) caused a activation of extracellular signal-regulated kinases 1 and 2 (ERK1/2) and increase expression of p21(82). In 2012, Denard demonstrated the mechanism of action of doxorubicin, the first line chemotherapy in OS treatment. Doxorubicin stimulates proteolytic activation of CREB3L1 by Site-1 and Site-2 Protease, causing N-terminal domain (nuclear form) to enter the nucleus. Nuclear form of CREB3L1 is a transcription factor of p21, a cell cycle inhibitor gene (101) so the antiosteosarcoma mechanism of cardiac glycosides via stimulation of p21 is most likely due to sharing the same mechanism with doxorubicin, the most effective chemotherapy in osteosarcoma. Doxorubicin has effectiveness around 60-70% in osteosarcoma in cases with *CREB3L1* expression but in cases that have no *CREB3L1* expression, cardiac glycosides may be potential drugs that can substitute doxorubicin in patients who do not response to doxorubicin or synergist the effect of doxorubicin by activation of p21 dependently from *CREB3L1* expression. However, the possible mechanisms of antiosteosarcoma effects of cardiac glycosides should be studied in the future to understand underlying pathomechanisms. Moreover, all kinds of cardiac glycosides should be tested to obtain the most efficient compound that has antiosteosarcoma effect.

Another issue that should be concerned is a narrow margin of safety of cardiac glycoside dosage because it may affect the contractile function of the heart so it structure may be modified or it may be tagged with antibody that specific to osteosarcoma protein such as GD2 which expresses in all osteosarcoma and brain (102). If we can tag cardiac glycosides with antibody against GD2 and limit its blood-brain barrier crossing, cardiac glycoside may be a potential novel therapeutic agent in

osteosarcoma.

In conclusion, this is the first study that exhibits antiosteosarcoma effect of digoxin by comprehensive analysis of proteomic data in osteosarcoma. After *in vivo* and clinical studies, combination with standard chemotherapy or administration as a single agent of digoxin may improve the overall survival in osteosarcoma that reached the plateau for almost 20 years.



REFERENCES

1. Wiangnon S, Veerakul G, Nuchprayoon I, Seksarn P, Hongeng S, Krutvecho T, et al. Childhood cancer incidence and survival 2003-2005, Thailand: study from the Thai Pediatric Oncology Group. *Asian Pacific journal of cancer prevention : APJCP*. 2011;12(9):2215-20.
2. Rosen G, Marcove RC, Caparros B, Nirenberg A, Kosloff C, Huvos AG. Primary osteogenic sarcoma: the rationale for preoperative chemotherapy and delayed surgery. *Cancer*. 1979;43(6):2163-77.
3. Allison DC, Carney SC, Ahlmann ER, Hendifar A, Chawla S, Fedenko A, et al. A meta-analysis of osteosarcoma outcomes in the modern medical era. *Sarcoma*. 2012;2012:704872.
4. Meyers PA, Gorlick R. Osteosarcoma. *Pediatric clinics of North America*. 1997;44(4):973-89.
5. Fletcher CD. The evolving classification of soft tissue tumours - an update based on the new 2013 WHO classification. *Histopathology*. 2014;64(1):2-11.
6. Hu F, Wang W, Zhou HC, Shang XF. High expression of periostin is dramatically associated with metastatic potential and poor prognosis of patients with osteosarcoma. *World journal of surgical oncology*. 2014;12:287.
7. Martin JW, Squire JA, Zielenska M. The genetics of osteosarcoma. *Sarcoma*. 2012;2012:627254.
8. Nakajima H, Sim FH, Bond JR, Unni KK. Small cell osteosarcoma of bone. Review of 72 cases. *Cancer*. 1997;79(11):2095-106.

9. Malhas AM, Sumathi VP, James SL, Menna C, Carter SR, Tillman RM, et al. Low-grade central osteosarcoma: a difficult condition to diagnose. *Sarcoma*. 2012;2012:764796.
10. PosthumaDeBoer J, Witlox MA, Kaspers GJ, van Royen BJ. Molecular alterations as target for therapy in metastatic osteosarcoma: a review of literature. *Clinical & experimental metastasis*. 2011;28(5):493-503.
11. Ruijs MW, Verhoef S, Rookus MA, Pruntel R, van der Hout AH, Hogervorst FB, et al. TP53 germline mutation testing in 180 families suspected of Li-Fraumeni syndrome: mutation detection rate and relative frequency of cancers in different familial phenotypes. *Journal of medical genetics*. 2010;47(6):421-8.
12. Walkley CR, Qudsi R, Sankaran VG, Perry JA, Gostissa M, Roth SI, et al. Conditional mouse osteosarcoma, dependent on p53 loss and potentiated by loss of Rb, mimics the human disease. *Genes & development*. 2008;22(12):1662-76.
13. Soussi T, Beroud C. Significance of TP53 mutations in human cancer: a critical analysis of mutations at CpG dinucleotides. *Human mutation*. 2003;21(3):192-200.
14. Eliyahu D, Michalovitz D, Eliyahu S, Pinhasi-Kimhi O, Oren M. Wild-type p53 can inhibit oncogene-mediated focus formation. *Proceedings of the National Academy of Sciences of the United States of America*. 1989;86(22):8763-7.
15. Goto A, Kanda H, Ishikawa Y, Matsumoto S, Kawaguchi N, Machinami R, et al. Association of loss of heterozygosity at the p53 locus with chemoresistance in osteosarcomas. *Japanese journal of cancer research : Gann*. 1998;89(5):539-47.

16. Tsuchiya T, Sekine K, Hinohara S, Namiki T, Nobori T, Kaneko Y. Analysis of the p16INK4, p14ARF, p15, TP53, and MDM2 genes and their prognostic implications in osteosarcoma and Ewing sarcoma. *Cancer genetics and cytogenetics*. 2000;120(2):91-8.
17. Wunder JS, Gokgoz N, Parkes R, Bull SB, Eskandarian S, Davis AM, et al. TP53 mutations and outcome in osteosarcoma: a prospective, multicenter study. *Journal of clinical oncology : official journal of the American Society of Clinical Oncology*. 2005;23(7):1483-90.
18. Chen X, Bahrami A, Pappo A, Easton J, Dalton J, Hedlund E, et al. Recurrent somatic structural variations contribute to tumorigenesis in pediatric osteosarcoma. *Cell reports*. 2014;7(1):104-12.
19. Venkatanarayan A, Raulji P, Norton W, Chakravarti D, Coarfa C, Su X, et al. IAPP-driven metabolic reprogramming induces regression of p53-deficient tumours in vivo. *Nature*. 2015;517(7536):626-30.
20. Flores ER, Sengupta S, Miller JB, Newman JJ, Bronson R, Crowley D, et al. Tumor predisposition in mice mutant for p63 and p73: evidence for broader tumor suppressor functions for the p53 family. *Cancer cell*. 2005;7(4):363-73.
21. Su X, Chakravarti D, Cho MS, Liu L, Gi YJ, Lin YL, et al. TAp63 suppresses metastasis through coordinate regulation of Dicer and miRNAs. *Nature*. 2010;467(7318):986-90.
22. Su X, Gi YJ, Chakravarti D, Chan IL, Zhang A, Xia X, et al. TAp63 is a master transcriptional regulator of lipid and glucose metabolism. *Cell metabolism*. 2012;16(4):511-25.

23. Tomasini R, Tsuchihara K, Wilhelm M, Fujitani M, Rufini A, Cheung CC, et al. TAp73 knockout shows genomic instability with infertility and tumor suppressor functions. *Genes & development*. 2008;22(19):2677-91.
24. Yang A, Kaghad M, Wang Y, Gillett E, Fleming MD, Dotsch V, et al. p63, a p53 homolog at 3q27-29, encodes multiple products with transactivating, death-inducing, and dominant-negative activities. *Molecular cell*. 1998;2(3):305-16.
25. Brekhman V, Lugassie J, Zaffryar-Eilot S, Sabo E, Kessler O, Smith V, et al. Receptor activity modifying protein-3 mediates the protumorigenic activity of lysyl oxidase-like protein-2. *FASEB journal : official publication of the Federation of American Societies for Experimental Biology*. 2011;25(1):55-65.
26. Chatchawit Apornthewan AM. Connection up-and down-regulation expression analysis of microarrays (CU-DREAM): a physiogenomic discovery tool. *Asian Biomedicine*. 2011;5(2):257-62.
27. Guo QC, Shen JN, Jin S, Wang J, Huang G, Zhang LJ, et al. Comparative proteomic analysis of human osteosarcoma and SV40-immortalized normal osteoblastic cell lines. *Acta pharmacologica Sinica*. 2007;28(6):850-8.
28. Folio C, Mora MI, Zalacain M, Corrales FJ, Segura V, Sierrasesumaga L, et al. Proteomic analysis of chemo-naive pediatric osteosarcomas and corresponding normal bone reveals multiple altered molecular targets. *Journal of proteome research*. 2009;8(8):3882-8.
29. Liu X, Zeng B, Ma J, Wan C. Comparative proteomic analysis of osteosarcoma cell and human primary cultured osteoblastic cell. *Cancer investigation*. 2009;27(3):345-52.

30. Zhang Z, Zhang L, Hua Y, Jia X, Li J, Hu S, et al. Comparative proteomic analysis of plasma membrane proteins between human osteosarcoma and normal osteoblastic cell lines. *BMC Cancer*. 2010;10:206.
31. Hua Y, Jia X, Sun M, Zheng L, Yin L, Zhang L, et al. Plasma membrane proteomic analysis of human osteosarcoma and osteoblastic cells: revealing NDRG1 as a marker for osteosarcoma. *Tumour biology : the journal of the International Society for Oncodevelopmental Biology and Medicine*. 2011;32(5):1013-21.
32. Posthumadeboer J, Piersma SR, Pham TV, van Egmond PW, Knol JC, Cleton-Jansen AM, et al. Surface proteomic analysis of osteosarcoma identifies EPHA2 as receptor for targeted drug delivery. *British journal of cancer*. 2013;109(8):2142-54.
33. Gemoll T, Epping F, Heinrich L, Fritzsche B, Roblick UJ, Szymczak S, et al. Increased cathepsin D protein expression is a biomarker for osteosarcomas, pulmonary metastases and other bone malignancies. *Oncotarget*. 2015;6(18):16517-26.
34. Spreafico A, Frediani B, Capperucci C, Chellini F, Paffetti A, D'Ambrosio C, et al. A proteomic study on human osteoblastic cells proliferation and differentiation. *Proteomics*. 2006;6(12):3520-32.
35. Suehara Y, Kondo T, Fujii K, Hasegawa T, Kawai A, Seki K, et al. Proteomic signatures corresponding to histological classification and grading of soft-tissue sarcomas. *Proteomics*. 2006;6(15):4402-9.

36. Kawai A, Kondo T, Suehara Y, Kikuta K, Hirohashi S. Global protein-expression analysis of bone and soft tissue sarcomas. *Clin Orthop Relat Res.* 2008;466(9):2099-106.
37. Li Y, Liang Q, Wen YQ, Chen LL, Wang LT, Liu YL, et al. Comparative proteomics analysis of human osteosarcomas and benign tumor of bone. *Cancer Genet Cytogenet.* 2010;198(2):97-106.
38. Rao UN, Hood BL, Jones-Laughner JM, Sun M, Conrads TP. Distinct profiles of oxidative stress-related and matrix proteins in adult bone and soft tissue osteosarcoma and desmoid tumors: a proteomics study. *Hum Pathol.* 2013;44(5):725-33.
39. Bona A, Papai Z, Maasz G, Toth GA, Jambor E, Schmidt J, et al. Mass spectrometric identification of ancient proteins as potential molecular biomarkers for a 2000-year-old osteogenic sarcoma. *PLoS One.* 2014;9(1):e87215.
40. Flores RJ, Li Y, Yu A, Shen J, Rao PH, Lau SS, et al. A systems biology approach reveals common metastatic pathways in osteosarcoma. *BMC Syst Biol.* 2012;6:50.
41. Chen X, Yang TT, Zhou Y, Wang W, Qiu XC, Gao J, et al. Proteomic profiling of osteosarcoma cells identifies ALDOA and SULT1A3 as negative survival markers of human osteosarcoma. *Mol Carcinog.* 2014;53(2):138-44.
42. Tang J, Shen L, Yang Q, Zhang C. Overexpression of metadherin mediates metastasis of osteosarcoma by regulating epithelial-mesenchymal transition. *Cell Prolif.* 2014;47(5):427-34.

43. Sau A, Filomeni G, Pezzola S, D'Aguanno S, Tregno FP, Urbani A, et al. Targeting GSTP1-1 induces JNK activation and leads to apoptosis in cisplatin-sensitive and -resistant human osteosarcoma cell lines. *Mol Biosyst.* 2012;8(4):994-1006.
44. Arai K, Sakamoto R, Kubota D, Kondo T. Proteomic approach toward molecular backgrounds of drug resistance of osteosarcoma cells in spheroid culture system. *Proteomics.* 2013;13(15):2351-60.
45. Izbicka E, Campos D, Marty J, Carrizales G, Mangold G, Tolcher A. Molecular determinants of differential sensitivity to docetaxel and paclitaxel in human pediatric cancer models. *Anticancer Res.* 2006;26(3A):1983-8.
46. Kang JH, Park KK, Lee IS, Magae J, Ando K, Kim CH, et al. Proteome analysis of responses to ascochlorin in a human osteosarcoma cell line by 2-D gel electrophoresis and MALDI-TOF MS. *J Proteome Res.* 2006;5(10):2620-31.
47. Chang YC, Park WH, Min KS, Kim T, Kim CH, Kang JH. Proteome profiling of U2OS cell line in response to a prenylphenol antibiotic isolated from a phytopathogenic fungus. *Biol Pharm Bull.* 2008;31(9):1696-703.
48. Xie XB, Yin JQ, Wen LL, Gao ZH, Zou CY, Wang J, et al. Critical role of heat shock protein 27 in bufalin-induced apoptosis in human osteosarcomas: a proteomic-based research. *PLoS One.* 2012;7(10):e47375.
49. Kubota D, Mukaihara K, Yoshida A, Tsuda H, Kawai A, Kondo T. Proteomics study of open biopsy samples identifies peroxiredoxin 2 as a predictive biomarker of response to induction chemotherapy in osteosarcoma. *J Proteomics.* 2013;91:393-404.

50. Kansara M, Teng MW, Smyth MJ, Thomas DM. Translational biology of osteosarcoma. *Nat Rev Cancer*. 2014;14(11):722-35.
51. Annunen-Rasila J, Ohlmeier S, Tuokko H, Veijola J, Majamaa K. Proteome and cytoskeleton responses in osteosarcoma cells with reduced OXPHOS activity. *Proteomics*. 2007;7(13):2189-200.
52. D'Alessandro A, Marrocco C, Rinalducci S, Peschiaroli A, Timperio AM, Bongiorno-Borbone L, et al. Analysis of TAp73-dependent signaling via omics technologies. *J Proteome Res*. 2013;12(9):4207-20.
53. Klevebring D, Fagerberg L, Lundberg E, Emanuelsson O, Uhlen M, Lundberg J. Analysis of transcript and protein overlap in a human osteosarcoma cell line. *BMC Genomics*. 2010;11:684.
54. Kirkwood KJ, Ahmad Y, Larance M, Lamond AI. Characterization of native protein complexes and protein isoform variation using size-fractionation-based quantitative proteomics. *Mol Cell Proteomics*. 2013;12(12):3851-73.
55. Gemei M, Corbo C, D'Alessio F, Di Noto R, Vento R, Del Vecchio L. Surface proteomic analysis of differentiated versus stem-like osteosarcoma human cells. *Proteomics*. 2013;13(22):3293-7.
56. Larance M, Ahmad Y, Kirkwood KJ, Ly T, Lamond AI. Global subcellular characterization of protein degradation using quantitative proteomics. *Mol Cell Proteomics*. 2013;12(3):638-50.
57. Niforou KM, Anagnostopoulos AK, Vougas K, Kittas C, Gorgoulis VG, Tsangaris GT. The proteome profile of the human osteosarcoma U2OS cell line. *Cancer Genomics Proteomics*. 2008;5(1):63-78.

58. Li G, Zhang W, Zeng H, Chen L, Wang W, Liu J, et al. An integrative multi-platform analysis for discovering biomarkers of osteosarcoma. *BMC Cancer*. 2009;9:150.
59. Li Y, Dang TA, Shen J, Perlaky L, Hicks J, Murray J, et al. Identification of a plasma proteomic signature to distinguish pediatric osteosarcoma from benign osteochondroma. *Proteomics*. 2006;6(11):3426-35.
60. Li Y, Dang TA, Shen J, Hicks J, Chintagumpala M, Lau CC, et al. Plasma proteome predicts chemotherapy response in osteosarcoma patients. *Oncol Rep*. 2011;25(2):303-14.
61. Savitskaya YA, Rico-Martinez G, Linares-Gonzalez LM, Delgado-Cedillo EA, Tellez-Gastelum R, Alfaro-Rodriguez AB, et al. Serum tumor markers in pediatric osteosarcoma: a summary review. *Clin Sarcoma Res*. 2012;2:9.
62. Jin S, Shen JN, Guo QC, Zhou JG, Wang J, Huang G, et al. 2-D DIGE and MALDI-TOF-MS analysis of the serum proteome in human osteosarcoma. *Proteomics Clin Appl*. 2007;1(3):272-85.
63. Stenkvist B, Bengtsson E, Eriksson O, Holmquist J, Nordin B, Westman-Naeser S. Cardiac glycosides and breast cancer. *Lancet*. 1979;1(8115):563.
64. Stenkvist B, Bengtsson E, Dahlqvist B, Eklund G, Eriksson O, Jarkrans T, et al. Predicting breast cancer recurrence. *Cancer*. 1982;50(12):2884-93.
65. Stenkvist B, Bengtsson E, Dahlqvist B, Eriksson O, Jarkrans T, Nordin B. Cardiac glycosides and breast cancer, revisited. *The New England journal of medicine*. 1982;306(8):484.

66. Bielawski K, Winnicka K, Bielawska A. Inhibition of DNA topoisomerases I and II, and growth inhibition of breast cancer MCF-7 cells by ouabain, digoxin and proscillaridin A. *Biological & pharmaceutical bulletin*. 2006;29(7):1493-7.
67. Yeh JY, Huang WJ, Kan SF, Wang PS. Effects of bufalin and cinobufagin on the proliferation of androgen dependent and independent prostate cancer cells. *The Prostate*. 2003;54(2):112-24.
68. Huang YT, Chueh SC, Teng CM, Guh JH. Investigation of ouabain-induced anticancer effect in human androgen-independent prostate cancer PC-3 cells. *Biochemical pharmacology*. 2004;67(4):727-33.
69. McConkey DJ, Lin Y, Nutt LK, Ozel HZ, Newman RA. Cardiac glycosides stimulate Ca²⁺ increases and apoptosis in androgen-independent, metastatic human prostate adenocarcinoma cells. *Cancer research*. 2000;60(14):3807-12.
70. Raghavendra PB, Sreenivasan Y, Ramesh GT, Manna SK. Cardiac glycoside induces cell death via FasL by activating calcineurin and NF-AT, but apoptosis initially proceeds through activation of caspases. *Apoptosis : an international journal on programmed cell death*. 2007;12(2):307-18.
71. Masuda Y, Kawazoe N, Nakajo S, Yoshida T, Kuroiwa Y, Nakaya K. Bufalin induces apoptosis and influences the expression of apoptosis-related genes in human leukemia cells. *Leukemia research*. 1995;19(8):549-56.
72. Daniel D, Susal C, Kopp B, Opelz G, Terness P. Apoptosis-mediated selective killing of malignant cells by cardiac steroids: maintenance of cytotoxicity and loss of cardiac activity of chemically modified derivatives. *International immunopharmacology*. 2003;3(13-14):1791-801.

73. Jing Y, Ohizumi H, Kawazoe N, Hashimoto S, Masuda Y, Nakajo S, et al. Selective inhibitory effect of bufalin on growth of human tumor cells in vitro: association with the induction of apoptosis in leukemia HL-60 cells. *Japanese journal of cancer research : Gann.* 1994;85(6):645-51.
74. Kawazoe N, Watabe M, Masuda Y, Nakajo S, Nakaya K. Tiam1 is involved in the regulation of bufalin-induced apoptosis in human leukemia cells. *Oncogene.* 1999;18(15):2413-21.
75. Newman RA, Yang P, Hittelman WN, Lu T, Ho DH, Ni D, et al. Oleandrin-mediated oxidative stress in human melanoma cells. *Journal of experimental therapeutics & oncology.* 2006;5(3):167-81.
76. Newman RA, Kondo Y, Yokoyama T, Dixon S, Cartwright C, Chan D, et al. Autophagic cell death of human pancreatic tumor cells mediated by oleandrin, a lipid-soluble cardiac glycoside. *Integrative cancer therapies.* 2007;6(4):354-64.
77. Mijatovic T, Op De Beeck A, Van Quaquebeke E, Dewelle J, Darro F, de Launoit Y, et al. The cardenolide UNBS1450 is able to deactivate nuclear factor kappaB-mediated cytoprotective effects in human non-small cell lung cancer cells. *Molecular cancer therapeutics.* 2006;5(2):391-9.
78. Frese S, Frese-Schaper M, Andres AC, Miescher D, Zumkehr B, Schmid RA. Cardiac glycosides initiate Apo2L/TRAIL-induced apoptosis in non-small cell lung cancer cells by up-regulation of death receptors 4 and 5. *Cancer research.* 2006;66(11):5867-74.
79. Kulikov A, Eva A, Kirch U, Boldyrev A, Scheiner-Bobis G. Ouabain activates signaling pathways associated with cell death in human neuroblastoma. *Biochimica et biophysica acta.* 2007;1768(7):1691-702.

80. Lopez-Lazaro M, Pastor N, Azrak SS, Ayuso MJ, Austin CA, Cortes F. Digitoxin inhibits the growth of cancer cell lines at concentrations commonly found in cardiac patients. *Journal of natural products*. 2005;68(11):1642-5.
81. Kaplan JG. Membrane cation transport and the control of proliferation of mammalian cells. *Annual review of physiology*. 1978;40:19-41.
82. Kometiani P, Liu L, Askari A. Digitalis-induced signaling by Na⁺/K⁺-ATPase in human breast cancer cells. *Molecular pharmacology*. 2005;67(3):929-36.
83. Paul RJ, Bauer M, Pease W. Vascular smooth muscle: aerobic glycolysis linked to sodium and potassium transport processes. *Science*. 1979;206(4425):1414-6.
84. Rahimtoola SH, Tak T. The use of digitalis in heart failure. *Current problems in cardiology*. 1996;21(12):781-853.
85. Xie Z, Askari A. Na⁽⁺⁾/K⁽⁺⁾-ATPase as a signal transducer. *European journal of biochemistry / FEBS*. 2002;269(10):2434-9.
86. Hashimoto S, Jing Y, Kawazoe N, Masuda Y, Nakajo S, Yoshida T, et al. Bufalin reduces the level of topoisomerase II in human leukemia cells and affects the cytotoxicity of anticancer drugs. *Leukemia research*. 1997;21(9):875-83.
87. Johnson PH, Walker RP, Jones SW, Stephens K, Meurer J, Zajchowski DA, et al. Multiplex gene expression analysis for high-throughput drug discovery: screening and analysis of compounds affecting genes overexpressed in cancer cells. *Molecular cancer therapeutics*. 2002;1(14):1293-304.
88. Manna SK, Sreenivasan Y, Sarkar A. Cardiac glycoside inhibits IL-8-induced biological responses by downregulating IL-8 receptors through altering membrane fluidity. *Journal of cellular physiology*. 2006;207(1):195-207.

89. Gillet JP, Calcagno AM, Varma S, Marino M, Green LJ, Vora MI, et al. Redefining the relevance of established cancer cell lines to the study of mechanisms of clinical anti-cancer drug resistance. *Proceedings of the National Academy of Sciences of the United States of America*. 2011;108(46):18708-13.
90. Gazdar AF, Gao B, Minna JD. Lung cancer cell lines: Useless artifacts or invaluable tools for medical science? *Lung cancer*. 2010;68(3):309-18.
91. Burdall SE, Hanby AM, Lansdown MR, Speirs V. Breast cancer cell lines: friend or foe? *Breast cancer research : BCR*. 2003;5(2):89-95.
92. Castell JV, Gomez-Lechon MJ. Liver cell culture techniques. *Methods in molecular biology*. 2009;481:35-46.
93. Roskelley CD, Srebrow A, Bissell MJ. A hierarchy of ECM-mediated signalling regulates tissue-specific gene expression. *Current opinion in cell biology*. 1995;7(5):736-47.
94. Bull ND, Johnson TV, Welsapar G, DeKorver NW, Tomarev SI, Martin KR. Use of an adult rat retinal explant model for screening of potential retinal ganglion cell neuroprotective therapies. *Investigative ophthalmology & visual science*. 2011;52(6):3309-20.
95. Parajuli N, Doppler W. Precision-cut slice cultures of tumors from MMTV-neu mice for the study of the ex vivo response to cytokines and cytotoxic drugs. *In vitro cellular & developmental biology Animal*. 2009;45(8):442-50.
96. Li WC, Ralphs KL, Tosh D. Isolation and culture of adult mouse hepatocytes. *Methods in molecular biology*. 2010;633:185-96.
97. Jones JC. Reduction of contamination of epithelial cultures by fibroblasts. *CSH protocols*. 2008;2008:pdb prot4478.

98. Dairkee SH, Deng G, Stampfer MR, Waldman FM, Smith HS. Selective cell culture of primary breast carcinoma. *Cancer research*. 1995;55(12):2516-9.
99. Clement V, Marino D, Cudalbu C, Hamou MF, Mlynarik V, de Tribolet N, et al. Marker-independent identification of glioma-initiating cells. *Nature methods*. 2010;7(3):224-8.
100. O'Brien J, Wilson I, Orton T, Pognan F. Investigation of the Alamar Blue (resazurin) fluorescent dye for the assessment of mammalian cell cytotoxicity. *European journal of biochemistry / FEBS*. 2000;267(17):5421-6.
101. Denard B, Lee C, Ye J. Doxorubicin blocks proliferation of cancer cells through proteolytic activation of CREB3L1. *eLife*. 2012;1:e00090.
102. Dobrenkov K, Cheung NK. GD2-targeted immunotherapy and radioimmunotherapy. *Seminars in oncology*. 2014;41(5):589-612.
103. Morello R, Bertin TK, Chen Y, Hicks J, Tonachini L, Monticone M, et al. CRTAP is required for prolyl 3- hydroxylation and mutations cause recessive osteogenesis imperfecta. *Cell*. 2006;127(2):291-304.
104. Asharani PV, Keupp K, Semler O, Wang W, Li Y, Thiele H, et al. Attenuated BMP1 function compromises osteogenesis, leading to bone fragility in humans and zebrafish. *American journal of human genetics*. 2012;90(4):661-74.
105. Symoens S, Malfait F, D'Hondt S, Callewaert B, Dheedene A, Steyaert W, et al. Deficiency for the ER-stress transducer OASIS causes severe recessive osteogenesis imperfecta in humans. *Orphanet journal of rare diseases*. 2013;8:154.

106. Cho TJ, Lee KE, Lee SK, Song SJ, Kim KJ, Jeon D, et al. A single recurrent mutation in the 5'-UTR of IFITM5 causes osteogenesis imperfecta type V. *American journal of human genetics*. 2012;91(2):343-8.
107. Alanay Y, Avaygan H, Camacho N, Utine GE, Boduroglu K, Aktas D, et al. Mutations in the gene encoding the RER protein FKBP65 cause autosomal-recessive osteogenesis imperfecta. *American journal of human genetics*. 2010;86(4):551-9.
108. Cabral WA, Chang W, Barnes AM, Weis M, Scott MA, Leikin S, et al. Prolyl 3-hydroxylase 1 deficiency causes a recessive metabolic bone disorder resembling lethal/severe osteogenesis imperfecta. *Nature genetics*. 2007;39(3):359-65.
109. van Dijk FS, Nesbitt IM, Zwikstra EH, Nikkels PG, Piersma SR, Fratantoni SA, et al. PPIB mutations cause severe osteogenesis imperfecta. *American journal of human genetics*. 2009;85(4):521-7.
110. Lapunzina P, Aglan M, Temtamy S, Caparros-Martin JA, Valencia M, Leton R, et al. Identification of a frameshift mutation in Osterix in a patient with recessive osteogenesis imperfecta. *American journal of human genetics*. 2010;87(1):110-4.
111. Puig-Hervas MT, Temtamy S, Aglan M, Valencia M, Martinez-Glez V, Ballesta-Martinez MJ, et al. Mutations in PLOD2 cause autosomal-recessive connective tissue disorders within the Bruck syndrome--osteogenesis imperfecta phenotypic spectrum. *Human mutation*. 2012;33(10):1444-9.
112. Shaheen R, Alazami AM, Alshammari MJ, Faqeih E, Alhashmi N, Mousa N, et al. Study of autosomal recessive osteogenesis imperfecta in Arabia reveals a

- novel locus defined by TMEM38B mutation. *Journal of medical genetics*. 2012;49(10):630-5.
113. Becker J, Semler O, Gilissen C, Li Y, Bolz HJ, Giunta C, et al. Exome sequencing identifies truncating mutations in human SERPINF1 in autosomal-recessive osteogenesis imperfecta. *American journal of human genetics*. 2011;88(3):362-71.
114. Christiansen HE, Schwarze U, Pyott SM, AlSwaid A, Al Balwi M, Alrasheed S, et al. Homozygosity for a missense mutation in SERPINH1, which encodes the collagen chaperone protein HSP47, results in severe recessive osteogenesis imperfecta. *American journal of human genetics*. 2010;86(3):389-98.
115. Garbes L, Kim K, Riess A, Hoyer-Kuhn H, Beleggia F, Bevot A, et al. Mutations in SEC24D, encoding a component of the COPII machinery, cause a syndromic form of osteogenesis imperfecta. *American journal of human genetics*. 2015;96(3):432-9.
116. Mendoza-Londono R, Fahiminiya S, Majewski J, Care4Rare Canada C, Tetreault M, Nadaf J, et al. Recessive osteogenesis imperfecta caused by missense mutations in SPARC. *American journal of human genetics*. 2015;96(6):979-85.
117. Fahiminiya S, Majewski J, Mort J, Moffatt P, Glorieux FH, Rauch F. Mutations in WNT1 are a cause of osteogenesis imperfecta. *Journal of medical genetics*. 2013;50(5):345-8.
118. Sillence DO, Senn A, Danks DM. Genetic heterogeneity in osteogenesis imperfecta. *J Med Genet*. 1979;16(2):101-16.

119. Nishimura G, Haga N, Kitoh H, Tanaka Y, Sonoda T, Kitamura M, et al. The phenotypic spectrum of COL2A1 mutations. *Human mutation*. 2005;26(1):36-43.
120. Zankl A, Zabel B, Hilbert K, Wildhardt G, Cuenot S, Xavier B, et al. Spondyloperipheral dysplasia is caused by truncating mutations in the C-propeptide of COL2A1. *American journal of medical genetics Part A*. 2004;129A(2):144-8.
121. Richards AJ, Morgan J, Bearcroft PW, Pickering E, Owen MJ, Holmans P, et al. Vitreoretinopathy with phalangeal epiphyseal dysplasia, a type II collagenopathy resulting from a novel mutation in the C-propeptide region of the molecule. *Journal of medical genetics*. 2002;39(9):661-5.
122. Kannu P, O'Rielly DD, Hyland JC, Kokko LA. Avascular necrosis of the femoral head due to a novel C propeptide mutation in COL2A1. *American journal of medical genetics Part A*. 2011;155A(7):1759-62.
123. Biesecker LG, Biesecker BB. An approach to pediatric exome and genome sequencing. *Current opinion in pediatrics*. 2014;26(6):639-45.
124. Collins FS, Hamburg MA. First FDA authorization for next-generation sequencer. *The New England journal of medicine*. 2013;369(25):2369-71.
125. Koboldt DC, Ding L, Mardis ER, Wilson RK. Challenges of sequencing human genomes. *Briefings in bioinformatics*. 2010;11(5):484-98.
126. Mardis ER. The impact of next-generation sequencing technology on genetics. *Trends in genetics : TIG*. 2008;24(3):133-41.
127. Mardis ER. Next-generation sequencing platforms. *Annual review of analytical chemistry*. 2013;6:287-303.

128. Metzker ML. Sequencing technologies - the next generation. *Nature reviews Genetics*. 2010;11(1):31-46.
129. Morozova O, Marra MA. Applications of next-generation sequencing technologies in functional genomics. *Genomics*. 2008;92(5):255-64.
130. Liu L, Li Y, Li S, Hu N, He Y, Pong R, et al. Comparison of next-generation sequencing systems. *Journal of biomedicine & biotechnology*. 2012;2012:251364.
131. McMahon AP, Bradley A. The Wnt-1 (int-1) proto-oncogene is required for development of a large region of the mouse brain. *Cell*. 1990;62(6):1073-85.
132. Joeng KS, Lee YC, Jiang MM, Bertin TK, Chen Y, Abraham AM, et al. The swaying mouse as a model of osteogenesis imperfecta caused by WNT1 mutations. *Human molecular genetics*. 2014;23(15):4035-42.
133. Keupp K, Beleggia F, Kayserili H, Barnes AM, Steiner M, Semler O, et al. Mutations in WNT1 cause different forms of bone fragility. *American journal of human genetics*. 2013;92(4):565-74.
134. Heo JS, Lee SY, Lee JC. Wnt/beta-catenin signaling enhances osteoblastogenic differentiation from human periodontal ligament fibroblasts. *Molecules and cells*. 2010;30(5):449-54.
135. Fujita K, Janz S. Attenuation of WNT signaling by DKK-1 and -2 regulates BMP2-induced osteoblast differentiation and expression of OPG, RANKL and M-CSF. *Molecular cancer*. 2007;6:71.
136. Aldinger KA, Mendelsohn NJ, Chung BH, Zhang W, Cohn DH, Fernandez B, et al. Variable brain phenotype primarily affects the brainstem and cerebellum

in patients with osteogenesis imperfecta caused by recessive WNT1 mutations.

Journal of medical genetics. 2015.



APPENDIX



จุฬาลงกรณ์มหาวิทยาลัย
CHULALONGKORN UNIVERSITY

APPENDIX A

THE USE OF NEXT-GENERATION SEQUENCING IN DIAGNOSIS AND MANAGEMENT OF SKELETAL DYSPLASIAS

A.1 BACKGROUND AND RATIONALE

Skeletal dysplasia is a group of diseases consisting of more than 400 entities. Most of them have structural or functional defects in collagen type I and type II. Abnormalities in collagen type I cause osteogenesis imperfecta (OI) while abnormalities in collagen type II cause a spectrum of disorder which is collectively called type II collagenopathies.

The incidence of OI in the US is about 1:20,000 live births. Patients suffer from brittle bone that are prone to fracture. In severe cases, recurrent fractures lead to bone deformities and disabilities. They may suffered from acute or chronic pain, reduced quality of life, and depression. There is no cure for OI. The main treatment is aimed to increase the overall bone density, prevent fracture, and maintain joint mobility. Bisphosphonate is the only medication that is proved to reduce the fracture rate. However, some patients do not respond to bisphosphonate due to differences in underlying mechanisms of the diseases. Obtaining definite genetic diagnosis may provide a pathogenesis of OI leading to proper management and targeted therapy.

Type II collagenopathies lead to retardation of endochondral ossification. Moreover, it is a structure protein of many organs including inner ear, vitreous humor of eyeball, and nucleus pulposus. Type II collagenopathies range from *in utero* lethal to adults disorders. Obtaining underlying causative mutations not only help in the

clinical diagnosis of this disease, but also in providing precise genetic counselling to the patients and families.

The use of conventional mutation detection methods by PCR and Sanger sequencing would be time-consuming and expensive. In this articles, we show that WES is an efficient method to identify underlying mutations and can guide clinicians for proper managements.

A.2 REVIEW OF RELATED LITERATURES

A.2.1 Molecular pathology and phenotypic spectrum in osteogenesis imperfecta

OI is a heritable connective disease characterized by bone fragility and fracture susceptibility. More than 95% of OI have dominant mutations in *COL1A1* or *COL1A2*, but recessive forms caused by mutations in *CRTAP* (103), *BMP1* (104), *CREB3L1*(105), *IFITM5* (106), *FKBP10* (107), *LEPRE1* (108), *PPIB* (109), *SP7* (110), *PLOD2* (111), *TMEM38B* (112), *SERPINF* (113), *SERPINH1* (114), *SEC24D* (115), *SPARC* (116), *WNT1* (117). Mutations in *COL1A1* or *COL1A2* result in structural and quantitative defects of collagen type I while recessive forms result in abnormal post-translational modification and protein interaction. OI has been classified into many types according to clinical presentation and genetic alterations. Phenotypic spectrum in OI varies from intrauterine fracture and perinatal death to mild form with a few or no fracture (118).

A.2.2 Molecular pathology and phenotypic spectrum in type II collagenopathies

COL2A1 regulates the important components that required to construct α -chain of type II collagen. Type II collagen is the main structural protein in cartilage and bone. Phenotypic-genotype correlations of *COL2A1* mutations in triple-helical glycine region showed that glycine to serine substitutions caused variable phenotypes. Glycine to non-serine substitutions or in-frame derangement caused more severe phenotypes such as achondrogenesis type II (ACG2; OMIM# 200610), hypochondrogenesis, and spondyloepiphyseal dysplasia congenital (SEDC; OMIM#183900). Missense mutations locating near N- or C-terminal usually cause HCG, while mutations of SEDC spread throughout the gene (119). Truncating mutations in the triple helical or N-propeptide region cause Stickler syndrome type I (STL1; OMIM# 108300) or Kniest dysplasia (OMIM# 156550) (119). Mutations in C-propeptide region cause unique phenotypes which range from *in utero* lethal to mild joint dysplasia including platyspondylic lethal skeletal dysplasia, Torrance type (PLSDT# OMIM 151210), spondyloperipheral dysplasia (SPPD) (OMIM# 271700) (120), vitreoretinopathy with phalangeal epiphyseal dysplasia (VPED) (121), or avascular necrosis of the femoral head (ANFH; OMIM# 608805) (122).

A.2.3 The use of whole-exome sequencing as a molecular diagnostic tool in skeletal dysplasias

Using WES, a next-generation sequencing (NGS), DNA is fragmented into millions of small fragments, followed by massively parallel sequencing of all exons in the genome. WES is suitable for detection of single nucleotide substitutions, small insertions, or deletions that less than 8-10 bases (123). WES and whole-genome

sequencing can be used to identify new disease genes. After the first use of NGS in 2010, 28 novel causative genes of skeletal dysplasia were identified. Moreover, incidental actionable pathogenic variants may be identified (124). The cost of NGS decreased dramatically from hundreds millions of dollars in 2001 to less than thousand dollars now. Compared to conventional methods by PCR and Sanger sequencing in mutation detection, NGS is not only less time consuming, but also less expensive. Skeletal dysplasias have more than 200 disorders. Molecular diagnosis using conventional methods would prohibitively expensive and time-consuming. However, there are many important points in using this technology. NGS has high calling error rates when compared with conventional method by PCR and Sanger sequencing but increasing the read depth of sequencing can eliminate the false positive (125). However, conventional methods such as Sanger sequencing are still needed to confirm the results of NGS.

A.2.4 Synthesis approach NGS by Illumina technology

Illumina NGS technology is sequencing by synthesis. Four nucleotide including A, T, C, and G are added to the DNA template and DNA polymerase in a flow cell channels. The flow cell is covered with adaptor library. Each of nucleotides has unique fluorescent label. When these nucleotides are added, fluorescent signal is captured.

This NGS technique library starts with fragmentation of genomic DNA into short sequences with approximately 200-500 base pairs. The end of these DNA fragments will be ligated with adapters which contain primer binding site and complementary region of oligo in the flow cell. Next process is clustering. Clustering

is the utilization of solid-phase amplification to produce randomly distributed, clonally amplified clusters from the flow cell. The surface of flow cell has two types of adaptor-specific adaptor oligo. The first oligo is hybridized to the adapter region on one surface of fragment strand. When DNA templates pass through the lane, the fragment strand will bind to the surface of oligo. After that, DNA polymerase will synthesize the complementary DNA sequencing of the hybridized fragments. The next process is denaturation of these double strand fragments into single strand fragments. These single strand fragments divided into original DNA template and synthesized complement DNA fragments. The original template is washed away. Only synthesized complement DNA fragments are left on the glass slide. Then, these fragments fold over and adapter regions hybridize to the second oligo type. DNA polymerase generates the complementary strands to form double strand bridges. These bridges are denatured to be two copy of single strands DNA template. These processes are called bridge amplification and repeated for millions cycles simultaneously. After the bridge amplification, reverse strands are cleaved and washed away, leaving the forward strand on the surface. Sequencing processes are started with hybridization of the first primer on the complementary regions on the adapter of DNA template. Fluorescent tagged nucleotides are then added to elongate the sequences. After that, these fluorescent tagged nucleotides are excited by a light source and will emit the unique characteristic of each fluorescence. Length of each read is determined by the number of cycle while base calling is determined by the number of cycles. All identical strands are read simultaneously to generate enough emission signal for detection. Hundreds millions of strands are sequenced to obtain billions of forward sequencing data. After the first read, the products are washed away

and 3' of sequences will be blocked. The DNA templates will fold over again to form bridge formation. DNA polymerase will synthesized the reverse strands as the same as was done in forward strands. All of the sequences are divided into groups based on the similarity of base calling. Forward and reverse strands are paired to obtain continuous sequence data and aligned to the reference genome (126-130)

A.3 MATERIALS AND METHODS

A.3.1 Study subjects

Thai children with skeletal dysplasia who were brought to the Genetics Clinic of King Chulalongkorn Memorial Hospital were included in this study. The medical data, pedigree, physical examination data, and laboratory results were recorded. The possible consequences of this study were thoroughly explained to the caregivers of the infant, and informed consent was obtained from them. Ethical approval was obtained from Chulalongkorn University Ethics Committee for the Faculty of Medicine.

A.3.2 Genomic DNA preparation and Truseq Custom Amplicon sequencing in the patient with OI

DNA was extracted from leukocyte of our proband and her mother using a Puregene blood kit (Qiagen, Hilden, Germany). Blood from the younger sister and the father were not available. Known 15 OI causing genes including *BMP1*, *COL1A1*, *COL1A2*, *CREB3L1*, *CRTAP*, *FKBP10*, *IFITM5*, *LEPRE1*, *PLOD2*, *PPIB*, *SERPINF1*, *SERPINH1*, *SP7*, *TMEM38B* and *WNT1* were amplified from 200 ng of genomic by using Truseq Amplicon Sequencing kit (Illumina, San Diego, CA). Target

genes comprised of 226 exons (30 kb). 268 amplicons which covered those all 226 exons were sequenced by Miseq (Illumina, San Diego, CA) using 2x250 paired-end reads. All reads were aligned against the University of California Santa Cruz human genome assembly hg19 using Burrows-Wheeler Alignment software (bio-bwa.sourceforge.net/). SNVs and Indel were detected by Miseq reporter software. Finally possible disease causing variants were confirmed by PCR and Sanger sequencing. PCR and Sanger sequencing using leukocyte-derived DNA of her mother were also performed.

A.3.3 Genomic DNA preparation and WES in the patient with type II collagenopathy

Genomic DNA was isolated from peripheral blood leukocytes obtained from the infant, using Puregene Blood kit (Qiagen, Hilden, Germany). WES of the genomic DNA was performed by Macrogen Inc. (Seoul, South Korea). DNA was captured on the SureSelect Human All Exon kit (v.4; Agilent Technologies, Santa Clara, CA, USA) and sequenced on an Agilent Hiseq2000 sequencer. Base calling was performed and the quality scores determined using the Real Time Analysis software (v.1.7; Illumina, San Diego, CA, USA). Sequence reads were aligned against UCSC hg19 using the Burrows-Wheeler Alignment software (<http://bio-bwa.sourceforge.net/>). Single nucleotide variants (SNVs) and insertion/deletions (InDels) were detected using SAMTOOLS (<http://samtools.sourceforge.net/>) and annotated by dbSNP&1000G. After quality filtering, we attempted to identify variants located in the coding regions of previously reported skeletal dysplasia genes for all potential pathogenic SNVs and InDels. Variant calling exclusion criteria included a coverage

<10X, quality score <20, minor allele frequency <1% in 1000 Genomes Project, and non-coding variants and synonymous exonic variants. The remaining variants were subsequently filtered using an in-house database of 165 unrelated Thai exomes. The variants were confirmed by PCR and Sanger sequencing.

Existing SNVs or known pathogenic mutations were filtered out using the Human Gene Mutation Database (HGMD; <http://www.hgmd.cf.ac.uk/ac/index.php>) and Exome Aggregation Consortium (ExAC; <http://exac.broadinstitute.org>). Deleterious SNVs were predicted by Polyphen-2 (<http://genetics.bwh.harvard.edu/pph2/>) and SIFT (<http://sift.jcvi.org>). Evolutionarily conserved sequences among species were analyzed using Clustal X v.2 (<http://clustal.org/clustal2/>).

A.3.3 A diagnosis of type II OI was made in the first child

The first child is a 14-year-old Thai girl who was born via cesarean section due to premature rupture of the membrane with a birth weight of 2,500 g. She is the first child of a consanguineous (second-degree relatives) couple. During her first year of life, she had delayed development and growth failure. At one year of age, she could not sit by herself and weighed 7.5 kg. (< 3rd centile). She presented to our hospital at 14 months of age with fractures of both femora without significant trauma. She was found to have ptosis of both eyes, normal teeth, no blue sclerae and small for her age. Her weight was 7.8 kg. (3rd centile) and her length was 68 cm. (< 3rd centile). Skeletal survey showed diffuse osteopenia, multiple healed fractures of the right humeral shaft, and both tibiae and fibulae. Spine radiograph showed flattening and indentation of vertebral bodies. Diagnosis of OI was made and intravenous bisphosphonate therapy was initiated and given every 3 months. Since then she had some of long bone

fractures from minor trauma. Multiple corrective osteotomies were performed to correct her deformities. At the last follow-up, she was 14 year-old with 20 kg of weight. She could not walk due to her long bone deformity (Figure 27). She could talk fluently appropriate for age and is in special education class due to physical disabilities. A diagnosis of type II OI was made in this patient.



Figure 54 Physical examination reveals short stature with complex long bone deformities. Radiograph of lower extremities revealed varus deformity of the femurs and valgus deformity of the tibias.

Her younger sister was found to have dilation of fourth ventricle by prenatal ultrasonography. She was born at term via cesarean section because of previous cesarean section and was diagnosed with hydrocephalus at birth. At 4 months of age, she had the first fracture without a history of a significant trauma. She was then diagnosed with OI. Physical examination revealed her head circumference of 38 cm (>95th centile) with wide anterior fontanelle (3x3 cm.) and blue sclerae. She had

delayed global development (could not hold her head) and hypotonia. MRI of the brain demonstrated large posterior fossa cyst connecting with fourth ventricular system, moderately hydrocephalus, hypoplasia of cerebellar hemisphere with absent of cerebellar vermis, and hypoplasia of corpus callosum. She was also diagnosed with vesicoureteral reflux grade 5 and gastroesophageal reflux requiring feeding tube. Many hospitalizations occurred because of recurrent urinary tract infection and pneumonia. She expired at 1 year of age.

A.3.4 A diagnosis of type II OI was made in the first child

The second child is the first child of a non-consanguineous couple. He was born by cesarean section due to breech presentation with a birth weight of 2640 g. He was referred to genetic clinic, Chulalongkorn University Hospital at age of 9 months. Physical examination revealed short stature (51 cm), flat midface, pectus carinatum, rhizomelia, limited range of motion of elbows, and left indirect inguinal hernia (Figure 28A). Radiographic studies revealed global delay ossification. The anteroposterior radiograph showed broad and bell-shaped thorax (Fig.2B) while lateral chest radiograph showed anterior rib flaring and platyspondyly (Figure 2C). Delayed ossification of pubic bones and small iliac wings were observed. No ossification centers were seen at femoral heads, necks, and around the knees. Long tubular bones have short appearance (Figure 28B, D). His parents and siblings have no dysmorphic feature. SEDC, a type II collagenopathy, was diagnosed in this patient.



Figure 55 Clinical and radiographic feature of the patient with SEDC. A. Physical examination reveals flat midface, pectus carinatum, rhizomelia, and left inguinal hernia. B. Chest AP radiograph reveals a bell-shaped thorax and short humeri. C. Chest lateral radiograph reveals anterior rib flaring and platyspondyly. D. Pelvic radiograph reveals delayed ossification of pubic bones, femoral heads, and necks, and short small iliac bones.

A.4 Results

A.4.1 Truseq Custom Amplicon sequencing revealed a novel homozygous one base pair frameshift deletion in *WNT1* in OI child.

Truseq Custom Amplicon sequencing of the proband revealed homozygous, c.3delG, pLeu3Serfs*36 in *WNT1*. These mutations have never been reported in Human Gene Mutation Database (HGMD; <http://www.hgmd.cf.ac.uk/ac/index.php>). PCR and Sanger sequencing using DNA of leukocytes from the patient and her

mother showed that the patient was homozygous, while her mother were heterozygous for the mutation.

A.4.2 WES revealed a *de novo* missense mutation in *COL2A1*

A non-synonymous variant, c.G2024A: p.G675D was indentified in *COL2A1*. PCR and Sanger sequencing of DNA extracted from leukocytes revealed that the patient was heterozygous for the mutation while his parents expressed wild type allele (Figure 29A). Prediction software including Polyphen-2 and SIFT (<http://sift.jcvi.org>) predicted that this mutation is damaging, with a score of 0.999 and deleterious, with a score of 0.001 respectively. Clustal X v.2 (<http://clustal.org/clustal2/>) this mutation is in evolutionary conserved region among species (Figure 29B). This mutation was absent in the HGMD (<http://www.hgmd.cf.ac.uk/ac/index.php>) and ExAC (<http://exac.broadinstitute.org>) databases, and our 165 in-house exome database.

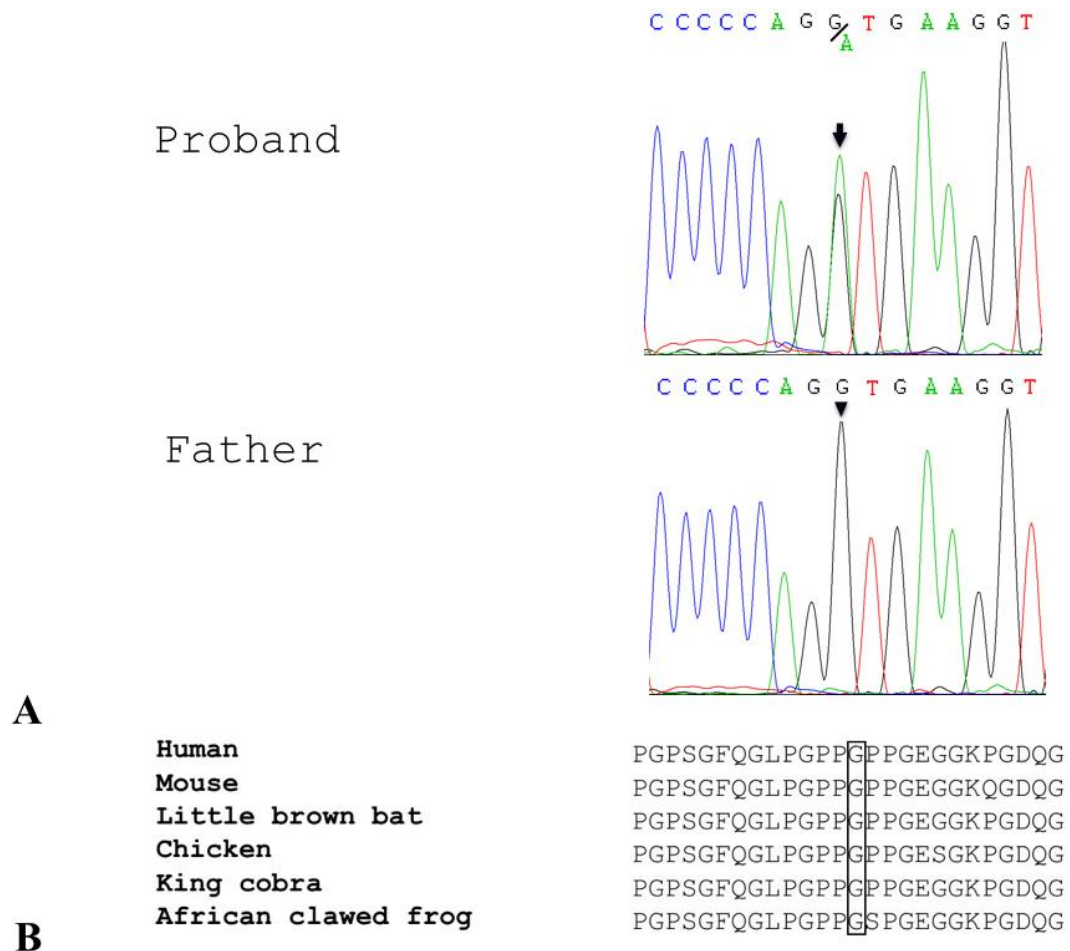


Figure 56 Mutation analysis A. Direct sequencing reveals that proband is heterozygous for a de novo c.G2024A (p.G675D) mutation (upper panel). His father expresses only wild type allele. B. This mutation is in the highly conserved region among species.

A.5 Discussion

WNT1 mutations were identified as a cause of malformation of mid brain and cerebellum in early brain development in mice for long before identified as a cause of OI in humans (131). Until in 2014, Swaying (*Wnt1^{sw/sw}*) mice that carry mutation in *WNT1*, had OI phenotypes including bone fragility and severe osteopenia (132).

Altered *WNT1* proteins fail to interact with its coreceptor, LRP5, which requires for frizzled receptor (FDZ) and activate WNT-regulated β -catenin signaling pathway (133). A homozygous loss of function mutations in *LRP5* resulting in osteoporosis-pseudoglioma syndrome (OPPG) characterized by low bone mass and pseudoglioma. Moreover, *SP7* (Osterix) and *ALPI* which are crucial for osteoblast differentiation and bone mineralization, are the downstream genes of Wnt signaling pathway (134, 135). An Egyptian child from a consanguineous family carrying homozygous one base pair deletion in *SP7* diagnosed OI type III so alteration in *WNT1* gene may effect *SP1* expression resulting in defective osteoblast differentiation (110). All of the above emphasize that *WNT1* is important for bone formation and homeostasis.

The patients describe here have an autosomal recessive form of OI caused by homozygous truncating mutation in *WNT1*. From our review, this mutation is the shortest truncating mutation due to out-of frame G deletion in starting codon of *WNT1* which expected to have nonsense-mediated mRNA decay (NMD). While our proband has only OI phenotype, her younger sister also suffered from brain anomalies showing significant variability in neurological involvement in between affected siblings (136) with identical *WNT1* alleles suggesting that *WNT1* might be subject to modifier alleles, non-genetic or epigenetics factors in human brain development.

In the second case, a previously undescribed heterozygous mutation c.G2024 in *COL2A1* which should cause an amino acid substitution, p.G675D. This mutation is in the triple-helical region. Many lines of evidences suggested that this is the causative mutation: First, this mutation is a *de novo* mutation. Second, it was absent in our 165 in-house Thai exome database. Third, this mutation is in the very highly

conserved region among species. Fourth, prediction software predicted that it should be pathogenic variant.

COL2A1 regulates the production of components to construct the α -chain of pro-collagen type II. It is a very important structural protein component of bones, cartilages, nucleus pulposus, and vitreous humor of the eye. Genotype-phenotype correlation studies shows that glycine to serine substitutions create variable phenotype while glycine to non-serine substitutions create more severe phenotypes such as HCG and SEDC. Missense mutations in HCG usually located near N- or C- terminal boundaries of triple-helical region but missense mutation in SEDC randomly spread throughout the exons (119). Mutation observed in our patient is in the triple-helical region. It is a glycine to non-serine substitutions. All patients carry this kind of mutations in triple-helical region always ocular abnormalities such as retinal detachment, vitreous degeneration, severe myopia, or blindness. This information led us to highly recommend a thorough eye examination in this patient. However, no ocular abnormality is detected now.

In conclusion, the use of NGS in molecular diagnosis not only fulfills the knowledge of skeletal dysplasias, but also leads the clinician for the definite diagnosis, proper management, precise genetic counselling.

VITA

Name	Apiruk Sangsin
Date of Birth	November 11, 1983
Place of Birth	Phrae, Thailand
Home Address	90/82 Moo 5, Kankongchonpratan Rd., Tambon Suthep, Muang district, Chiang Mai, Thailand 50200 Telephone 66-53810-800

EDUCATION

2002-2008 Doctor of medicine, Chiang Mai University, Chiang Mai, Thailand (M.D.)(First degree honors)

2008-2009 Internship training, Faculty of Medicine, Chiang Mai University, Chiang Mai, Thailand

2009-2012 Residency in Orthopedic Surgery, Faculty of Medicine, Chiang Mai University, Chiang Mai, Thailand

2013 Visiting research fellowship in Musculoskeletal oncology, Keio University, Tokyo, Japan

2013-2014 Clinical fellowship in Musculoskeletal oncology, Department of Orthopaedics, Faculty of Medicine, Chiang Mai University, Chiang Mai, Thailand

RESEARCH PUBLICATIONS

Apiruk Sangsin, Chalurmporn Srichomtong, Monnat Pongpanich, Kanya Suphapeetiporn, Vorasuk Shotelersuk. Whole exome sequencing reveals a novel COL2A1 mutation in a patient with spondyloepiphyseal dysplasia congenita. *Genetics and Molecular Research* 2016